STREAM-AQUIFER INTERACTIONS: ITS EFFECTS ON NUTRIENT VARIABILITY, ITS ROLE ON STREAMFLOW PERMANENCE AND THE EFFECTS OF TEMPERATURE MEASUREMENT RESOLUTION ON ITS QUANTIFICATION

by

Carlos Daniel Soto López

A Dissertation Submitted to the Faculty of the

DEPARTMENT OF HYDROLOGY AND ATMOSPHERIC SCIENCES

In Partial Fulfillment of the Requirements

For the Degree of

DOCTOR OF PHILOSOPHY

In the Graduate College

THE UNIVERSITY OF ARIZONA

2018

THE UNIVERSITY OF ARIZONA
GRADUATE COLLEGE

As members of the Dissertation Committee, we certify that we have read the dissertation prepared by Carlos Daniel Soto López, titled Stream-Aquifer Interactions: Its Effects On Nutrient Variability, Its Role On Streamflow Permanence And The Effects Of Temperature Measurement Resolution On Its Quantification and recommend that it be accepted as fulfilling the dissertation requirement for the Degree of Doctor of Philosophy.

Thomas Meixner — Date: July 27, 2018

Ty P.A. Ferré — Date: July 27, 2018

Jennifer McIntosh — Date: July 27, 2018

Jon Pelletier — Date: July 27, 2018

Final approval and acceptance of this dissertation is contingent upon the candidate's submission of the final copies of the dissertation to the Graduate College.

I hereby certify that I have read this dissertation prepared under my direction and recommend that it be accepted as fulfilling the dissertation requirement.

Dissertation Director: Thomas Meixner — Date: July 27, 2018

STATEMENT BY AUTHOR

This dissertation has been submitted in partial fulfillment of the requirements for an advanced degree at the University of Arizona and is deposited in the University Library to be made available to borrowers under rules of the Library.

SIGNED: Carlos Daniel Soto López

ACKNOWLEDGMENTS

I would like to first thank my advisor, Dr. Thomas Meixner, for his continued support and commitment throughout my graduate studies. He has been instrumental on my journey and without his guidance and patience this work would not have happened.

I would also like to thank my dissertation committee members, Dr. Ferré, Dr. McIntosh and Dr. Pelletier. Their insights, guidance and feedback have been key in the completion of this dissertation.

I am very thankful to the National Science Foundation Graduate Research Fellowship Program, which provided funding for part of graduate studies and research.

Finally and most importantly, I would like to thank my dear wife, Dr. Angélica Vázquez Ortega, for being the pillar and driver I needed at a point when I thought none was needed. Thank you!

DEDICATION

I dedicate this work to my wife, Angélica, to my children, Adrián and Paola, and to my parents, Ramón and Sylvia. This is a product of your unconditional love and support.

TABLE OF CONTENTS

ABSTRACT

In semi-arid river systems, the connectivity and interaction between the stream and its aquifer is an important hydrologic linkage that affects the presence and quantity of streamflow, and the biogeochemical processes occurring in the stream, its streambed and aquifer. The work presented here builds upon and intends to expand on the knowledge base of stream-aquifer interaction by focusing on three main study areas. First, a descriptive and process based study evaluates how changes in basin groundwater (BGW) contribution to streamflow in the San Pedro River translate to changes in its chemical composition (nitrogen, metals and dissolved organic carbon) and proposes mechanisms that could explain the observed relationships. Second, an experimental and process based study evaluates how an empirically derived predictive model can use and predict streamflow permanence (wet/dry areas) on the San Pedro River from a set of geomorphic and hydrologic variables. Third, a methodological investigation of an idealized system that evaluates the effect of temperature measurement resolution on the estimations of stream-aquifer flux using temperature as a tracer. Major findings of this work show that in the San Pedro River: 1) BGW contribution and its variability increases with downstream distance and time since last flooding; 2) the concentrations, variability and spatial dependence of several chemical species are associated and follow similar patterns with BGW contribution; and 3) an empirical model using variables that describe bedrock elevation, the shape and width of the floodplain, the land surface elevation, and late spring streamflow can be used to correctly predict 80-87% of the wet/dry location in the river. In addition, this study found that temperature measurement resolution introduces large estimation errors when temperature amplitude is used as a predictor of stream-

aquifer flux, and that it limits the range over which vertical stream-aquifer fluxes can be accurately estimated more than temperature measurement, placement and thermal parameter uncertainty.

1 INTRODUCTION

At its most basic level, streams can be considered hydrologic conduits in which surface water, following the path of least resistance, is able to accumulate and be transported downhill. These conduits are not impervious and to different magnitudes and time scales allow for the exchange of water, mater and energy between the atmosphere, the biota, and the water bearing porous geologic formations (aquifers) within the stream catchment [*Chen,* 2007; *Covino,* 2017; *Jones and Mulholland,* 2000; *Wohl,* 2014]. Similar to streams, aquifers are able to exchange water, mater and energy back to the stream, or store and transport them within the aquifer [*Brutsaert,* 2005; *Chen,* 2007; *Jones and Mulholland,* 2000; *Karamouz et al.,* 2011; *Pinder and Celia,* 2006; *Wohl,* 2014]. These interactions make the stream and its aquifer linked elements of the hydrologic cycle that not only affect the discharge and recharge processes of the stream and aquifer, but also the biogeochemical processes that occur in them [*Dent and Grimm,* 1999; *Dent et al.,* 2001; *Holmes et al.,* 1994; *Jones et al.,* 1995a; *Jones et al.,* 1995b; *Sophocleous,* 2002].

How, where and when these interactions occur, the magnitude and directionality of these interaction, and what effects will these interactions have on the stream and the aquifer are controlled by the local and regional climatic, hydrogeologic, geomorphic and biologic conditions of the system [*Jones and Mulholland,* 2000; *Sophocleous,* 2002]. This has provided fertile grounds for research into stream-aquifer (SA) interactions and because of this the body of published research focusing SA interactions has seen a dramatic increase since the early 1990. This period of prolific growth has not only increased our knowledge in the field of SA interactions but in some instances it helped to

shift the focus of research from broad issue research, that identified knowledge gaps and proposed conceptual models, to more descriptive, empirical, process and method based studies [*Wondzell,* 2015]. In general, the work presented here falls in line with the latter category of studies and focuses on the SA interactions of the San Pedro River National Conservation Area, a mostly perennial and undammed semi-arid river and riparian system in southeastern Arizona, United States.

The San Pedro River, like other semi-arid river systems of the southwestern United States, has two characteristics that make it ideal to study SA interactions. First, these systems experience extended periods were potential evapotranspiration far exceed precipitation rates and during these periods streamflow is sustained by aquifer inputs (baseflow) [*Pool and Coes,* 1999; *Thomas et al.,* 2006]. Second, summer flooding and overland connectivity between the river and hillslopes occurs during the summer monsoon season (June to October) [*Pool and Coes,* 1999; *Thomas et al.,* 2006]. Both of these characteristics result in a reduction in the interactions and potential sources that support and control streamflow and its chemical composition. Furthermore, and thanks to over two decades of research, our understanding of the San Pedro River system is fairly mature [*Stromberg and Tellman,* 2009]. For example studies have: Characterized the aquifer system [*Gettings and Houser,* 2000; *Gungle et al.,* 2016; *Hopkins et al.,* 2014; *Lacher et al.,* 2014; *Pool and Coes,* 1999; *Robertson,* 1992]; Mapped and characterized the effects streamflow intermittency [*Stromberg et al.,* 2005; *Turner and Richter,* 2011], Analyzed the effects of flooding on the river and aquifer [*Brooks and Lemon,* 2007; *Brooks et al.,* 2007; *Simpson,* 2011]; Characterized the river and streamflow [*Baillie et al.,* 2007; *Haas,* 2003; *Hereford,* 1993; *Pool and Coes,* 1999; *Thomas et al.,* 2006];

Characterized the sources of streamflow and aquifer recharge [*Baillie et al.,* 2007; *Wahi et al.,* 2008]; and the effects of climate change [*Dixon et al.,* 2009; *Stromberg and Tellman,* 2009]. This existing knowledge base allows research and development to focus on more complex question in the San Pedro River system.

This work aims to build upon this growing body of research to describe how the chemical composition of streamflow evolves with increased SA interaction and propose processes that could explain the observed patters, generate an empirical model that is able to replicate observed streamflow permanence survey and identify the variables that are significant predictors of streamflow permanence, and lastly describe the effects temperature measurement resolution in the estimation of stream-aquifer flux for an idealized system.

1.1 Dissertation Format

This dissertation contains a summary section entitled Present Study in which the three manuscripts that will be or have been submitted for publication are briefly introduced, described and summarized. Each of the three appendices that follow the initial section contains fully formatted and independent manuscripts. Each manuscript describes in detail the background, motivation, methods, results, and discussion of each study.

The manuscripts submitted on this dissertation (Appendices A-C) as well as the supporting materials (Appendices D-F) were developed solely by the primary author. The coauthor(s) provided insight and direction throughout the studies as well as editorial feedback during the development and refinement of all three manuscripts.

2 PRESENT STUDY

The present study is divided into three manuscripts that are included in this dissertation as Appendices A, B and C with supporting information for each manuscript included in Appendices D through F. The main subject of this work is Stream-Aquifer (SA) interactions and its effects on stream nutrient concentrations, its role on streamflow permanence and the effects of measurement resolution on its quantification using temperature as a tracer. Specifically, Appendix A investigates how the chemical composition of streamflow evolves as the basin groundwater contribution to streamflow changes in the San Pedro River, Appendix B investigates which physical, spatial and temporal properties of semi-arid river systems influence streamflow permanence and Appendix C expands the analysis of recently published work to include the effects of temperature measurement resolution on estimates of vertical SA interaction using recorded temperature time series of the stream and its streambed. The following is a summary of each manuscript.

2.1 Summary of Manuscript 1: On the Controls of Temporal Variation of Nitrogen, Metals and DOC Concentration in a Semi-Arid River; San Pedro, Arizona

The objective of this manuscript is to describe how the chemical composition of streamflow evolves as the basin groundwater contribution to streamflow changes in the San Pedro River. Specifically this manuscript aims to answer the following three questions: Do changes in basin groundwater contribution to streamflow translate to changes in its chemical composition (Nitrogen, Metals and Dissolved Organic Carbon)? 2) Would, simple mixing between two chemically distinct sources explain the observed variability? and 3) What do the relationships between SA Interactions and the chemical

composition of streamflow indicate about the underlying processes controlling nutrient concentrations in a semi-arid stream? We hypothesized that increases in basin groundwater (BGW) contribution to streamflow would be accompanied by decreases in the concentration of nitrogen, metals and dissolved organic carbon. To answer these questions streamflow water samples of the San Pedro River were collected and analyzed to determine the dissolved concentrations of their major anions (Cl, NO_2, NO_3, and SO4), metals (Ca, K, Mg, Na, Si, and Sr), Total Nitrogen (TN), and dissolved organic carbon (DOC).

As expected, this study shows that basin groundwater (BGW) contribution to streamflow changes both spatially and temporally. Specifically, BGW contribution increases with time since last flooding and downstream distance. This study found that changes in BGW contribution are in fact associated with changes in the concentration, variability, and spatial dependence of ten different chemical species in streamflow during the study period. Although, most of the chemical species did not follow the expected decrease in concentration with increases in BGW contribution hypothesized in this study, the results showed that multiple chemical species had similar patterns in the relationship between their average concentration and variability with BGW contribution. In general our results show that K, Na and DOC decrease their concentration while F and TN increase their concentration with increases in BGW contribution. On the other hand, the results show that the concentrations of Ca, Mg, Si, Sr and IN do change with changes in BGW contribution and that the direction of that relationship (inverse or direct) depends on the degree of BGW contribution to streamflow and 2) the threshold value for the inversion in the relationship is a proximately 42% and 3) the concentration of Ca, Mg, Si,

Sr and IN increase significantly when BGW contribution is highest, and streamflow is lowest. Also, the results show that mixing between BGW and floodwater inputs to baseflow appears to control the observed variability in the in-stream concentrations of Mg, Si, Sr, K, and DOC. Finally, all chemical species exhibited spatial dependence (autocorrelation) at either the 10Km or 1Km sampling reaches with the range of spatial auto correlation trending smaller with increases in BGW contribution.

We argue that the similar response of the chemical species concentration, variability and spatial dependence to changes in BGW contribution in the San Pedro River may point to the sources or mechanism controlling those chemical species in streamflow. Based on past published research three groups of potential processes or mechanism that could explain the observed patterns are proposed.

For example, the inversion in the relationship exhibited by Ca, Mg, Si, Sr and IN when BGW contribution exceeded ~42% suggest that the sources and processes controlling these chemical species in streamflow shift from one of dilution or in-stream consumption, to one of concentration or in-stream production when BGW contribution is at the extremes. However, there is a threshold that triggers an apparent switch in the source and processes controlling Ca, MG, Si, Sr and IN as the stream becomes more BGW dominated. In the San Pedro river, we argue this process could associated with one or more of the following events: changes in the in-stream biological activity, an increase in parafluvial areas of the streambed due do decreases in streamflow, the relative increase in basin groundwater flow and changes in the physical or chemical characteristics of stream waters (e.g. temperature, pH, DO, etc.). However, we acknowledge that determining which of the potential process or combination of processes that are

effectively controlling the chemical species observed in streamflow waters of the San Pedro River would require a specific set of experimental measures that have not been conducted.

2.2 Summary of Manuscript 2: An Empirical Model for Predicting Flow Permanence on the San Pedro River

The objective of this manuscript was to answer the following 3 questions: First, what physical, spatial and temporal properties of semi-arid river systems influence streamflow permanence (wet/dry patterns)? Two, how sensitive is streamflow permanence to changes in streamflow? Three, what do these results indicate about the underlying processes controlling streamflow permanence in arid and semi-arid regions? We claim that major factors that control proximity of the water table to the ground surface (i.e.: bedrock topography, surface concavity, channel geomorphology and contributing area) as well as minor factors (i.e.: stream channel slope, stream channel sinuosity, flood plain width, streamflow and precipitation) will be significant predictors of the location and spatial distribution of streamflow permanence in the San Pedro River.

To answer these questions a logistic regression model was generated and used to test if several geomorphic and hydrologic explanatory variables are significant predictors of streamflow permanence observed and recorded in the San Pedro River for the years of 1999-2011. The creation of the logistic regression model was followed by an overall assessment of the logistic regression, the fit of the model to actual outcomes, and an evaluation of its predicted probabilities. Lastly, the calibrated and validated logistic regression model was used to assess the effects of future scenarios on the patterns of river

reaches predicted wet by looking at historical highs, lows and average values for streamflow and precipitation in the basin.

The results show that a logistic regression using ten (10) hydrologic and geomorphic explanatory variables can be used to predict streamflow permanence on the San Pedro River National Conservation Area. Analysis of the logistic regression model revealed that late spring streamflow as well as variables that describe bedrock elevation, variables that describe the shape and width of the floodplain and variables that describe the land surface elevation are significant predictors of streamflow permanence in the San Pedro River. These variables either directly or indirectly describe: the surface-groundwater-vegetation interaction of late spring baseflow, the shape and thickness of the aquifer underlying the river, the channel morphology and how it varies along the river, and the shape and form of the stream surface. Making use of those explanatory variables the logistic regression model was able to correctly predict 80.1-86.7% of the wet/dry locations of the study site during the validation period of 2006 to 2011 at a resolution of 10 meters. The logistic regression model was also able to show that increasing late spring streamflow would result in a downstream expansion of river segments classified as wet centered on areas that remain perennial.

2.3 Summary of Manuscript 3: Effects of Measurement Resolution on the Analysis of Temperature Time Series for Stream-Aquifer Flux Estimation

The objectives of this manuscript is to expand on recent published work and study the effects of temperature measurement discretization (measurement resolution) on the estimation of vertical SA fluxes as well as suggest a modified approach to make those estimations using temperature amplitude and phase shift information. In order to achieve

these objective this work expands on recently published work to generate a series of synthetic thermographs using an analytical solution to a one-dimensional conduction-advection-dispersion equation at two different depths beneath an idealized stream-streambed interface. The synthetic thermographs were generated in response to a range of synthetic thermal front velocities and a daily sinusoidal surface temperature signal generated at one-minute intervals for a system with constant thermal diffusivity.

The results of this study show that errors in thermal front velocity estimation introduced by discretizing thermographs differ when amplitude or phase shift data are used to estimate vertical fluxes. More importantly, the results also show that under similar conditions, sensor resolution will limit the range over which vertical velocities can be accurately reproduced more than combined effects of uncertainty in temperature measurements, uncertainty in sensor separation distance, and uncertainty in the thermal diffusivity. The study also shows that errors introduced by measurement discretization represent the baseline error present and thus the best-case scenario when discrete temperature measurements are used to infer vertical fluxes. Although the errors associated with measurement resolution would be minimized by using the highest resolution sensors available, a thoughtful experimental design could allow users to select the most cost-effective temperature sensors to fit their measurement needs.

2.4 Conclusions

This research adds to the growing understanding of the role stream-aquifer interactions play in the San Pedro River. More specifically how they relate to the chemical evolution of streamflow, how they can be inferred from a set of geomorphic and hydrologic variables in an empirical model, and how they can be accurately quantified using

temperature as a tracer. The research presented here allows us to conclude three main points.

First, this research shows that in the San Pedro River increased contribution of basin groundwater during the dry season was associated with changes in the concentration, variability, and spatial dependence of several chemical species in streamflow (K, Na, DOC, F, TN, Ca, Mg, Si, Sr and IN). More importantly, basin groundwater contribution and the concentration of these species followed either a direct, inverse or a threshold (direct then inverse) relationship. It is argued that the relationship of concentration and basin groundwater contribution may suggest to the sources or processes controlling those chemical species in streamflow. For example, the decreases in the pool size and leaching rates of allochthonous particulate and organic matter, increases biogeochemical uptake rates, decreases of autochthonous organic matter and DOC production rates, and increases of groundwater inputs are proposed as possible processes controlling the concentration in streamflow of K, Na, DOC, F, TN. On the other hand the increase in parafluvial areas in the stream (decrease in streamflow permanence), changes in the in-stream biological activity as well as changes in temperature, dissolved oxygen and pH in streamflow were proposed as the threshold process that could trigger the observed inversion in the relationship between basin groundwater contribution and the concentration Ca, MG, Si, Sr and IN. However, it is acknowledged that more research is needed to categorically identify which of these proposed processes is responsible for the observed changes.

Second, streamflow permanence is controlled by the connectivity between the stream and its aquifer, the directionality of the hydrologic gradient, and the in-stream balance

between inputs and outputs. However, this work was able to predict, with a good degree of accuracy, streamflow permanence using a logistic regression model that does not include direct observations of groundwater levels, hydrologic gradients, or streambed hydraulic properties as explanatory variables. Instead the model infers streamflow permanence by making use of variables that describe bedrock elevation, variables that describe the shape and width of the floodplain, variables that describe the land surface elevation as well as late spring streamflow. We propose that in the San Pedro River these variables describe, represent or act as a proxy of: the surface-groundwater-vegetation interaction of late spring baseflow, the shape and thickness of the aquifer underlying the river, the variability of the channel morphology, and the variation of shape and form of the stream surface. This is important because is suggest that in the absence of direct observations of the aquifer, proxy variables could be used to infer connectivity and interactions between the stream and its aquifer.

Third, there are several methodologies for the estimation of stream-aquifer fluxes, these include: flow-mass balance, Darcy Flux (hydraulic gradients), direct measurements of flux (seepage meters), and tracer-based (matter or energy based). The suitability of each of these methods will depend on the scale of project, accessibility to the site, resources needed, and the required accuracy. This work suggests a modified approach to make estimations of vertical stream-aquifer flux utilizing temperature as a tracer. This study found that temperature sensor resolution introduces large errors in the estimation of stream-aquifer flux when amplitude is used as the predictor instead of phase shift. Therefore it is recommended that phase shift be used to estimate the magnitude, whereas amplitude should be used to estimate directionality of the stream-aquifer flux. In

addition, tools and recommendations are made available to help in the planning and the collection of data so that the user is able to make the most accurate estimates of stream-aquifer flux possible

In conclusion, the works presented in this dissertation independently provide insights into stream-aquifer interactions. Each work focuses on different aspect of the interactions giving a descriptive-process based, an empirical-process based, and a method based investigation into stream-aquifer interactions

3 REFERENCES

Baillie, M. N., J. F. Hogan, B. Ekwurzel, A. K. Wahi, and C. J. Eastoe (2007), Quantifying water sources to a semiarid riparian ecosystem, San Pedro River, Arizona, *J. Geophys. Res., 112*.

Brooks, P. D., P. A. Haas, and A. K. Huth (2007), Seasonal variability in the concentration and flux of organic matter and inorganic nitrogen in a semiarid catchment, San Pedro River, Arizona, *J. Geophys. Res. -Biogeosci., 112*, G03S04.

Brooks, P. D. and M. M. Lemon (2007), Spatial variability in dissolved organic matter and inorganic nitrogen concentrations in a semiarid stream, San Pedro River, Arizona, *J. Geophys. Res. (G Biogeosci.), 112*.

Brutsaert, W., (2005), *Hydrology: An Introduction*, Cambridge University Press, Cambridge; New York.

Chen, X. (2007), Hydrologic connections of a stream-aquifer-vegetation zone in south-central Platte River valley, Nebraska, *J. Hydrol., 333*, 554-568.

Covino, T. (2017), Hydrologic connectivity as a framework for understanding biogeochemical flux through watersheds and along fluvial network, *Geomorphology, 277*, 133-144.

Dent, C. L. and N. B. Grimm (1999), Spatial heterogeneity of stream water nutrient concentrations over successional time, *Ecology, 80*, 2283-2298.

Dent, C. L., N. B. Grimm, and S. G. Fisher (2001), Multiscale effects of surface-subsurface exchange on stream water nutrient concentrations, *J. N. Am. Benthol. Soc., 20*, 162-181.

Dixon, M. D., J. C. Stromberg, J. T. Price, H. Galbraith, A. K. Fremier, and E. W. Larsen (2009), Potential effects of climate change on the upper san pedro riparian ecosystem, in *Ecology and Conservation of the San Pedro River*, edited by J. C. Stromberg and B. Tellman, University of Arizona Press, Tucson.

Gettings, M. E. and B. B. Houser (2000), Depth to bedrock in the Upper San Pedro Valley, Cochise County, southeastern Arizona, *U. S. Geological Survey Open-File Report, 00-138, Version 1.0*.

Gungle, B., J. B. Callegary, N. V. Paretti, J. R. Kennedy, C. J. Eastoe, D. S. Turner, J. E. Dickinson, L. R. Levick, and Z. P. Sugg (2016), Hydrological conditions and evaluation of sustainable groundwater use in the Sierra Vista Subwatershed, Upper San Pedro Basin, southeastern Arizona, *Scientific Investigations Report*, 106.

Haas, P. A. (2003), Changes in Concentration and Composition of dissolved and Particulate Organic Matter in the Upper San Pedro River, Arizona in Resposnse to Chanes in Flow Regime, 1-175.

Hereford, R. (1993), Entrenchment and Widening of the Upper San Pedro River, Arizona, *Geological Society of America Special Papers, 282*, 1-47.

Holmes, R. M., S. G. Fisher, and N. B. Grimm (1994), Parafluvial nitrogen dynamics in a desert stream ecosystem, *J. N. Am. Benthol. Soc., 13*, 468-478.

Hopkins, C. B., J. C. McIntosh, C. Eastoe, J. E. Dickinson, and T. Meixner (2014), Evaluation of the importance of clay confining units on groundwater flow in alluvial basins using solute and isotope tracers: the case of Middle San Pedro Basin in southeastern Arizona (USA), *Hydrogeol. J., 22*, 829-849.

Jones, J. B. and P. J. Mulholland (Eds.) (2000), *Streams and Ground Waters*, Acuatic Ecology Series, 425 pp., Academic Press, San Diego, California.

Jones, J. B.,Jr, S. G. Fisher, and N. B. Grimm (1995a), Nitrification in the hyporheic zone of a desert stream ecosystem, *J. N. Am. Benthol. Soc., 14*, 249-258.

Jones, J. B.,Jr, S. G. Fisher, and N. B. Grimm (1995b), Vertical hydrologic exchange and ecosystem metabolism in a Sonoran Desert stream, *Ecology, 76*, 942-952.

Karamouz, M., A. Ahmadi, and M. Akhbari (2011), *Groundwater Hydrology: Engineering, Planning, and Management*, CRC Press, Boca Raton, FL.

Lacher, J. L., S. D. Turner, B. Gungle, M. B. Bushman, and E. H. Richter (2014), Application of Hydrologic Tools and Monitoring to Support Managed Aquifer Recharge Decision Making in the Upper San Pedro River, Arizona, USA, *Water, 6*.

Pinder, G. F. and M. A. Celia (2006), *Subsurface Hydrology*, John Wiley & Sons, Incorporated, Hoboken.

Pool, D. R. and A. L. Coes (1999), Hydrogeologic investigations of the Sierra Vista subwatershed of the Upper San Pedro Basin, Cochise County, southeast Arizona: Water Resources Investigation Report, *99-4197*, 41 p.

Robertson, F. N. (1992), Radiocarbon dating of groundwater in a confined aquifer in southeast Arizona, *Radiocarbon, 34*, 664-676.

Simpson, S. C. (2011), Impacts of Floods on Riparian Groundwater and Post-Event Streamflow Across Spatial and Temporal Scales, PhD thesis, University of Arizona, Tucson, AZ.

Sophocleous, M. (2002), Interactions between groundwater and surface water: the state of the science, *Hydrogeol. J., 10*, 52-67.

Stromberg, Juliet C.,Tellman, Barbara., (2009), *Ecology and Conservation of the San Pedro River*, University of Arizona Press, Tucson.

Stromberg, J. C., K. J. Bagstad, J. M. Leenhouts, S. J. Lite, and E. Makings (2005), Effects of stream flow intermittency on riparian vegetation of a semiarid region river (San Pedro River, Arizona), *River Research and Applications, 21*, 925-938.

Thomas, B. E., D. R. Pool, and Geological Survey (U.S.) (2006), Trends in streamflow of the San Pedro River, southeastern Arizona, and regional trends in precipitation and streamflow in southeastern Arizona and southwestern New Mexico.

Turner, D. S. and H. E. Richter (2011), Wet/Dry Mapping: Using Citizen Scientists to Monitor the Extent of Perennial Surface Flow in Dryland Regions, *Environ. Manage.*, *47*, 497-505.

Wahi, A. K., J. F. Hogan, B. Ekwurzel, M. N. Baillie, and C. J. Eastoe (2008), Geochemical quantification of semiarid mountain recharge, *Ground Water*, *46*, 414-425.

Wohl, E. (2014), *Rivers in the Landscape : Science and Management*, Wiley-Blackwell, Somerset.

Wondzell, S. M. (2015), Groundwater–surface-water interactions: perspectives on the development of the science over the last 20 years, *Freshwater Science, 34*, 368-376.

APPENDIX A: ON THE CONTROLS OF TEMPORAL VARIATION OF NITROGEN, METALS AND DOC CONCENTRATION IN A SEMI-ARID RIVER; SAN PEDRO, ARIZONA

Carlos D. Soto-López[1], Thomas Meixner[1] and Scott Simpson [2]

[1] Department of Hydrology and Atmospheric Sciences

University of Arizona

1133 E James E Rogers Way

Building 11, Room 122

Tucson, Arizona, 85722, USA.

[2]Tetra Tech

Atlanta, Ga, USA

To be submitted for publication to Biogeochemistry

1 Abstract

The chemical composition of streamflow is the result of complex hydrological and biogeochemical processes of different spatiotemporal scales that occur inside the stream, its aquifer and along its hillslopes. Perennial semi-arid river systems of the southwestern United States are characterized by undergoing extended periods of time where potential evaporation rates greatly exceed precipitation rates ("dry season"). This implies that: 1) during the dry season perennial flow in these systems occurs only in locations where water is supplied by the river's aquifer, and 2) during the dry season the river system is effectively disconnected from its hillslope. Therefore, during the dry season these characteristics reduce the complexity of the interactions as well as the potential sources of water to the stream. This makes semi-arid rivers, like the San Pedro River in southeastern Arizona, an ideal system to study the concentration, variability and controls of chemical species in streamflow. In this study we aim to understand if changes in basin groundwater (BGW) contribution to streamflow translate to changes in its chemical composition (Nitrogen, Metals and DOC). Streamflow water samples were collected at sampling intervals (250, 100, 2.5 and 1 meters) along different locations of a 10 Km reach of the San Pedro River National Conservation Area in March 2007, May 2007, November 2007 and April 2008. Making use of SO_4/Cl ratios as a proxy of BGW contribution we found that BGW contribution and its variability increased with downstream distance and time since last flooding with a maximum BGW contribution of approximately 49% during May 2007 and a minimum BGW contribution of approximately 30% during November 2007. In addition, we found that the concentration, variability and spatial dependence of several chemical species were associated with

changes in BGW contribution and that multiple chemical species had similar patterns in the relationship between their average concentration and variability with BGW contribution. For instance, we found that the concentrations of K, Na and DOC had an inverse relationship with BGW contribution, whereas F and TN had a direct relationship with BGW contribution. However, the relationship in the concentration of Ca, Mg, Si, Sr and inorganic N BGW changed from inverse to direct when BGW contribution exceeded a threshold value of approximately 42% BGW contribution. In addition, we found direct evidence to suggest simple mixing or enrichment is responsible for the variations in the concentration of Mg, Si, F, K and Na. Finally, the observed relationships between BGW contribution and the changes in concentration, variability and spatial dependence of the chemical species measured in this study are then put into context of relevant literature in an attempt to identify potential sources or mechanism controlling those chemical species in streamflow.

2 Introduction

Streams integrate waters of different sources that have been subjected to a complex series of hydrological interactions and biogeochemical processes [*Covino*, 2017; *Williamson Craig et al.*, 2008]. These processes and interactions exchange energy and matter across a wide range of spatial and temporal scales in the stream, its aquifer and the hillslopes of its watershed [*Wohl*, 2014]. Therefore, the chemical composition of streamflow and its evolution in both time and space will be a function of the hydrological interactions, biogeochemical processes, and the relative contribution and connectivity of these different sources and processes. It is then evident that a prior and robust awareness of the interactions and water sources contributing to streamflow is necessary in order to

understand the processes controlling the chemical composition of streamflow. However, if the complexity of the system under study were to be naturally reduced it would eliminate some of the interactions and sources confounding the processes controlling streamflow chemical composition.

In semi-arid river systems of the southwestern United States stream-aquifer (SA) interactions are an important process that during periods of little to no atmospheric inputs (i.e. dry season) controls the presence, quantity and chemical composition of streamflow [*Jones and Mulholland,* 2000]. During the dry season in these systems precipitation rates are much smaller than potential evaporation rates. Therefore, flow occurs only in locations where water is supplied by the local and regional groundwater system thus effectively disconnecting the river from its hillslope. In these systems research has shown that during the dry season the locations where SA interactions occur can be characterized as biogeochemical control points [*Bernhardt et al.,* 2017]. These control points may act as sink or source of organic and inorganic nutrients, as well as be permanent or activated features of the landscape depending on directionality, length and magnitude of the interaction [*Bernhardt et al.,* 2017]. For example, oxygen rich stream water entering the subsurface can activate and enhance high respiration rates of organic matter bearing sediments or dissolved organic matter (DOM) carried by the flow. As this water moves through streambed sediments it can become enriched in mineralized forms of nutrients that then may return to the stream when the directionality of flow changes fueling primary productivity and starting the cycle again [*Dent,* 2001; *Dent and Grimm* 1999; Jones et. al., 1995; *Holmes et al.,* 1994].

The San Pedro River in southeastern Arizona is one such system and one of the last undammed mostly perennial river systems of the southwest. In the San Pedro River, monsoon season generated streamflow (floods) usually occurs from the months of June to October, while groundwater controlled streamflow (baseflow) is dominant during dry periods leading to the monsoon season (Figure 1) [*Thomas and Pool,* 2006; *Pool and Coes,* 1999]. Floodwaters generated during the monsoon period, when compared to streamflow during periods of baseflow, are mostly derived from precipitation event waters [*Brooks and Lemmon,* 2007]. They dominate dissolved and particulate C and N fluxes [*Dent and Grimm,* 1999; *Martí et al.,* 1997] and carry large concentrations of dissolved organic carbon (DOC), dissolved organic nitrogen (DON), dissolved inorganic nitrogen (DIN) and particulate organic carbon and nitrogen (POC and PON), which decrease during baseflow periods [*Brooks and Lemmon,* 2007]. More importantly, in the San Pedro River floodwaters are responsible for 96% of the annual organic carbon (DOC + POC) and 97% annual nitrogen (DIN + DON + PON) fluxes with a large fraction of organic carbon and nitrogen being transported as particulates [*Brooks et al*., 2007]. The large fluxes of C and N are caused by the accumulation and subsequent transport of terrestrially derived nutrients by the summer rains, which connect the hillslope with the stream via overland flow [*Bernhardt et al.,* 2017; *Brooks and Lemon,* 2007; *Westerhoff and Anning,* 2000a]. These floodwaters and nutrients recharge the alluvial aquifer, which later returns to the stream during periods of baseflow [*Simpson,* 2011; *Baillie et al.,* 2007] and suggest that it is the connection of the river with its hillslope that drives nutrient and dissolved matter concentrations during both the wet (flooding) and dry (baseflow) periods in the river.

Studies in other semi-arid river systems have shown that during periods of baseflow the variability of nitrate concentration in streamflow is inversely related to time since last flooding [*Dent*, 2001; *Dent and Grimm*, 1999]. In addition, research has shown that nitrate concentration as well as nitrification and respiration rates in the subsurface and parafluvial zones increase as time since flooding increases [*Dent*, 2001; *Dent and Grimm* 1999; Jones et al., 1995; *Holmes et al.*, 1994]. As ground water moves towards the surface and emerges as baseflow it interacts with these regions and may act as discrete or distributed sources of dissolved nutrients to the stream depending on local hydrogeologic conditions [*Dent* 2001]. However, time since flooding is a relative term that depends on a subjective definition of a flooding event which may change in time and magnitude. More importantly, it is not known if changes in nutrient concentration observed in the stream and streambed of other river systems occur in the San Pedro River.

In the San Pedro River, research has shown that sulfate to chloride mass ratios (SO_4/Cl ratios) can be used to estimate the relative contribution of basin groundwater and floodwater to streamflow. Baillie et al., [2007] showed that basin groundwater has SO_4/Cl mass ratio of ~1.7, whereas summer runoff has SO_4/Cl mass ratios of ~17.1 and that mixing of this two sources explains streamflow in the river. In addition, Baillie et al., [2007] demonstrated that as the San Pedro River flows north the relative contribution of basin groundwater to streamflow increases. These findings show that there is a spatial component to the contribution of basin groundwater and floodwater to streamflow along the river and suggest that there may also be a temporal component to the relative contributions of basin groundwater/floodwater to streamflow in the San Pedro River. In

other words, as time since flooding increases the contribution of basin groundwater to streamflow would also increase.

The objective of this study is to describe how the chemical composition of streamflow during baseflow evolves as basin groundwater contribution to streamflow changes in the San Pedro River. Specifically, do changes in basin groundwater contribution to streamflow translate to changes in its chemical composition (Nitrogen, Metals and DOC)? Would, simple mixing between two chemically distinct sources explain the observed variability? What do these results indicate about the underlying processes controlling nutrient concentrations in a semi-arid stream? Since basin groundwater (BGW) and floodwater (summer runoff) are two chemically distinct sources of baseflow to the river, a relative increase of basin groundwater contribution in the stream would, by a process of mixing, shift the chemical composition of streamflow (**Figure 2**). We hypothesize that an increase in the contribution BGW to streamflow would be accompanied by a steady decrease in the concentration of nitrogen, metals and DOC (**Figure 2**).

3 Methods

3.1 Study Site

The study site consists of four river reaches nested inside a 10 Km river stretch in the San Pedro River National Conservation Area (SPRNCA), located to the east of the town of Sierra Vista, Arizona (Figure 3). The 10 km river stretch is centered at the intersection of Arizona State Route 90 and the river (31°33’7” N - 110°8’18” W). The four river reaches are organized in a nested hierarchy, so that each smaller scale is a subset of the

preceding scale. Each river reach was divided and sampling stations were set-up using the following definitions: 1) 10 Km reach with a sampling interval of 250 m, 2) 1 Km reach with a sampling interval of 25 m, 3) 100 m reach with a sampling interval of 2.5 m, and 4) 40 m reach with a sampling interval of 1 m.

3.2 Hydrogeological Setting

The San Pedro River flows northward with an overall gradient of 2.43 m per km and at the downstream end of SPRNCA the river drains an area of approximately 5,011 km^2. The river flows along a variable depth alluvium filled extensional basin that is bounded by the Mule Mountains and Tombstone Hills on the east and by the Huachuca Mountains on the west with altitudes ranging from 1,524 to 2,256 m and from 1,524 to 2,896 m above sea level, respectively [*Pool and Coes,* 1999]. Inside SPRNCA the overall thickness of the alluvial deposits decreases as downstream distance increases and it ranges from zero (exposed bedrock) near the Tombstone Hills to 1.46 km at the upstream end of SPRNCA [*Gettings and Houser,* 2000].

There are two distinct wet seasons and one dry season in the San Pedro River watershed [*Hereford,* 1993]. The first wet season is characterized by high rainfall intensity, average daily rainfall and rainfall probability and operationally occurs from mid-June to mid-October. These precipitation events are driven mainly by the southwestern monsoon and by cut-off low-pressure systems [*Hereford,* 1993]. The second wet season is characterized by low rainfall and snowfall intensity from early December to late March. A dry period occurs each year from early April to early June and is characterized by the almost complete absence of precipitation. Streamflow records from 1915-1987 at the Tombstone gauging station show that flooding and increased

streamflow in the Upper San Pedro River are mainly associated with the mid-June to mid-October wet period, with 87% of the flooding events occurring during this period. During the dry season and in the absence of atmospheric inputs, perennial river flow is sustained and controlled by baseflow inputs from the alluvial and basin fill aquifers.

3.3 Surface Water Sample Collection

Surface water samples were collected at the thalweg of the stream during four different sampling campaigns: 1) March 18, 2006, 6.3 months after the last summer flood and prior to Cottonwood leaf out; 2) May 21, 2006, 8.4 months after the last summer flood and after Cottonwood leaf out; 3) November 18, 2006, 2.2 months after the last summer flood and during Cottonwood leaf fall; and 4) April 21, 2007, 7.3 months after the last summer flood and after Cottonwood leaf out (Figure 4). Water samples for all chemical species with the exception of dissolved organic carbon (DOC) were collected in the field with 125mL HDPE bottles. Water samples were then filtered at the laboratory and analyzed to determine the dissolved concentrations of their major anions (F, Cl, NO_2, NO_3, and SO_4) using ion chromatography (IC), metals (Ca, K, Mg, Na, Si, and Sr) using inductively coupled plasma optical emission spectrometry (ICP-OES), and total nitrogen (TN) and dissolved organic carbon (DOC) using high temperature combustion catalytic oxidation method.. The surface water samples were managed and analyzed according to the standard methods outlined by [*Eaton et al.,* 2005] for each chemical species group (ions, metals and TN/DOC).

3.4 Data Analysis: BGW Contribution and Chemical Composition Changes

In order to describe how the chemical composition of streamflow in the San Pedro River evolves with changes of BGW contribution this study uses SO_4/Cl ratios as a proxy

of BGW contribution *[Baillie et al., 2007]*. Therefore, the SO_4/CL ratios for all the samples were calculated. Initially, the data were grouped by chemical species and sampling campaign and a one-way analysis of variance and a multiple comparison test for each chemical species was performed to test if the means of each chemical species were significantly different for each sampling campaign.

Finally, in order to describe how the chemical composition of streamflow evolves as the BGW contribution to streamflow changes in the San Pedro River the entire dataset was merged and then clustered into 10 groups using SO_4/CL ratios as the clustering variable and a k-means clustering algorithm. The k-means clustering algorithm was performed using Matlab's *kmeans* function with the following parameters: 1) dataset records with no SO_4/Cl data were ignored, 2) data were clustered into 10 groups, 3) the distance method used was squared Euclidean distance (each group centroid is the mean of the data points in that cluster), 4) if a cluster population dropped to zero the cluster group was dropped, 5) the initial cluster centroids were chosen by randomly selecting 10 points in the dataset, and 6) the process was iterated 2500 times before choosing the best set of clusters that minimized the distance between all the points and their respective group centroids. The resulting clustered groups were then plotted to assess if any patterns in the concentration of the chemical species as a function of SO_4/Cl ratios (as a proxy of BGW contribution) exist.

3.5 Data Analysis: Spatial trends and Spatial Auto-Correlations

The data were analyzed to assess if any of the chemical species exhibited: spatial trends with downstream distance and/or spatial auto-correlation at the 10Km and 1Km sampling reaches. The spatial trend assessment was performed by calculating the

Pearson product-moment correlation coefficient and by performing linear correlation regression. For these an analysis of covariance and a multiple comparison test was performed to test if the correlation coefficients were significantly different between sampling campaigns. The spatial auto-correlation assessment for the 10Km and 1Km reaches was performed by calculating the empirical semi-variance and graphing it in a semi-variogram. If any of the chemical species exhibited a significant linear trend with downstream distance it was de-trended before calculating the semi-variances. For each chemical species semi-variance was calculated using Equation 1 for all separation distances (h) less than or equal to 4000m and 400m for the 10km and 1km sampling reaches, respectively. Once the semi-variogram was created, a simple bounded linear model, linear model or a random model was fitted to the data to help determine objectively the separation distance limit at which chemical species are auto-correlated (semi-variogram range) [*Webster and Oliver*, 2007]. If semi-variances increased continually without leveling into a maximum value (linear), then the range was set to be larger than the maximum separation distance of that variogram (i.e. 4000m or 400m). If semi-variance values followed a horizontal trend (random), then the range was set to be smaller than the minimum separation distance of that variogram (i.e. 250m or 25m).

Equation 1: $\widehat{\boldsymbol{\gamma}}(\boldsymbol{h}) = \frac{\mathbf{1}}{\mathbf{2}} \cdot \frac{\mathbf{1}}{\boldsymbol{n(h)}} \sum_{\boldsymbol{i=1}}^{\boldsymbol{n(h)}} \left(\boldsymbol{z(Xi+h)} - \boldsymbol{z(Xi)}\right)^{\mathbf{2}}$

Where:

$\hat{\gamma}(h)$ is the semi-variance at a separation distance *h*,

n(h) is the number of data pairs at separation

distance (*h*),

$\big(z(Xi+h)-z(Xi)\big)$ is the difference between all the data pairs with a separation distance (h).

4 Results

4.1 Descriptive Summary Statistics and General Patterns

On average 144 samples were analyzed for each sampling campaign and in order to simplify the interpretation of the data, the summary statistics (mean, standard deviation, sample count, minimum and maximum) for each chemical species were calculated and the values were grouped by sampling campaign and in turn each sampling campaign was sorted using the SO_4/CL ratios in increasing order (Table 1 and Table 2). The data shows that there is a significant difference in the mean concentration of SO_4/Cl, Ca, K, Si, F, SO_4 and DOC between all four sampling campaigns (Table 1). The mean concentration of Mg, Na, Sr, Cl and TN is significantly different between three sampling campaigns whereas the mean concentration of inorganic nitrogen (NO_3-N + NO_2-N) is only significantly different for two sampling campaigns (Table 1). Average SO_4/Cl ratios range from 3.27 in May 2006 to 5.09 in November of 2006 (Table 1) with overall minimum and maximum values of 2.59 and 6.09, respectively (Table 2). During that same period the variability of SO_4/Cl ratios as measured by the standard deviation decreased from 0.2 to 0.15(Table 1).

4.2 Longitudinal Correlation and Spatial Auto-Correlation Trends

A linear regression analysis of all the chemical species against downstream sampling distance for the longest sampling reach shows that only SO_4/CL ratios exhibit, a

consistent and significant (p-value<0.05) inverse linear correlation with downstream distance [m] for all sampling campaigns (Figure 5and Table 3). Other chemical species do exhibit significant linear correlation with downstream distance during all or some of the sampling campaigns. However, in some cases the slope of the relationship is not consistent or the linear model is not the best fit for the data (Table 3). In the case of SO_4/Cl ratios and downstream distance (m), the slope values for the linear relationship are between $-7.0x10^{-5}$ and $-9.0x10^{-5}$ with coefficient of determination values (r^2) between 64.1 and 80.3 % (Figure 5 and Table 3). Although, the individual slope values are significant for each sampling campaign and appear to differ slightly, the analysis of covariance (ANCOVA) showed that there is no statistical difference in the slope values when comparing them across sampling campaigns (Figure 5 and Table 3). The sampling campaign of May 2006 had the lowest average flows, the lowest average SO_4/CL ratio and the highest number of months since the last flood (Table 1). Conversely, the sampling campaign of November 2006 had the highest average flows, the largest average SO_4/CL ratio and lowest number of months since the last flood (Table 1). In fact, the data show a statistically significant inverse linear relationship between SO_4/Cl ratios and time since last flooding (Figure 6)

A semi-variogram analysis of all chemical species sampled at the 10km and 1km sampling reaches show that all of the chemical species exhibit spatial auto-correlation characteristics at either the 10Km or 1Km sampling reaches for one or more of the sampling campaigns (Table 5). In general, the results show that the semi-variograms for all chemical species had 3 basic patterns: First, a linearly structured semi-variogram that is best fitted by a sloping line (Figure 7A); Second, range limited linearly structured

semi-variograms that were best fitted by a range-bounded sloping line (Figure 7B); Finally, random semi-variograms best fit by a flat horizontal line (Figure 7C). Of these three patterns, only the chemical species with linearly structured (bounded and unbounded) semi-variograms exhibited characteristics of being spatially auto-correlated. The data show that amongst all chemical species, sampling campaigns and sampling reaches the most common semi-variogram type was the bounded linear semi-variogram, followed by the random and then by the linear semi-variogram (Table 5). The fitted semi-variogram range values for each chemical species (Table 6) were ranked, in ascending order, across all sampling campaigns and then summed across sampling campaigns (Table 7). The total ranked ranges values (Table 7) show that the range of spatial autocorrelation tends to decrease with time and SO_4/Cl ratios. Specifically, the sampling campaigns of May 2006 and April 2007 had the lowest and highest overall ranges, respectively. However, due to the low number of points (four) the correlation between ranked ranges SO_4/Cl ratios was not statistically significant.

4.3 Correlation and Patterns in the Relationship Between the Chemical Species Concentration and their Variability with SO_4/Cl

A multivariate correlation analysis showed that several chemical species exhibit a significant (p-value<0.05) positive or negative correlation when compared to the other chemical species evaluated in this study (Table 4). Examination of the correlation coefficient (R) values reveals that in general the positive-correlated chemical species have a stronger correlation than the negative-correlated species. For example, the R-values for the top five positive-correlated variables (ignoring SO_4/Cl correlation with SO4 and Cl) are between 0.82 and 0.91, whereas the R-values for the top five negative-

correlated variables are between -0.52 and -0.57 (Table 4). The data also shows that the top two highest positive and negative correlations occur with SO_4/Cl ratios as one of the chemical species, with SO_4/Cl ratios exhibiting a strong and positive correlation ($0.85 \leq R \leq 0.91$) with K and DOC (Figure 8 H-J and Table 4), and a weak and negative correlation ($-0.57 \leq R \leq -0.56$) with F and TN (Figure 8 F-G and Table 4). The chemical species pairs of SO_4/Cl-Na, Ca-Sr, Na-K and K-DOC also exhibit medium to strong positive ($0.77 < R < 0.85$) correlations (Table 4).

The clustering of the chemical species based on their SO_4/Cl ratios and the subsequent visualization of the mean cluster values and coefficient of variation in scatterplots showed that concentration and variability of several of the chemical species exhibited similar relationship patterns with SO_4/Cl ratios (Figure 8 and Figure 10). In terms of concentration, the most common pattern is the non-linear relationship exhibited by Ca, Mg, Si, Sr and NO_3-N + NO_2-N (IN) which is characterized by a decrease in the mean concentration of the chemical species as SO_4/Cl ratios decrease from a value 5.12 to a value of 3.84 and then by an increase in the mean concentration of the chemical species as SO_4/Cl ratios further decrease from a value of 3.84 to a value of 2.77 (Figure 8A-E). The second most common pattern is the medium to strong linear relationship exhibited by K, Na and DOC which is characterized by an increase in mean chemical species concentration with corresponding increases in SO_4/Cl ratios (Figure 8H-J, Table 4). The final pattern is the weak inverse linear pattern exhibited by TN and F which is characterized by high mean concentration values when SO_4/Cl are low with roughly equal concentration when SO_4/Cl ratios are between 4.12 and 5.12 (Figure 8F-G). The mean concentrations of Ca, Mg, Si, F, K and Na as a function of SO_4/Cl ratios when

compared with data published in the same study area [*Pool et al.*, 1999], reveals that for the most part, the observed concentrations fall within the reference range data of baseflow in the San Pedro River (Figure 9) [*Pool et al.*, 1999]. This shows that the observed concentrations for Ca, Mg, Si, K and Na are not unique. However, there are several observed values of Ca, Mg, K, and Na that are outside of reference ranges of streamflow during baseflow (**Error! Reference source not found.**Figure 9A-B, E-F).

In terms of the variability in the concentration of the chemical species, the most common pattern is the one exhibited by Ca, Mg, Si, Sr, K and Na (Figure 10A-E, H, I) which is characterized by a positive linear correlation between all pairs, ($R>0.75$ and p-value<0.025) and by high variability when SO_4/Cl ratios are between 3.5 and 4.0. This same region is where the inversion occurs in the relationship between concentration and SO_4/Cl occurs for Ca, Mg, Si and Sr. The second most common pattern is the increased variability at low SO_4/Cl ratios exhibited by F, TN and SO_4/Cl (Figure 10F-G, K). The third pattern is characterized by high variability of IN (NO_3-N + NO_2-N) at high SO_4/Cl ratios (Figure 10E). Finally, the variability pattern of DOC is characterized low variability when SO_4/Cl ratios are between 3.5 and 4.0 (Figure 10J).

5 Discussion

In order to determine if changes in groundwater contribution to streamflow translate to changes in its chemical composition (Nitrogen, Metals and DOC) we have used the results of chemical analysis from water samples collected during four different periods along the SPRNCA. Overall, results of this study show that within the study site the contribution of basin groundwater to streamflow increases with distance downstream and time since last flooding. In addition, the results show that the concentration and

variability of several chemical species is associated with the contribution of basin groundwater to the stream. However and most notable, the results show that the majority of chemical species did not follow the expected decrease in concentration with increased contribution of basin groundwater to the stream

5.1 Basin Groundwater Contribution

An analysis of the spatial and temporal relationships of SO_4/Cl ratios shown in the results (Figure 5, Figure 6, Table 1 and Table 3) and the fact that SO_4/Cl ratios in the San Pedro River can be used as a proxy of basin groundwater contribution [*Baillie et al.,* 2007] suggest that during non-flood periods the amount of basin groundwater in streamflow increases significantly with downstream distance (longitudinally) (Figure 5 and Table 3) and with time since last flooding (Figure 6). The trends and ranges observed in this study and especially for the sampling campaign of May 2006 are well within the ones reported by [*Baillie et al.,* 2007]. Although the individual slopes and intercepts of each longitudinal profile are statistically significant, an analysis of covariance revealed that the difference between slopes is not significantly different from zero (Table 3). In other words the rate of change of SO_4/Cl ratios as a function of downstream distance holds constant between all sampling campaigns despite the fact that the difference between the mean SO_4/Cl ratios (Table 1) and the regression's y-intercept for each sampling campaign are significantly different from zero (Figure 5). However, a digital extraction and analysis of the mixing diagram generated by *Baillie et al* [2007] reveals that a two-term power function can be used to estimate the percentage of basin groundwater (pBGW) contribution to streamflow as a function of SO_4/Cl (Equation 2). The non-linearity in the relationship between pBGW and SO_4/Cl made the slope of

pBGW vs downstream distance for the sampling campaign of May 2006 steeper (p-value <0.05) than the other campaigns. This suggests that actual inputs of BGW during the sampling campaign of May 2006 were higher when compared to the sampling campaigns of March-2006, November-2006 and April-2007. In addition, Equation 2 and the entire dataset of SO_4/Cl values reveals that the average BGW contribution to streamflow in the San Pedro River was approximately 38.1%, 48.9%, 30.5% and 33.3% during sampling campaigns of March 2006, May 2006, November 2006 and April 2007, respectively. At the same time the regression lines of SO_4/Cl as a function of downstream distance at the 10Km sampling extent (Figure 5) revealed that BGW contribution to streamflow at the downstream and upstream ends varied from: 1) 34.2 to 42.6% during March 2006, 2) from 44.9 to 59.2% during May 2006, 3) from 28.4 to 33.8% during November 2006, and 4) from 31.2 to 38.1% during April 2007.

Equation 2: $\mathbf{pBGW = 162.9 * (SO4/Cl)\text{^}(-0.5369) - 35.52}$; for $1.632 \leq SO_4/Cl \leq 10.094$. Where, pBGW is the percentage of basin groundwater in streamflow and SO_4/Cl is the SO_4/Cl ratio. Note this relationship has an R^2=0.9998 derived from [*Baillie et al.,* 2007].

The increase in the amount of basin groundwater contribution must be attributed to a relative increase of basin groundwater flow from the aquifer when compared to the other source of water (monsoon floodwaters) to the stream. Using data collected 2 to 5 years earlier by the US Geological Survey at one of their gauging stations and riparian well clusters (located near the center of the study site) show that decreases in streamflow leading to and including the late-spring and summer baseflow period (April to June) are

accompanied by a gradual increase in the vertical upward gradients (Figure 12). However, determining whether the increase in basin groundwater contributions is solely due to increases in flux or increases in the gaining areas of the stream, or both cannot be determined with the data collected during this study. The data collected in this study does show that the shift towards increased basin groundwater dominated streamflow is associated with an increase in the variability of the SO_4/Cl values as measured by the coefficient of variation (Figure 10K) and shortened spatial autocorrelation ranges at the 10 km sampling reach as measured by the semi-variograms (Table 6). These results and the fact at its highest average value, basin groundwater accounts for roughly 49% of streamflow in May (2006) suggest that there are significant inputs of monsoon floodwater to streamflow months after the last flood event. Furthermore, the increased variability in SO_4/Cl values and small autocorrelation ranges suggests that the spatial arrangement and magnitude of basin groundwater inputs (e.g. groundwater discharge) to the stream is less homogeneous along the length of the river when compared to the other sampling periods of this study. In other words, ground water discharge to the river becomes more localized during the period of highest BGW contribution.

5.2 Changes in the Chemical Composition of Streamflow with Changes in BGW Contribution

In order to determine if changes in groundwater contribution to streamflow translate to changes in its chemical composition (Nitrogen, Metals and DOC) we have used the results of chemical analysis from water samples collected during four different periods along the SPRNCA, The results presented in this study show that basin groundwater (BGW) contribution to streamflow, as measured by SO_4/Cl ratios, change both spatially

(Figure 5 and Table 1) and temporally (Figure 6, Table 3). More importantly, the results of this study show that the average concentration (Figure 8 and Figure 9) and variability (Figure 10) of most of the chemical species measured in this study change as BGW contribution (SO_4/Cl ratios) to streamflow changes.

As briefly mentioned before, the results show that K, Na, DOC exhibit a strong and significant direct relationship with SO_4/Cl ratios (Table 4 and Figure 8H-J) whereas F and TN exhibit a weak and significant inverse relationship with SO_4/Cl ratios (Table 4 and Figure 8F-G). This implies that K, Na and DOC, as hypothesized, decrease their concentration with increases in BGW contribution. F and TN, contrary to the hypothesis, increase their concentration with increases in BGW contribution. On the other hand, the results show that Ca, Mg, Si, Sr and IN exhibit a similar non-linear change in their concentration with changes in SO_4/Cl ratios (Table 4 and Figure 8A-E). For Ca, Mg, Si, Sr and IN the observed pattern can be outlined as a direct relationship when SO_4/Cl ratios are larger than 3.8 and an inverse relationship when SO_4/Cl ratios are less than 3.8. These results suggests that: 1) the type of relationship between the concentrations of Ca, Mg, Si, Sr and IN and changes in BGW contribution (inverse or direct) depends on the degree of BGW contribution to streamflow; 2)the concentration of Ca, Mg, Si, Sr and IN initially decrease but after a threshold value the concentrations increase significantly when BGW contribution is highest, and streamflow is lowest; and 3) the threshold value for the inversion in the relationship is approximately 42% BGW (Figure 8A-E and Equation 2).

5.2.1 Are the Changes in the Chemical Composition of Streamflow with Changes in BGW Due to Mixing?

Basin groundwater (BGW) and floodwater (summer runoff) are two chemically distinct sources of baseflow to the river (Figure 9). Therefore, a relative increase of basin groundwater contribution in the stream should, by a process of mixing, lower the concentration of nutrients, metals and DOC in streamflow (**Figure 2**). The results of this study show that with the exception of K, Na, and DOC (Table 4 and Figure 8H-J) the average concentration of most of the chemical species measured in this study (Figure 8) did not follow the expected decrease in concentration as BGW contribution in streamflow increased (**Figure 2**). However, the results do show that multiple chemical species had similar patterns in the relationship between their average concentration and variability with the changes BGW contribution as inferred from SO_4/Cl ratios (Figure 8 and Figure 10) suggesting linked sources or mechanism controlling those chemical species in streamflow. The reference data ranges for Ca, Mg, Si, F, K and Na (Figure 9) [*Pool et al.,* 1999] can be used in conjunction with the concentration values and the similar patterns observed in this study (Table 4 and Figure 8) to narrow down the potential processes, mechanisms or sources controlling those chemical species. When mixing is the primary process controlling the concentrations of chemical species in streamflow the observed concentration values should roughly approximate a linear pattern (mixing line) between the regional aquifer (also BGW) and floodwater endmembers. Assuming that there are no errors in the reference ranges or in the observed data, any vertical deviation from the mixing line of a chemical species is indicative of a relative enrichment or depletion with respect to simple mixing in streamflow. If enrichment/depletion is noted for a particular chemical species it would suggest that there is a series of in-stream or near-stream biogeochemical processes producing or consuming said chemical species.

The data shown on Figure 9 gives clear indication of mixing or enrichment of for 5 of the 10 chemical species measured in this study (Mg, Si, F, K and Na). First, the fairly linear evolution of the reference ranges for Si, and K suggest that concentrations of those species in streamflow during baseflow are primarily controlled by mixing of BGW and flood endmembers (Figure 9 C and E). Second and similar to Si and K, the reference ranges for Mg also suggest that mixing between BGW and flood endmembers is partially responsible for the observed concentrations (Figure 9 B). However, there is an apparent enrichment of Mg relative to the reference ranges when SO_4/Cl ratios are greater than 4.25 suggesting that there is an additional in-stream source of Mg to streamflow. Third, the large variability and overlapping reference ranges of Ca concentrations prevents determining if mixing is responsible for the observed concentrations (Figure 9 A). Fourth, the clear enrichment of F and Na in the reference range data and observed data suggest that there is an additional in-stream source of F and Na to streamflow (Figure 9 D and F). Finally, at very low SO_4/Cl ratios ($\leq$3.37) the concentrations of Ca, Mg and Si as opposed to K, F and Na are either inside reference areas of the regional aquifer or inside the overlap areas between regional aquifer and baseflow (Figure 9 A-C). This area corresponds to the inversion regions exhibited by Ca, Mg, Si, Sr and IN and suggests that the variability Ca, Mg and Si and by extension Sr and IN are strongly influenced by BGW inputs. We are unable to directly determine whether the observed changes in the concentration of Sr, IN, TN and DOC are the results of simple mixing because reference range data containing both SO_4/Cl ratios and concentrations of Sr, IN, TN and DOC could not be found. However, Sr and IN (Figure 8 D and E) exhibit a similar pattern to that of Ca, Mg and Si (Figure 8 A-C) with changes in SO_4/Cl ratios. Likewise, TN

(Figure 8G) exhibits a similar pattern to that of F (Figure 8F); while DOC (Figure 8J) exhibits a similar pattern to that of K and Na (Figure 8 H and I). Due to these similarities we argue that Sr and DOC and to smaller degree IN and TN concentrations during baseflow period could be controlled by mixing.

5.2.2 Potential Processes Behind the Enrichment or Depletion of the Observed Chemical Species.

Other than mixing, the decrease in the enriched concentrations with decreases in SO_4/Cl ratios relative to reference ranges of baseflow exhibited by K, Na and by extension DOC could be associated (Figure 8 H-J and Figure 9 E-F) with: 1) a decrease in the pool size of flood related pulses of allochthonous particulate and dissolved organic matter [*Brooks and Lemmon*, 2007], 2) a decrease in leaching of K, Na and DOC from senesced leaves [*Breymeyer and Van Dyne*, 1980; *Morgan and Tukey*, 1964; *Tukey*, 1970] or plant debris or due to a decrease in pool size, 3) decreased rates of in-stream or near-stream chemical weathering of K and Na rich minerals (Feldspars and Micas), 4) increases in biogeochemical uptake and processing when BGW contribution increases and/or 5) a decrease of the autochthonous organic matter and dissolved organic carbon (DOC) production rates[*Grimm and Petrone*, 1997; *Jones et al.*, 1995; *Westerhoff and Anning*, 2000b] due to decreasing streamflow and shrinking wetted regions. At the same time, the increase in the concentration and variability exhibited by F and TN with SO_4/Cl ratios (Figure 8 F-G and Figure 9 D) could indicate that the source of F is associated with a non-homogeneous increase in the inputs of a fluoride rich, long residence time groundwaters [*Hopkins et al.*, 2014], coupled and an increase in the mineralization/ mobilization of particulate or organic N previously trapped in the sediments.

The relationship exhibited by Ca, Mg, Si, Sr and IN is more intriguing because of the inversion in the relationship and enrichment when SO_4/Cl ratios in streamflow are less than 3.8 (pBGW ~42%). In the San Pedro River basin dissolved Ca, Mg, Si and Sr are the by-products of mineral weathering [*Robertson*, 1991] and the dissolution of Ca-Mg-Sr carbonates (caliche, calcite and dolomite). In addition, Ca, Mg and IN can be derived from mineralization of dissolved or particulate organic matter, or leached from submerged senesced leaves [*Breymeyer and Van Dyne*, 1980; *Morgan and Tukey*, 1964; *Tukey*, 1970]. The change in the relationship of Ca, Mg, Si, Sr and IN suggests that the sources and processes controlling Ca, Mg, Si, Sr and IN in streamflow shift from one of dilution or in-stream consumption, to one of concentration or in-stream production For these chemical species there appears to be a threshold by which the sources and processing shifts as the stream becomes more BGW dominated. In the San Pedro this process could associated with: 1) a decrease in streamflow, 2) an increase in parafluvial areas of the streambed, 3) a relative increase in basin groundwater flow, 4) changes in biological activity and/or 5) changes in the physical or chemical characteristics of stream waters (e.g. temperature, pH, DO, etc.). Research has shown that in the San Pedro River the ratio of Ca/Sr [ppm/ppm] have an inverse correlation with residence time and can therefore be used as qualitative indicator of groundwater residence times [*Hopkins et al.*, 2014]. The determination of Ca/Sr ratios with the data of this study reveals that Ca/Sr mass ratios (**Figure 11**) follow the same inversion in relationship exhibited by Ca, Mg, Si, Sr and IN (Figure 8A-E) with Ca/Sr ratios as high as 130 when SO_4/Cl ratios are 5.1, reaching a low of 95.6 when SO_4/Cl are 3.8 and then increasing to a value about 105 when SO_4/Cl ratios are 3.0. In general this suggest that the common low point exhibited

by Ca, Mg, Si, Sr and IN at a SO_4/Cl could be associated with a shift from relatively young to older waters, and then back to relatively younger groundwater inputs

There is a wide body of research focused on the biogeochemical processes controlling N concentrations in semi-arid streams[*Dahm et al.,* 1998; *Dent and Grimm,* 1999; *Dent et al.,* 2001; *Fisher et al.,* 1998; *Grimm,* 1987; *Grimm and Petrone,* 1997; *Holmes et al.,* 1994; *Holmes et al.,* 1996; *Jones et al.,* 1995; *Martí et al.,* 1997]. Two of those published studies have looked at changes in the concentration of nitrate in streamflow with some measure of the contribution of groundwater with a long spatial (10 Km) and temporal (weeks to several months) scale. The data published by Dent et al. (2001) and Dent and Grimm (1999) for Sycamore Creek, AZ in a limited way shows that the mean concentration of nitrate follows the same inversion pattern exhibited in this study when BGW contribution increases. Specifically, the results show that for a 10km section of river sampled every 25m, the average concentrations of nitrate are highest (0.219 mg/L NO_3-N) two weeks after flooding then decreasing to a low value (0.006 mg/L NO_3-N) two and a half months after flooding, and finally increase again (0.035 mg/L NO_3-N) nine months after the floods. As the data in this study shows, time since last flooding in baseflow dominated semi-arid streams, like the San Pedro River or Sycamore Creek (~250 Km NW of the San Pedro River), is generally directly correlated to groundwater contribution to streams.

Similar to [*Dent and Grimm,* 1999], this study proposes that the increase in IN concentrations observed when SO_4/Cl < 3.8 (May 2006) are the result of: high respiration and nitrification rates in the streambed and parafluvial zones [*Dent,* 2001; *Dent and Grimm,* 1999; *Jones et al.,* 1995; *Holmes et al*., 1994] coupled with a relative decrease in

river discharge when compared to a steady or increased groundwater discharge. This process causes the streambed to become enriched with IN, which is then advected with groundwater discharge to the stream. Although not for the same time period, the first part of this hypothesis is supported by the fact that vertical gradients nearest to the surface at one location near our study site increased markedly while streamflow decreased during the summer low-flow period (April-June) of 2001-2003 (Figure 12). Similarly, the second part of our hypothesis is supported by vertical NO_3 profile data collected shortly before and after a flood in the streambed of two gaining reaches of the study site and reported by [*Simpson*, 2011]. These vertical profiles show that in the topmost 1.4m of the streambed, nitrate concentration before the summer floods are consistently higher than those observed after the floods for two different years (Figure 13). The increased rates of organic matter (particulate/dissolved) respiration and subsequent mineralization / nitrification produce excess acidity. This acidity could help explain the increased concentration of Ca, Mg and Sr observed in the stream dissolving Ca-Mg-Sr carbonates that were either transported during the floods or previously precipitated in the in-stream or near-stream zones.

5.3 Does the Variability and Length of Spatial Auto-Correlation Changes with BGW Contribution?

As briefly mentioned earlier, the results show that the variability (as measured by the coefficient of variation) and the length of spatial auto correlation of the chemical species analyzed in this study change with BGW contribution. Overall the variability of BGW contribution increases and the degree of spatial auto correlations decreases as the river becomes more BGW dominated. As with concentration, several chemical species have

similar patterns in the relationship between the coefficient of variation (CV) and SO_4/Cl ratios (Figure 10). In review, Ca, Mg, Si, Sr, K, and Na exhibit a region of increased variability when BGW contribution is approximately ~42% BGW, which matches with regions of decreased concentrations observed for Ca, Mg, Si, Sr and IN. The variability of F and TN increases 3 to 5 fold when BGW contributions is highest, in contrast, the variability of IN increases 4 fold when BGW contribution is lowest and, the variability of DOC exhibits a region of decreased variability when BGW contribution is ~42%. Finally, the spatial autocorrelation analysis demonstrated that the concentration of all chemical species exhibited spatial dependence for all sampling campaigns at either the 10Km or 1Km sampling reaches, and that the length by which the chemical species were spatially dependent tended to decrease with increases in BGW contribution (Table 5, Table 6 and Table 7).

In regards to the variability of IN, our findings do not match those reported by [*Dent et al.*, 2001]and [*Dent and Grimm*, 1999]. In that study the authors showed that in another semi-arid river system, Sycamore Creek (~250 Km NW of the San Pedro River), the spatial and temporal variability of nitrate concentration in the stream during periods of baseflow increase with time since last flooding. The opposite pattern is present in the data collected for this study. Two aspects that might explain this discrepancy is the fact that during its lowest flow period the downstream connectivity is reduced significantly, something that did not occur during the sampling campaigns for this study. Second, in this study the concentrations of both NO_3 and NO_2 were combined and analyzed as one (inorganic Nitrogen, IN), whereas *Dent and Grimm*, [1999] and *Dent et al.*, [2001] used only NO_3. In Sycamore Creek researchers have proposed that the increased variability of

nutrients are due to increases in the heterogeneity of the vertical interaction between the stream and hyporheic zone [*Dent et al.,* 2001]. Our data make it obvious that such a statement is not globally applicable to all chemical species and that changes in the contribution of BGW are not able to explain the patterns observed.

Researchers have shown that floods in the San Pedro River and Sycamore Creek help homogenize the system and at the same time deliver significant quantities of materials to the stream which influences the nutrient conditions of the stream [*Brooks and Lemon,* 2007; *Brooks et al.,* 2007; *Martí et al.,* 2000; *Meixner et al.,* 2012]. The observations made in this study suggest that the degree of spatial dependence changes with changes in BGW contribution and with the target chemical species. This result implies that a study whose foundation is based on measurements of the stream's chemical properties must change and adapt their experimental design to ensure the samples accurately describe the variability of said chemical at the right scale. Otherwise, the researcher risks wasting resources by sampling too frequently or gathering not enough information by collecting too infrequently.

6 Conclusion

This study has used SO_4/Cl ratios of streamflow, from samples collected during four different sampling campaigns along a 10Km section of the San Pedro River, to infer the degree of basin groundwater contribution to streamflow. These results were then used to assess if changes in basin groundwater (BGW) contribution to streamflow translates to changes in its chemical composition, the variability of its chemical composition and the degree of spatial dependence of those chemical species.

The results of this study show that in the San Pedro River BGW contribution and its variability, as inferred from SO_4/Cl ratios, increased with downstream distance and time since last flooding. Specifically, streamflow from the month of May 2006 had the longest time after flooding, on average the largest proportion of BGW (~49%) and the highest variability in BGW contribution while the month of November 2006 had the shortest time after flooding, the smallest proportion of BGW (~30%) and lowest variability. This initial finding was expected due to the fact that the San Pedro River remains mostly perennial along the study site during extended periods of little to no atmospheric inputs while depending on aquifer discharge to sustain streamflow.

This study found that changes in BGW contribution are in fact associated with changes in the concentration, variability and spatial dependence of ten different chemical species in streamflow during the study period. Although, most of the chemical species did not follow the expected decrease in concentration with increases in BGW contribution hypothesized in this study, the results showed that multiple chemical species had similar patterns in the relationship between their average concentration and variability with BGW contribution. For example, the concentrations of K, Na and DOC, and the concentrations of F and TN had an inverse and direct relationship with BGW contribution, respectively. At the same time, the concentrations of Ca, Mg, Si, Sr and IN had a direct relationship with BGW contribution when the contribution of BGW was larger than 42% and an inverse relationship when BGW contribution was less than 42%. The variability in the concentration for F and TN, and IN was highest when the BGW contribution was highest and smallest, respectively. However, the variability of Ca, Mg, Si, Sr, K and Na was highest and the variability of DOC smallest when the contribution

of BGW as ~42%. Finally, all chemical species exhibited spatial autocorrelation at either the 10Km or 1Km sampling reaches with the range of spatial auto correlation trending smaller with increases in BGW contribution.

The relationship between BGW contribution and the changes in concentration, variability and spatial dependence of the chemical species measured in this study is important because it may point to the sources or mechanism controlling those chemical species in streamflow. This study found direct and evidence to suggest that mixing between BGW and floodwater are largely responsible for the observed variability in the in-stream concentrations of Mg, Si, Sr, K, and DOC. In addition, this study found that the concentrations of F, Na, IN and TN appear to be enriched over what would be expected by simple mixing, suggesting that in-stream biogeochemical processes are controlling those chemical species. For example, the increase in the concentration and variability exhibited by F and TN with SO_4/Cl ratios may suggest that the source of those species is linked to the non-homogeneous increase of fluoride rich, long residence time groundwater inputs [*Hopkins et al.,* 2014] and an increase in the mineralization/ mobilization of particulate or organic N previously trapped in the sediments and now moved to the stream with groundwater inputs. The inversion in the relationship exhibited by Ca, Mg, Si, Sr and IN when BGW contribution exceeded ~42% suggest that that the sources and processes controlling these chemical species in streamflow shift from one of dilution or in-stream consumption when BGW contribution is at the extremes. However, there is a threshold that triggers an apparent switch in the source and processes controlling Ca, MG, Si, Sr and IN as the stream becomes more BGW dominated. In the San Pedro river, we argue this process could be associated with one or more of the

following events: changes in the in-stream biological activity, an increase in parafluvial areas of the streambed due do decreases in streamflow, the relative increase in basin groundwater flow and changes in the physical or chemical characteristics of stream waters (e.g. temperature, pH, DO, etc.).

The determination of which processes previously described above are effectively controlling the chemical species observed in streamflow waters of the San Pedro River would require a specific set of experimental measures that are beyond the objective of this study. However, the results presented here add to the understanding about the concentration, variability and spatial distribution of key chemical species in the San Pedro River.

7 References

Baillie, M. N., J. F. Hogan, B. Ekwurzel, A. K. Wahi, and C. J. Eastoe (2007), Quantifying water sources to a semiarid riparian ecosystem, San Pedro River, Arizona, J. Geophys. Res. (G Biogeosci.), 112.

Bernhardt, E. S., J. R. Blaszczak, C. D. Ficken, M. L. Fork, K. E. Kaiser, and E. C. Seybold (2017), Control Points in Ecosystems: Moving Beyond the Hot Spot Hot Moment Concept, *Ecosystems, 20*, 665-682.

Breymeyer, A. I. and G. M. Van Dyne (1980), Grasslands, Systems Analysis, and Man, International Biological Programme, vol. 19, 950 pp., Cambridge University Press, Cambridge Eng.; New York.

Brooks, P. D. and M. M. Lemon (2007), Spatial variability in dissolved organic matter and inorganic nitrogen concentrations in a semiarid stream, San Pedro River, Arizona, Journal of Geophysical Research-Biogeosciences, 112, G03S05.

Brooks, P. D., P. A. Haas, and A. K. Huth (2007), Seasonal variability in the concentration and flux of organic matter and inorganic nitrogen in a semiarid catchment, San Pedro River, Arizona, J. Geophys. Res. -Biogeosci., 112, G03S04.

Covino, T. (2017), Hydrologic connectivity as a framework for understanding biogeochemical flux through watersheds and along fluvial network, *Geomorphology, 277*, 133-144.

Dahm, C., N. Grimm, P. Marmonier, H. Valett, and P. Vervier (1998), Nutrient dynamics at the interface between surface waters and groundwaters, Freshwat. Biol., 40, 427-451.

Dent, C. L. and N. B. Grimm (1999), Spatial heterogeneity of stream water nutrient concentrations over successional time, Ecology, 80, 2283-2298.

Dent, C. L., N. B. Grimm, and S. G. Fisher (2001), Multiscale effects of surface-subsurface exchange on stream water nutrient concentrations, J. N. Am. Benthol. Soc., 20, 162-181.

Eaton, A. D., M. A. H. Franson, American Public Health Association, American Water Works Association, and Water Environment Federation (2005), Standard Methods for the Examination of Water & Wastewater, 21 2005, Centennial ed., American Public Health Association, Washington, DC.

Fisher, S., N. Grimm, E. Marti, and R. Gomez (1998), Hierarchy, spatial configuration, and nutrient cycling in a desert stream, Aust. J. Ecol., 23, 41-52.

Grimm, N. B. (1987), Nitrogen Dynamics During Succession in a Desert Stream, Ecology, 68, 1157-1170.

Grimm, N. and K. Petrone (1997), Nitrogen fixation in a desert stream ecosystem, Biogeochemistry, 37, 33-61.

Hereford, R. (1993), Entrenchment and Widening of the Upper San Pedro River, Arizona, Geological Society of America Special Papers, 282, 1-47.

Holmes, R. M., S. G. Fisher, and N. B. Grimm (1994), Parafluvial nitrogen dynamics in a desert stream ecosystem, J. N. Am. Benthol. Soc., 13, 468-478.

Holmes, R., J. Jones, S. Fisher, and N. Grimm (1996), Denitrification in a nitrogen-limited stream ecosystem, Biogeochemistry, 33, 125-146.

Hopkins, C. B., J. C. McIntosh, C. Eastoe, J. E. Dickinson, and T. Meixner (2014), Evaluation of the importance of clay confining units on groundwater flow in alluvial basins using solute and isotope tracers: the case of Middle San Pedro Basin in southeastern Arizona (USA), Hydrogeol. J., 22, 829-849.

Jones, J. B. and P. J. Mulholland (Eds.) (2000), *Streams and Ground Waters*, Acuatic Ecology Series, 425 pp., Academic Press, San Diego, California.

Jones, J. B.,Jr, S. G. Fisher, and N. B. Grimm (1995), Nitrification in the hyporheic zone of a desert stream ecosystem, J. N. Am. Benthol. Soc., 14, 249-258.

Martí, E., S. G. Fisher, J. D. Schade, and N. B. Grimm (2000), Flood frequency and stream-riparian linkages in arid lands, in Streams and Ground Waters, edited by J. B. Jones and P. J. Mulholland, pp. 111-136, Academic Press, San Diego.

Martí, E., N. B. Grimm, and S. G. Fisher (1997), Pre- and Post-Flood Retention Efficiency of Nitrogen in a Sonoran Desert Stream, J. N. Am. Benthol. Soc., 16, 805-819.

Meixner, T., P. Brooks, J. Hogan, C. Soto, and S. Simpson (2012), Carbon and Nitrogen Export from Semiarid Uplands to Perennial Rivers: Connections and Missing Links, San Pedro River, Arizona, USA, Geography Compass, 6, 546-559.

Morgan, J. V. and H. B. Tukey (1964), Characterization of leachate from plant foliage, Plant Physiol., 39, 590-593.

Pool, D. R., A. L. Coes, Arizona. Dept. of Water Resources., Cochise County (Ariz.), and Geological Survey (U.S.) (1999), Hydrogeologic investigations of the Sierra Vista subwatershed of the upper San Pedro Basin, Cochise County, southeast Arizona.

Robertson, F. N (1991), Geochemistry of Ground Water in Alluvial Basins of Arizona and Adjacent Parts of Nevada, New Mexico, and California, vol. 1406-C, 90 pp., U.S. Dept. of the Interior, U.S. Geological Survey ;Denver, CO, Reston, Va.

Simpson, S. C. (2011), Impacts of Floods on Riparian Groundwater and Post-Event Streamflow Across Spatial and Temporal Scales, PhD thesis, University of Arizona, Tucson, AZ.

Thomas, B. E., D. R. Pool, and Geological Survey (U.S.) (2006), Trends in streamflow of the San Pedro River, southeastern Arizona, and regional trends in precipitation and streamflow in southeastern Arizona and southwestern New Mexico.

Tukey, H. B. (1970), Leaching of Substances from Plants, Annual Review of Plant Physiology, 21, 305-&.

Webster, R. and M. A. Oliver (2007), Geostatistics for Environmental Scientists, Statistics in Practice, 2nd ed., 315 pp., John Wiley, Chichester, England; Hoboken, NJ.

Westerhoff, P. and D. Anning (2000), Concentrations and characteristics of organic carbon in surface water in Arizona: influence of urbanization, J. Hydrol., 236, 202-222.

Williamson Craig, E., D. Walter, K. Kratz Timothy, and A. Palmer Margaret (2008), Lakes and streams as sentinels of environmental change in terrestrial and atmospheric processes, *Frontiers in Ecology and the Environment*, *6*, 247-254.

Wohl, E. (2014), *Rivers in the Landscape : Science and Management*, Wiley-Blackwell, Somerset.

8 List of Figures

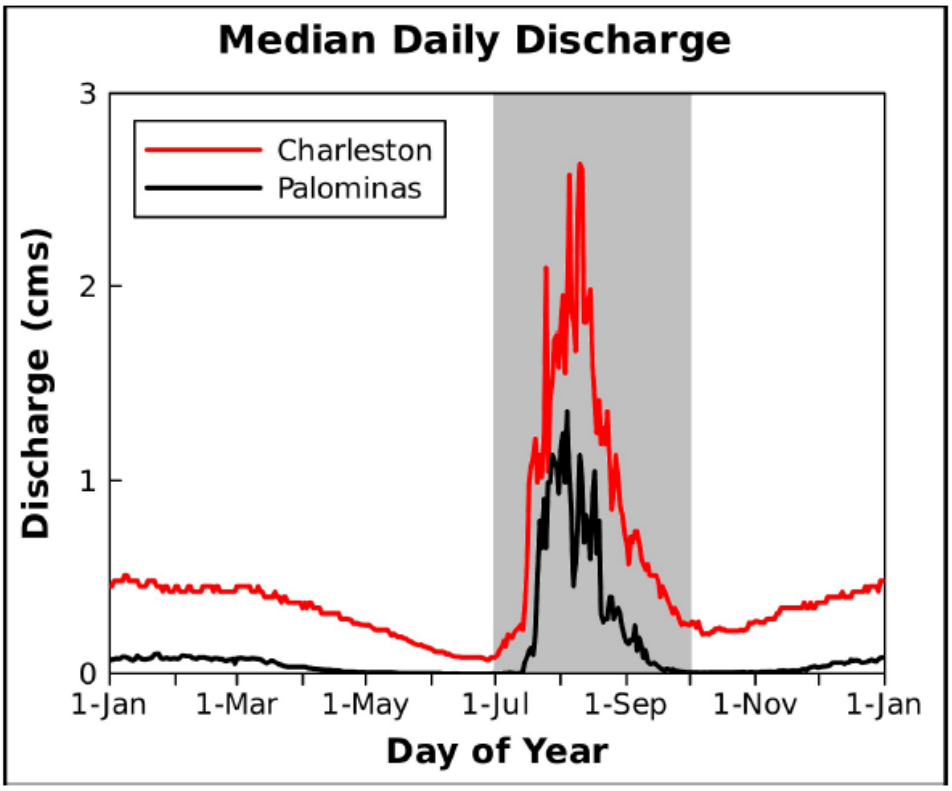

Figure 1: From *Simpson (2011)* Mean daily discharge in CMS (m^3 s^{-1}) at of the San Pedro River at Charleston (1905-2010) and at Palominas (1951-2010). The dark gray band is the period monsoon season (summer floods).

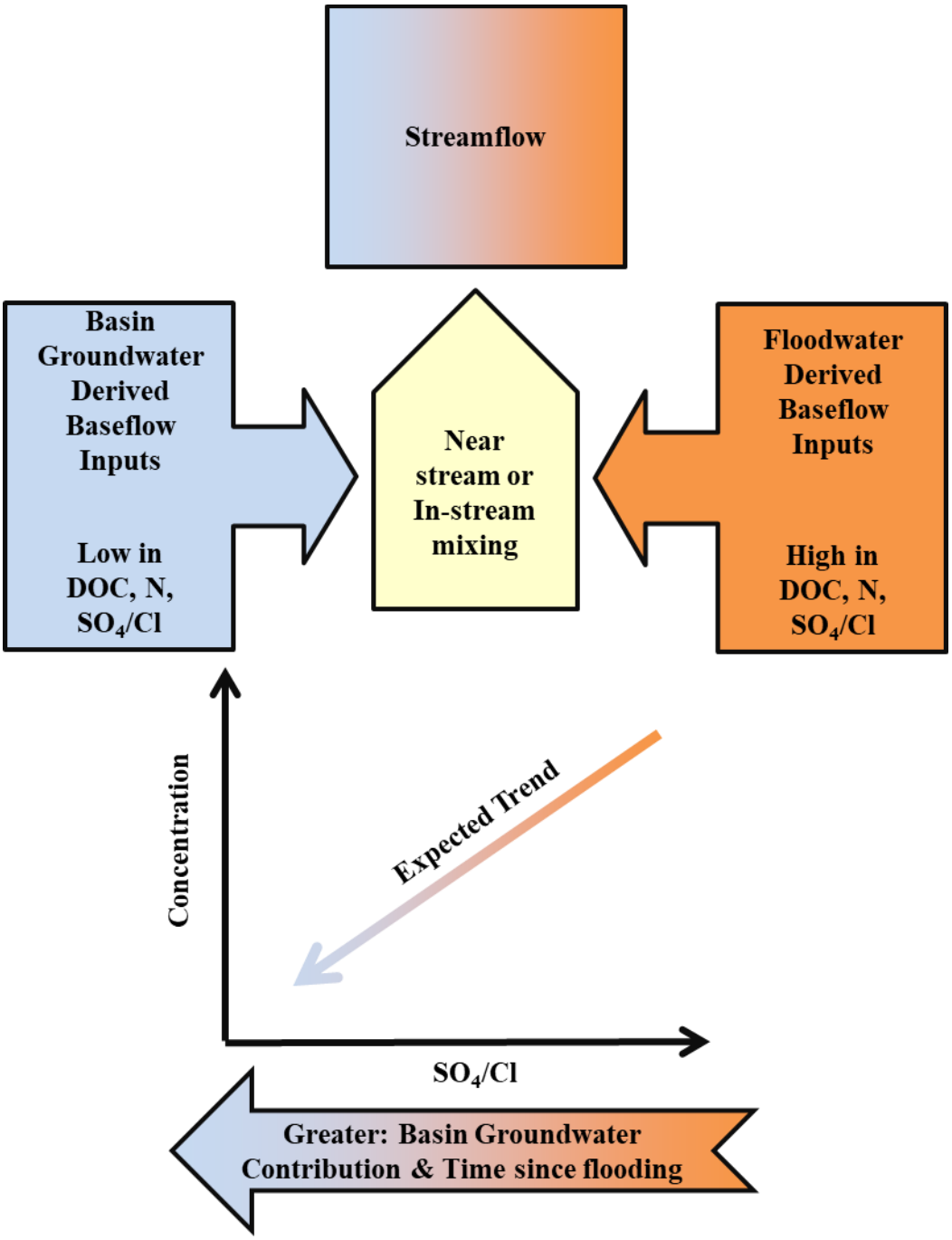

Figure 2: Conceptual Model

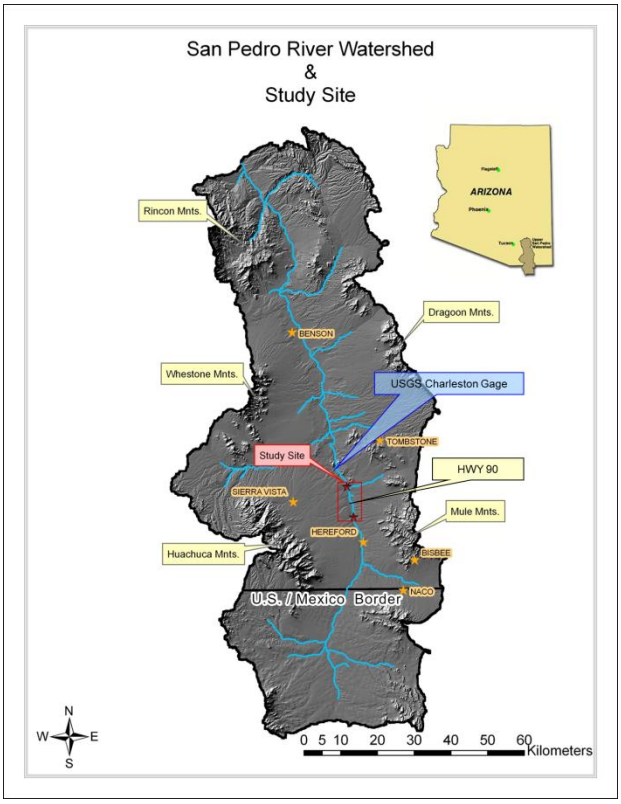

Figure 3: Map of study site

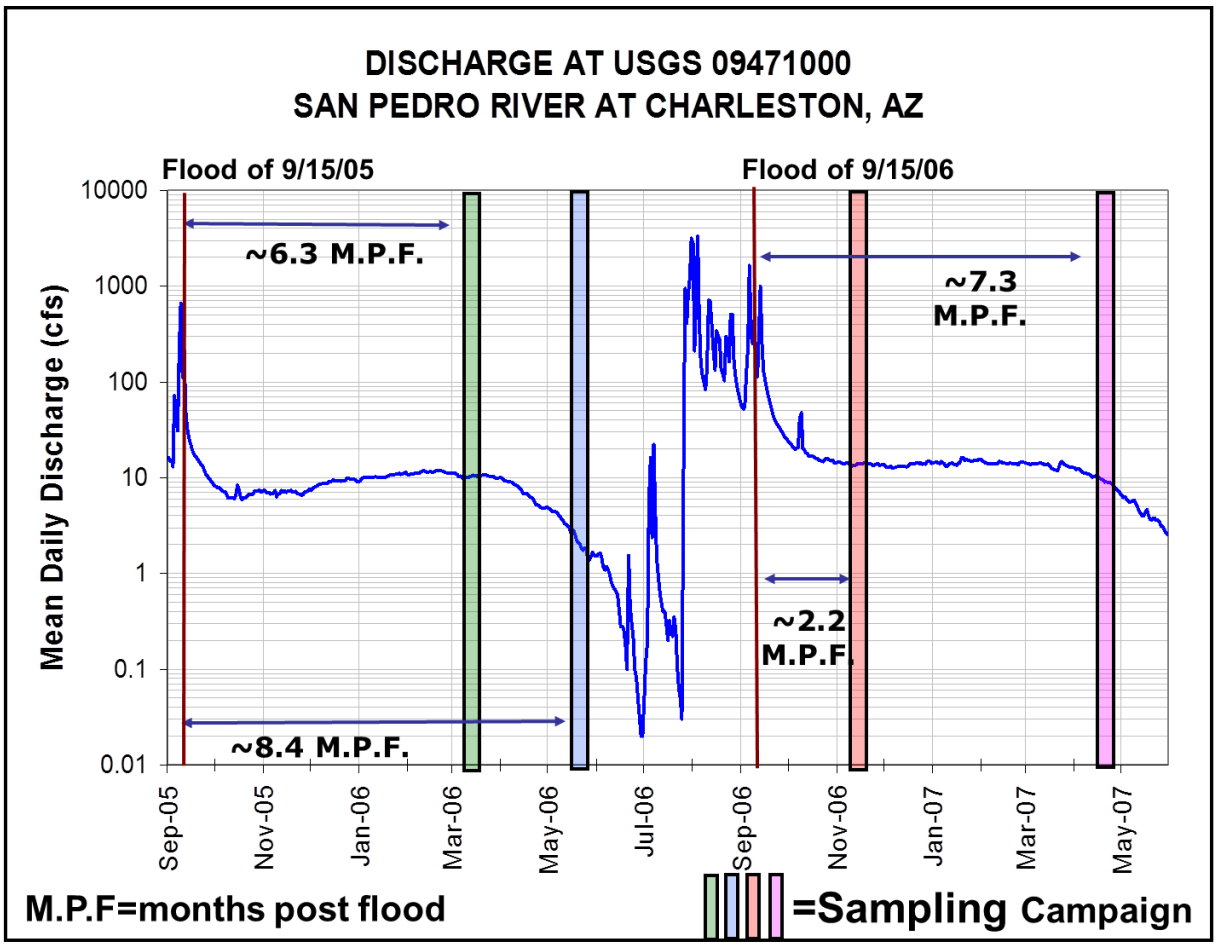

Figure 4: Hydrograph of the San Pedro River at Charleston, AZ for the study period.

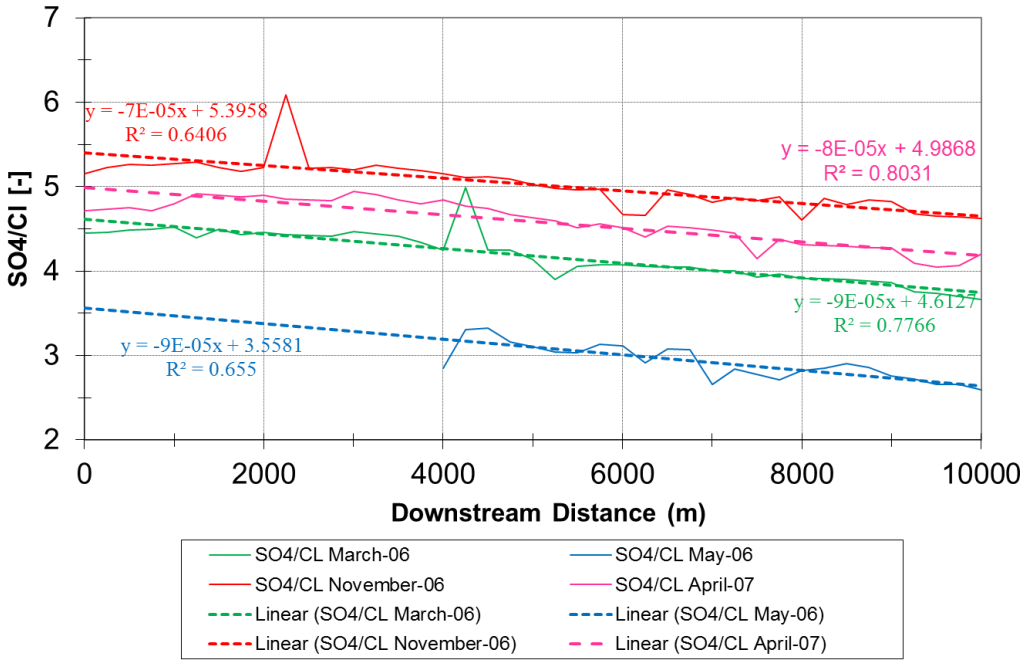

Figure 5: Streamflow Sulfate to Chloride ratio values as a function of downstream distance in the 10 km reach of the San Pedro River.

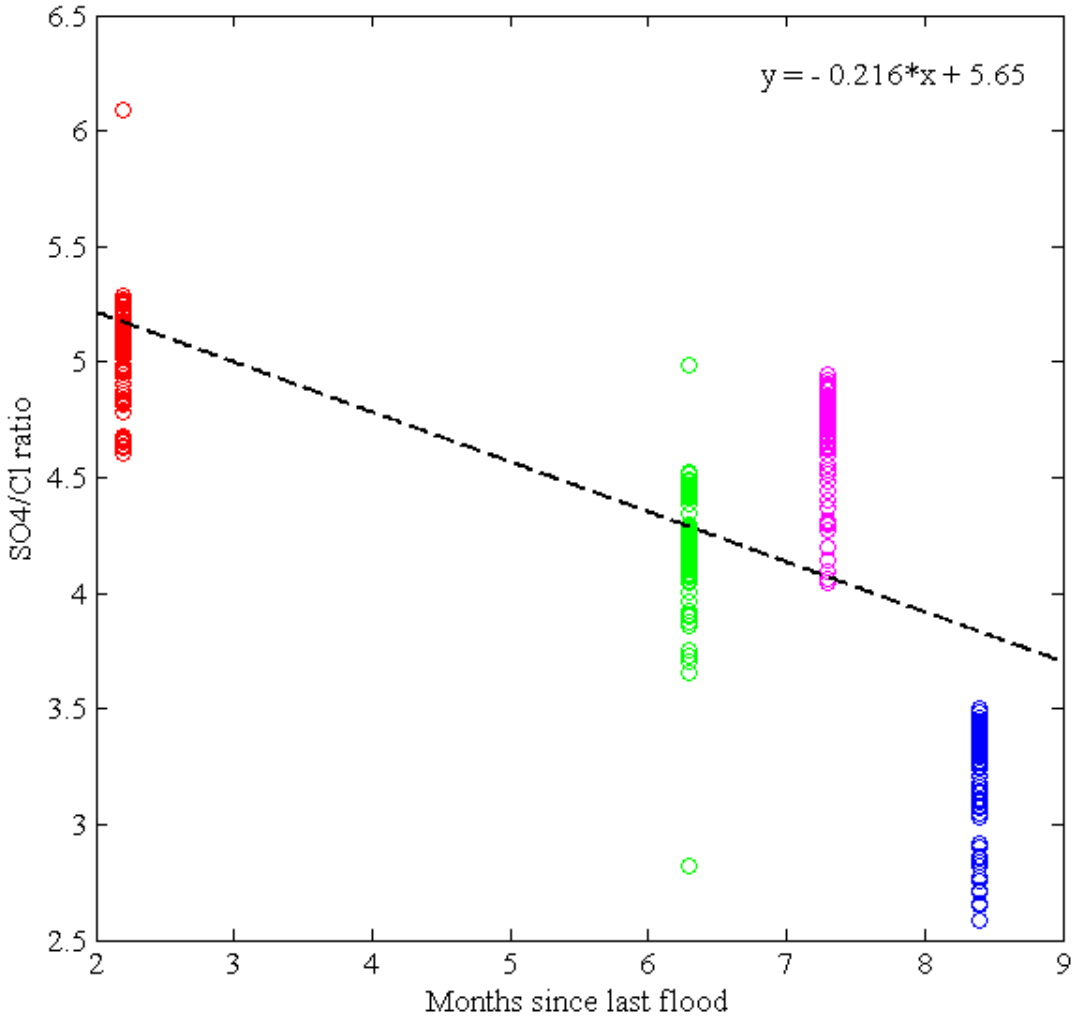

Figure 6: SO_4/Cl Ratios as a functions time since last flood for the entire dataset. The color of each group represents a different sampling campaign: March-2006 = Green, May-2006 = Blue, November-2006 = Red and April-2007 = Magenta. Note the linear relationship slope is statistically different from zero (p-value < 0.05) and the R^2 is 0.5344 . The Pearson's linear correlation coefficient (R) for the relationship is -0.7310 and it is also statistically different from zero (p-value < 0.05).

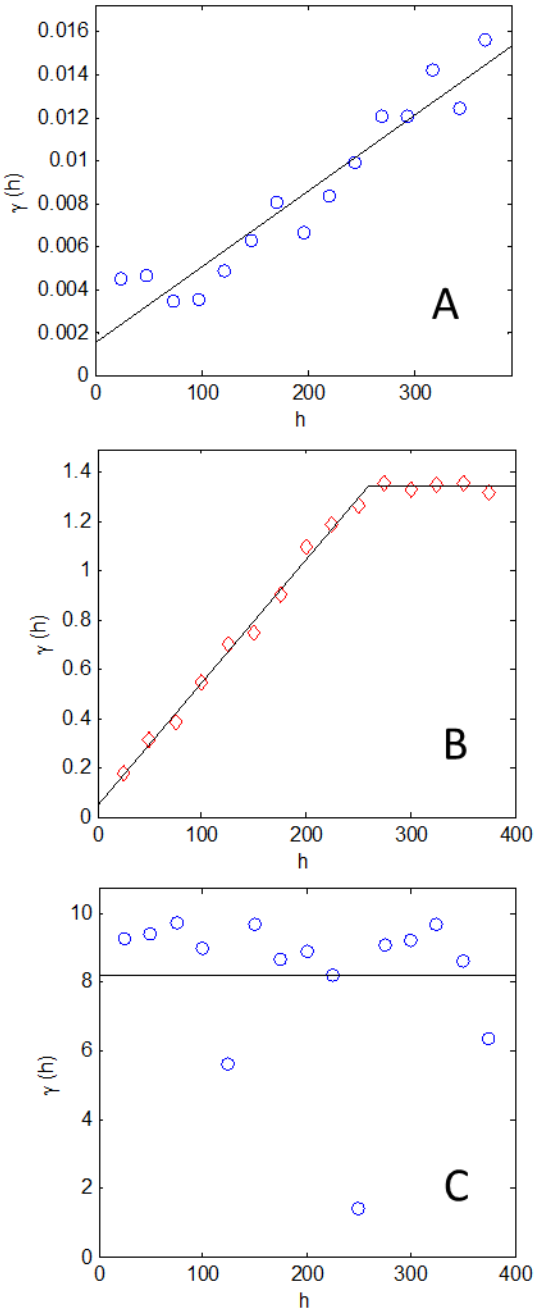

Figure 7: Examples of three empirical semi-variogram types (symbols) fitted model (solid line) for the 1km sampling reach : A) Semi-Variogram of SO_4/Cl for the sampling campaign of May 2006, B) Semi-Variogram of Na for the sampling campaign of November 2006 and C) Semi-Variogram of Cl for the sampling campaign of May 2006. These semi-variograms highlight the three different behaviors exhibited by all other chemical species: random, no auto-correlation (A), linear with range, auto-correlated (B and C) and, linear with no range, auto-correlated (D).

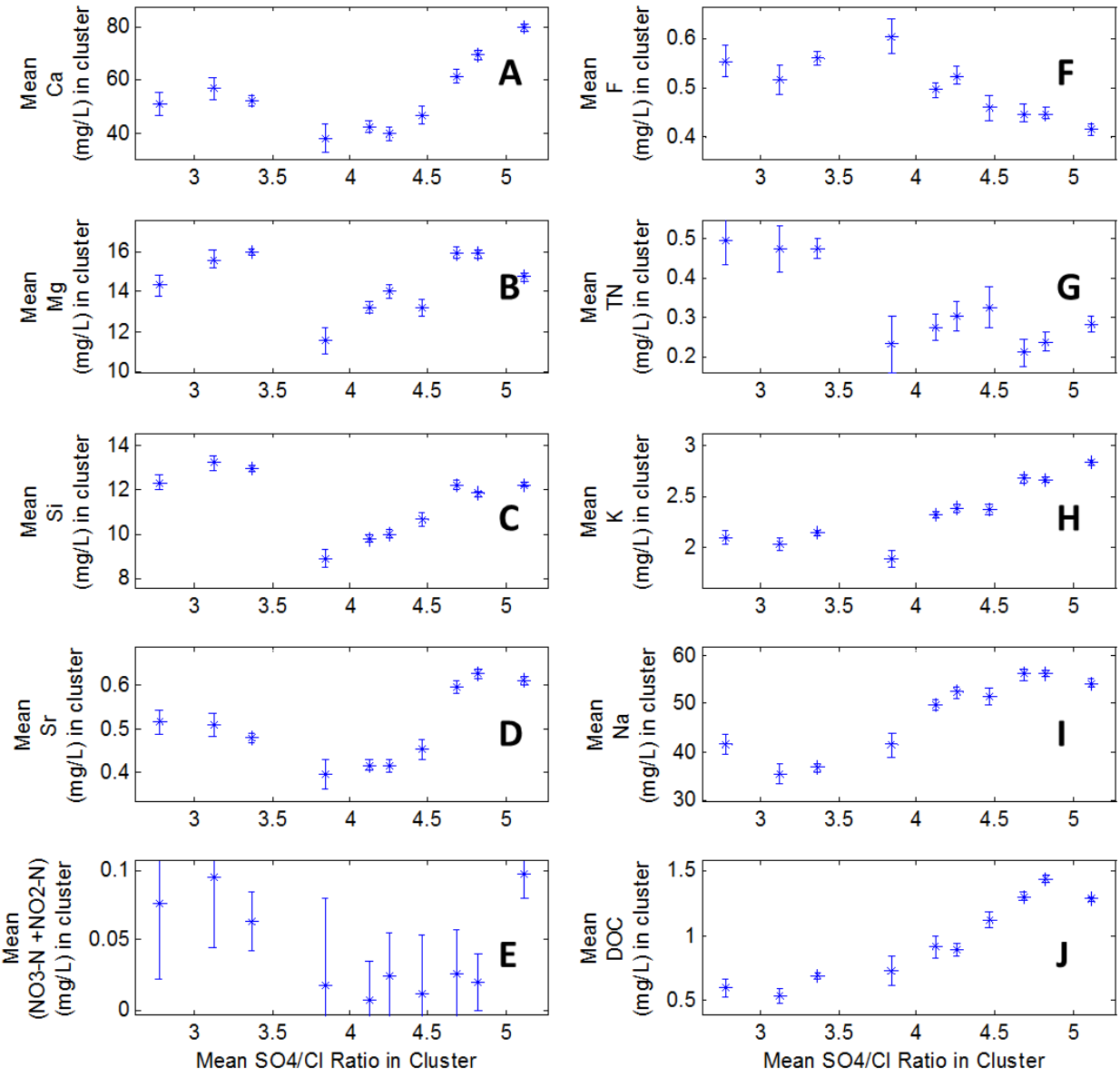

Figure 8: Clustered chemical species mean concentration as a function of mean SO_4/Cl ratio in the cluster. The asterisk represents the mean concentration value while the bars represent ±1.96 x (standard error). The means between two clusters are significantly different (p-value<0.05) if the error bars do not intersect.

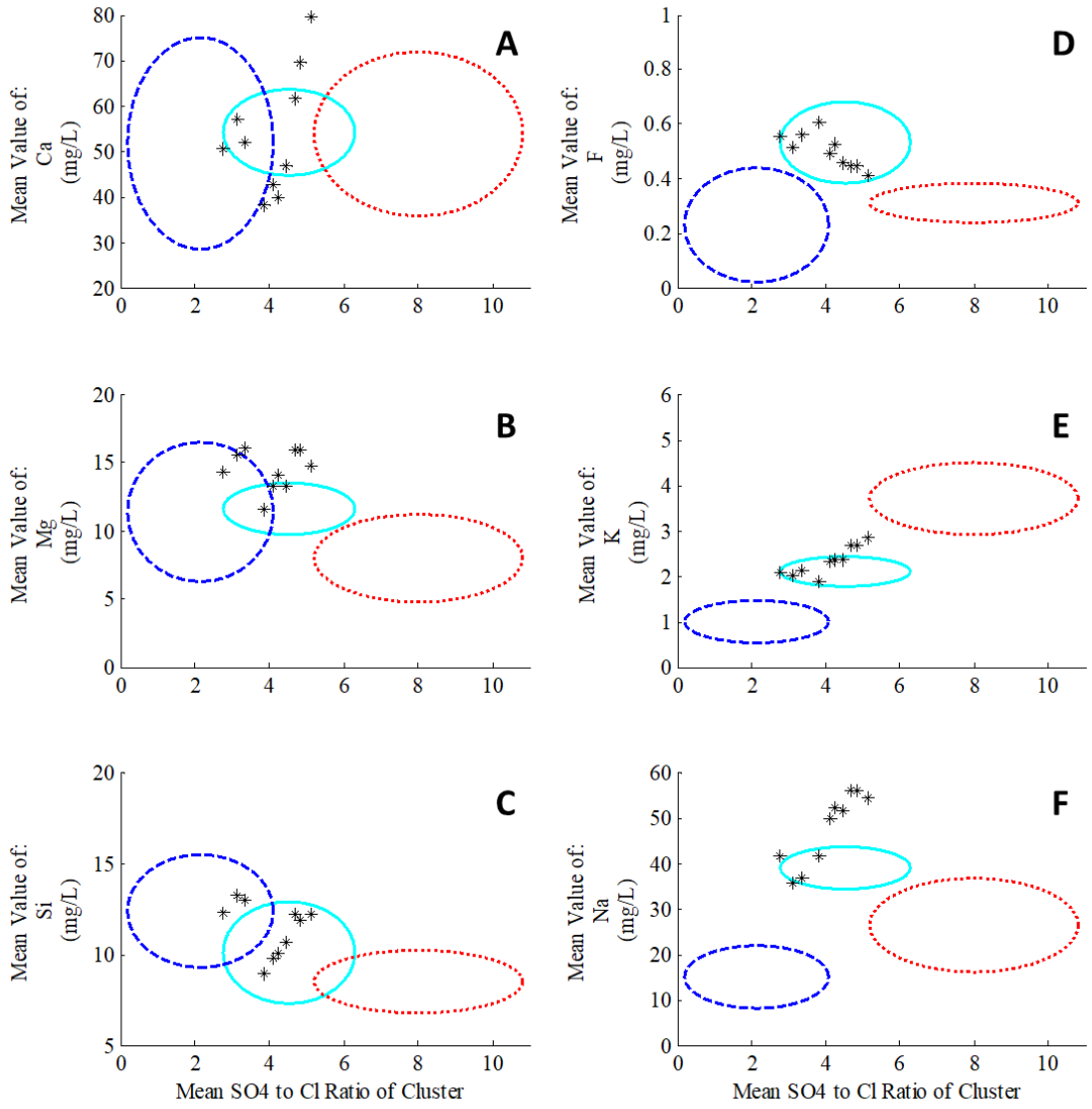

Figure 9 : Mean concentration of Ca, Mg, Si, F, K and Na with reference data ranges. The squares are the mean concentrations values shown in Figure 8. The reference regions represent the ranges (mean ± standard deviation) of the: Regional Aquifer (blue dashed line), streamflow during baseflow (cyan solid line) and streamflow during flood events (red dotted line) derived from [*Pool et al.*, 1999]

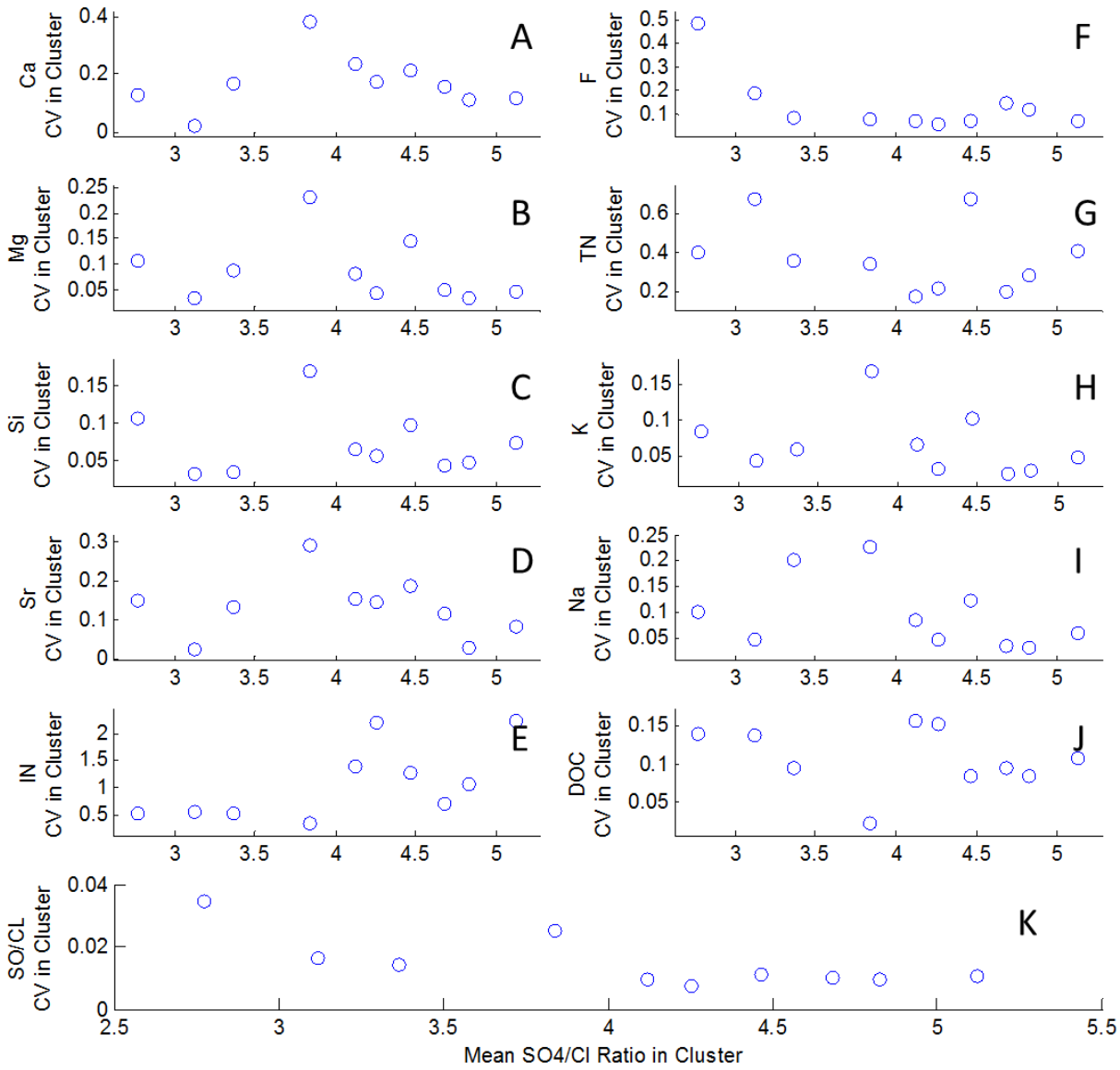

Figure 10: Clustered chemical species coefficient of variation as a function of the mean SO_4/Cl ratio in each cluster.

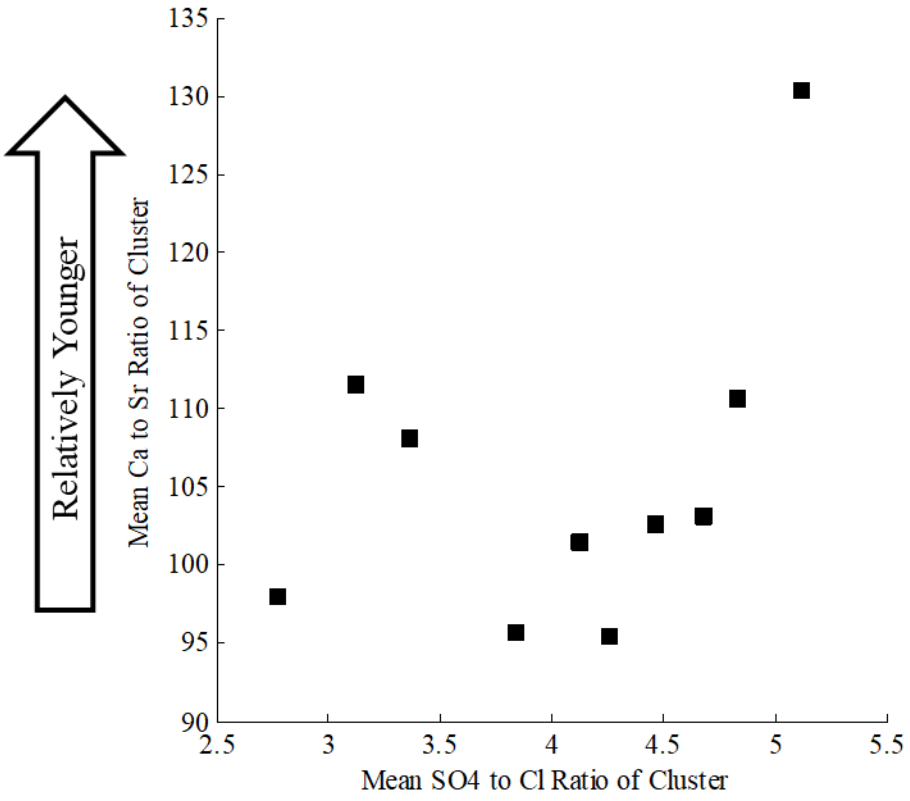

Figure 11: Mean Ca to Sr mass ratios (ppm/ppm) as a function of mean SO_4/Cl ratio in the cluster.

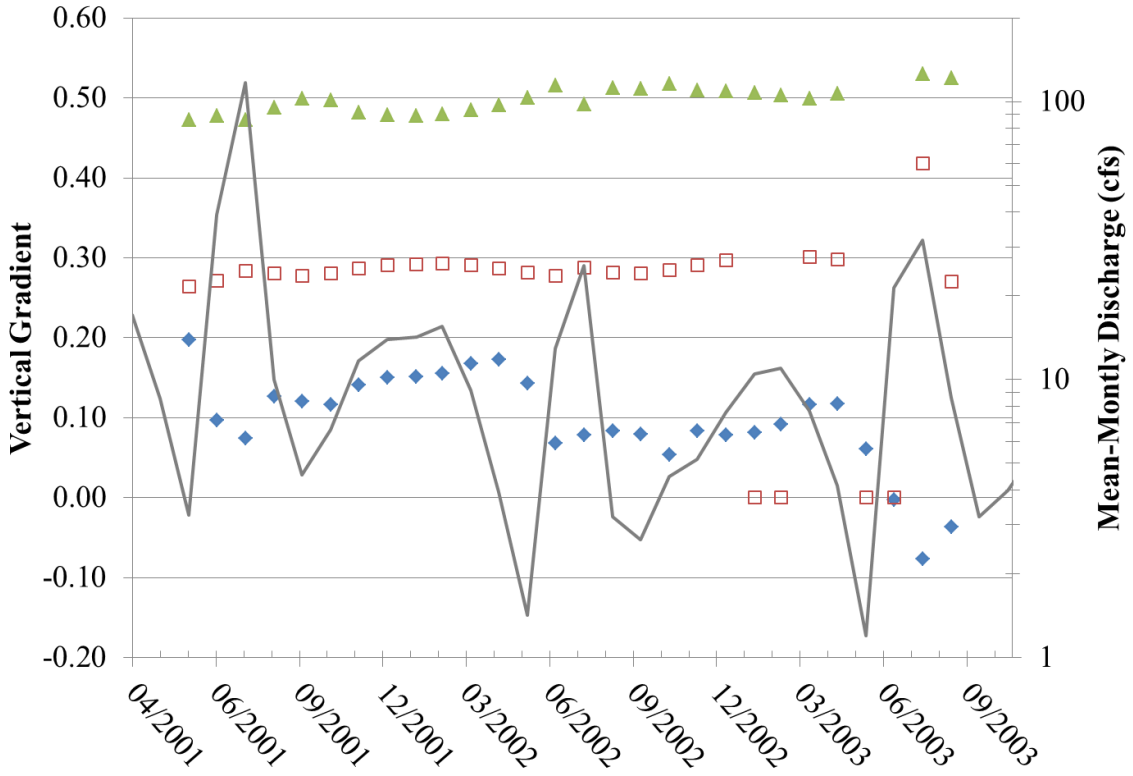

Figure 12: Vertical hydraulic gradients (symbols) at Riparian Wells in Cottonwood and mean monthly discharge (line) at Charleston as a function of time. The depth of each gradient measurement is 5.33, 10.23 and 11.15 meters for the diamond, square and triangle symbols, respectively. The well cluster is located approximately 4.5 km south of HWY90 bridge and the gauging station is located approximately 8.9 km north of HWY90 bridge. For the gradients positive value indicate upward flow.

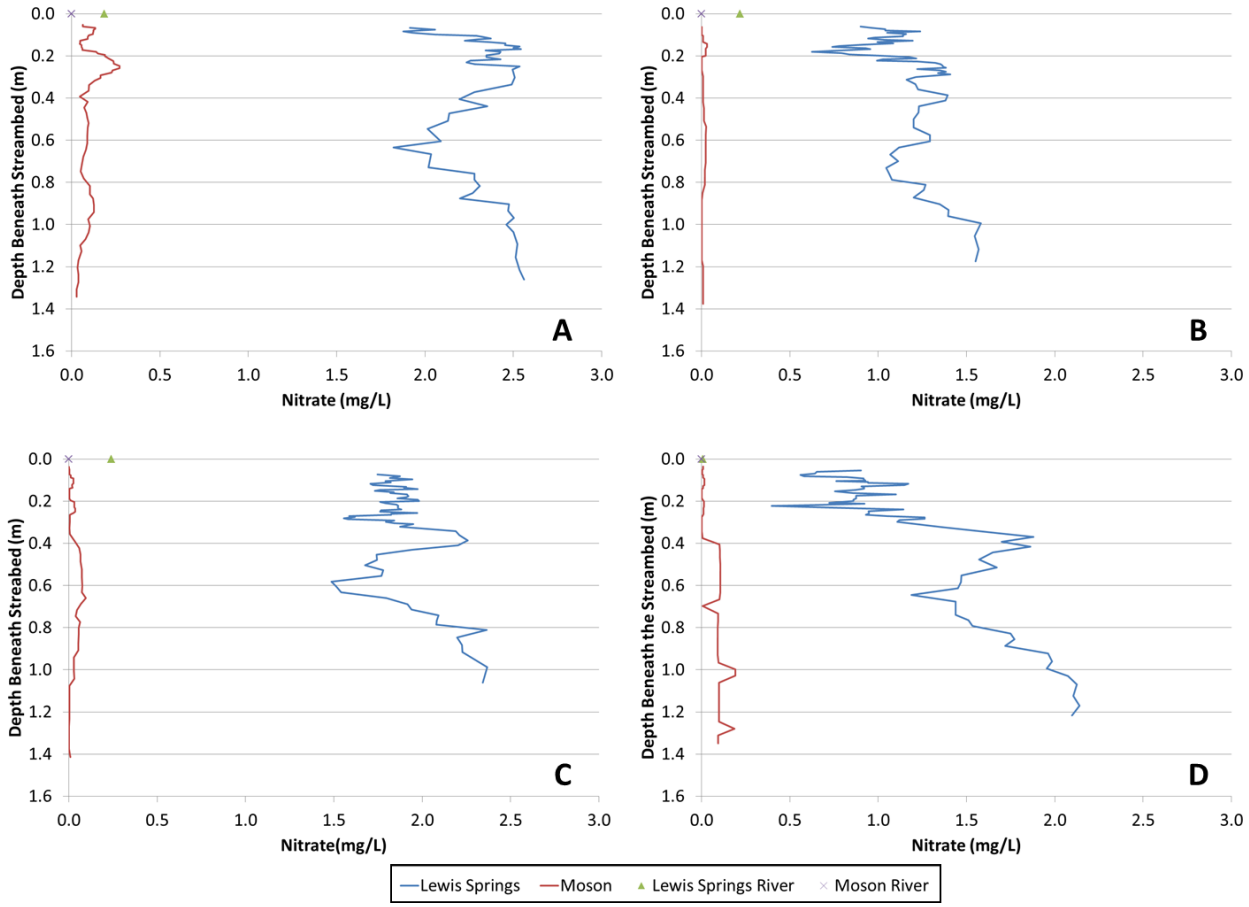

Figure 13: Nitrate concentrations profiles (mg/L) versus depth beneath the streambed (m) at two sites in the San Pedro River streambed. The data was collected A) June 2009, before summer floods; B) November 2009, shortly after summer floods; C) June 2010, before summer floods; and D) October 2010, shortly after summer floods. The symbols at depth zero represent the river streamwater nitrate concentration.

9 List of Tables

Table 1: Mean Concentration (Standard Deviation) and sample size for all chemical species per sampling period.

Chemical Species	May 2006	Mar 2006	Apr 2007	Nov 2006
Months Post-Flood	8.4	6.3	7.3	2.2
SO/CL (mg/L / mg/L)	3.27a (0.20) n=138	4.19b (0.22) n=131	4.73c (0.17) n=161	5.09d (0.15) n=162
Ca (mg/L)	52.85a (7.91) n=146	39.77b (8.44) n=131	64.97c (7.53) n=162	79.29d (10.05) n=138
K (mg/L)	2.11a (0.13) n=146	2.31b (0.22) n=131	2.61c (0.10) n=162	2.83d (0.12) n=138
Mg (mg/L)	15.80a (1.37) n=146	13.19b (1.46) n=131	15.75a (0.71) n=162	14.94c (0.82) n=138
Na (mg/L)	36.97a (6.51) n=146	50.54b (5.80) n=131	55.51c (2.82) n=162	54.43c (3.01) n=138
Si (mg/L)	12.96a (0.59) n=146	9.69b (0.63) n=131	11.73c (0.35) n=162	12.43d (0.87) n=138
Sr (mg/L)	0.49a (0.06) n=146	0.40b (0.05) n=131	0.61c (0.03) n=162	0.61c (0.06) n=138

Note the sampling campaigns are organized by the SO_4/CL in increasing order. Different super script letters for each of the chemical species mean value imply significant difference in the means with a p-value < 0.05.

Table 1(Cont.): Mean Concentration (Standard Deviation) and sample size for all chemical species per sampling period.

Chemical Species	May 2006	Mar 2006	Apr 2007	Nov 2006
F^- (mg/L)	0.55a (0.11) n=146	0.50b (0.05) n=132	0.46c (0.04) n=160	0.41d (0.06) n=162
Cl^- (mg/L)	8.45a (2.48) n=146	13.46b (1.28) n=132	13.65b (0.93) n=161	14.25c (0.67) n=162
SO_4^{-2} (mg/L)	28.89a (6.73) n=146	56.00b (8.14) n=132	64.66c (6.24) n=161	72.51d (4.79) n=162
IN (NO_3-N+NO_2-N) (mg/L)	0.07a (0.04) n=144	0.01b (0.02) n=130	0.02b (0.03) n=161	0.09a (0.21) n=160
TN (mg/L)	0.47a (0.20) n=143	0.30b (0.12) n=126	0.23c (0.06) n=161	0.27b (0.11) n=162
DOC (mg/L)	0.65a (0.09) n=107	0.85b (0.12) n=33	1.39c (0.16) n=157	1.28d (0.14) n=139

Note the sampling campaigns are organized by the SO_4/CL in increasing order. Different super script letters for each of the chemical species mean value imply significant difference in the means with a p-value < 0.05.

Table 2: Minimum – Maximum concentration for all chemical species per sampling period.

Chemical Species	May 2006	Mar 2006	Apr 2007	Nov 2006
Months Post-Flood	8.4	6.3	7.3	2.2
SO_4^{-2}/Cl^- (mg / mg)	2.59 / 3.50	2.82 / 4.99	4.05 / 4.95	4.61 / 6.09
Ca (mg/L)	8.99 / 14.21	4.40 / 10.66	11.10 / 12.79	7.95 / 15.09
K (mg/L)	33.15 / 63.57	16.47 / 68.40	47.98 / 76.20	34.34 / 94.71
Mg (mg/L)	8.96 / 20.00	6.00 / 14.71	12.96 / 17.01	12.23 / 16.90
Na (mg/L)	8.99 / 14.21	4.40 / 10.66	11.10 / 12.79	7.95 / 15.09
Si (mg/L)	0.33 / 0.63	0.25 / 0.58	0.52 / 0.67	0.34 / 0.68
Sr (mg/L)	2.59 / 3.50	2.82 / 4.99	4.05 / 4.95	4.61 / 6.09

Note the sampling campaigns are organized by the SO_4/CL values in increasing order as identified in (Table 1).

Table 2 (cont): Minimum – Maximum concentration for all chemical species per sampling period.

Chemical Species	May 2006	Mar 2006	Apr 2007	Nov 2006
F^- (mg/L)	0.03 / 0.86	0.41 / 0.69	0.38 / 0.65	0.18 / 0.57
Cl^- (mg/L)	2.2E-3 / 10.72	10.12 / 18.63	10.72 / 14.65	12.15 / 15.46
SO_4^{-2} (mg/L)	0.44 / 0.86	0.64 / 1.15	0.96 / 1.78	0.51 / 1.55
IN (NO_3-N+NO_2-N) (mg/L)	0.03 / 0.86	0.41 / 0.69	0.38 / 0.65	0.18 / 0.57
TN (mg/L)	2.2E-3 / 10.72	10.12 / 18.63	10.72 / 14.65	12.15 / 15.46
DOC (mg/L)	1.42 / 35.32	0.01 / 71.91	45.62 / 72.36	56.79 / 86.66

Note the sampling campaigns are organized by the SO_4/CL values in increasing order as identified in (Table 1).

Table 3: Linear coefficient (slope) and (R^2) for each chemical species as a function of downstream distance at the 10 Km Reach.

Chemical Species	May 2006	Mar 2006	Apr 2007	Nov 2006
SO_4^{-2}/Cl^- (mg / mg)	-9.16E-5*[a] (0.65)	-8.64E-5*[a] (0.78)	-8.06E-5*[a] (0.80)	-7.44E-5*[a] (0.64)
Ca (mg/L)	-2.20E-3* (0.54)	-6.22E-4 a(0.02)	-7.40E-5 (0.00)	-8.11E-4 (0.03)
K (mg/L)	-3.39E-6 (0.00)	-4.77E-5*[a] (0.17)	-5.46E-5*[a] (0.88)	-2.60E-5*[a] (0.50)
Mg (mg/L)	-4.38E-4*[a] (0.32)	-2.08E-5 (0.00)	1.65E-5 (0.00)	2.38E-4*[b] (0.74)
Na (mg/L)	1.22E-3*[a] (0.37)	-1.15E-3*[bcd] (0.14)	-1.61E-3*[bc] (0.89)	-5.02E-4*[bd] (0.59)
Si (mg/L)	-3.03E-4*a (0.33)	-1.10E-4*a (0.10)	-2.28E-5 (0.05)	9.14E-5*b (0.47)
Sr (mg/L)	6.14E-6 (0.05)	-1.07E-6 (0.00)	-4.38E-6* (0.14)	-1.22E-6 (0.00)
F^- (mg/L)	4.50E-5 (0.12)	2.24E-5*a (0.79)	2.22E-5*a (0.85)	1.65E-5*a (0.36)
Cl^- (mg/L)	-8.02E-5 (0.00)	-4.05E-4*ab (0.79)	-4.35E-4*a (0.85)	-1.79E-4*b (0.61)
SO_4^{-2} (mg/L)	-9.43E-4 (0.05)	-2.72E-3*abc (0.81)	-3.00E-3*ab (0.86)	-1.89E-3*ac (0.70)
IN (NO_3-N+NO_2-N) (mg/L)	-8.49E-6 (0.11)	1.75E-6* (0.18)	5.56E-6 (0.08)	7.63E-8 (0.00)
TN (mg/L)	1.41E-5 (0.01)	-2.07E-5* (0.11)	-1.20E-6 (0.00)	-2.67E-6 (0.02)
DOC (mg/L)	-7.08E-6 (0.02)	-4.27E-5*a (0.82)	-5.50E-5*a (0.79)	-1.18E-5 (0.04)

*Denotes that the correlation coefficient is significant for the campaign to a p-value less than 0.05 for each campaign. If the correlation is significant for the campaign, then letter superscript denotes if the two slopes are significantly different to p-value <0.05. Note the sampling campaigns are organized by the SO_4/CL values in increasing order as identified in (Table 1)

Table 4: Statistically significant correlation coefficient matrix for the complete dataset and chemical species.

	SO/CL	Ca	K	Mg	Na	Si	Sr	F	Cl	SO4	IN	TN
Ca	0.626											
K	0.910	0.710										
Mg	-0.154	0.160	--									
Na	0.815	0.423	0.796	--								
Si	-0.272	0.326	--	0.563	-0.302							
Sr	0.605	0.844	0.663	0.394	0.567	0.264						
F	-0.569	-0.421	-0.538	0.189	-0.430	--	-0.340					
Cl	0.911	0.448	0.814	-0.149	0.784	-0.396	0.446	-0.316				
SO4	0.980	0.568	0.891	-0.170	0.819	-0.336	0.548	-0.486	0.970			
IN	--	--	-0.121	-0.184	-0.214	-0.118	-0.172	--	--	--		
TN	-0.564	-0.311	-0.474	--	-0.509	0.207	-0.445	0.320	-0.500	-0.538	0.134	
DOC	0.851	0.545	0.775	--	0.762	-0.238	0.659	-0.519	0.791	0.843	-0.122	-0.530

Note all listed correlation coefficients values are statistically significant (p-value<0.05). The "--" implies that the correlation coefficient is not statistically significant (p-value>0.05)

Table 5: Semi-Variogram type for each chemical species and sampling campaign at the 10 Km and 1Km sampling reaches.

Chemical Species	May 2006	Mar 2006	Apr 2007	Nov 2006
10 Km Sampling Reach				
SO/CL	Bounded Linear*	Bounded Linear*	Bounded Linear*	Bounded Linear*
Ca	Random*	Bounded Linear	Bounded Linear	Bounded Linear
K	Bounded Linear	Bounded Linear*	Bounded Linear*	Bounded Linear*
Mg	Bounded Linear*	Bounded Linear	Linear	Bounded Linear*
Na	Random*	Bounded Linear*	Bounded Linear*	Bounded Linear*
Si	Random*	Random*	Bounded Linear	Bounded Linear*
Sr	Linear	Bounded Linear	Bounded Linear*	Bounded Linear
F	Bounded Linear	Bounded Linear*	Bounded Linear*	Linear*
Cl	Bounded Linear	Linear*	Bounded Linear*	Linear*
SO4	Bounded Linear	Linear*	Bounded Linear*	Bounded Linear*
IN	Bounded Linear	Bounded Linear*	Random	Random
TN	Bounded Linear	Random*	Bounded Linear	Bounded Linear
DOC	Bounded Linear	Random*	Bounded Linear*	Bounded Linear
1 Km Sampling Reach				
SO/CL	Linear*	Bounded Linear	Random*	Linear*
Ca	Bounded Linear*	Linear	Bounded Linear	Bounded Linear*
K	Bounded Linear*	Random*	Linear*	Bounded Linear*
Mg	Linear*	Linear	Bounded Linear*	Linear*
Na	Random*	Bounded Linear*	Linear*	Bounded Linear*
Si	Random*	Bounded Linear	Linear	Bounded Linear*
Sr	Linear*	Bounded Linear	Bounded Linear*	Bounded Linear*
F	Random	Linear*	Random	Linear*
Cl	Random	Linear*	Bounded Linear*	Bounded Linear*
SO4	Random	Bounded Linear*	Bounded Linear*	Linear*
IN	Bounded Linear	Random*	Bounded Linear*	Random
TN	Random	Random	Random	Random
DOC	Bounded Linear*	Bounded Linear	Bounded Linear*	Random

* Denotes that the data was first de-trended before calculating the semi-variances and generating the semi-variograms.

Table 6: Fitted semi-variogram ranges (m) for each chemical species and sampling campaign at the 10 Km and 1Km sampling reaches.

Chemical Species	May 2006	Mar 2006	Apr 2007	Nov 2006
10 Km Sampling Reach				
SO/CL	*960*	3147	2962	1500
Ca	<250	701	1657	599
K	634	2500	3099	2837
Mg	*803*	2014	>4000	1500
Na	*<250*	1000	2750	2750
Si	<250	250	2717	921
Sr	>3000	621	3039	1146
F	*401*	2579	2323	>4000
Cl	*440*	>4000	3098	>4000
SO4	419	>4000	3024	2162
IN	1014	2133	*<250*	*<250*
TN	1392	*<250*	731	*1000*
DOC	608	*<250*	1553	*1500*
1 Km Sampling Reach				
SO/CL	>400	75	*<25*	>400
Ca	236	>400	137	193
K	125	*<25*	>400	175
Mg	>400	>400	49	>400
Na	*<25*	77	>400	260
Si	*<25*	57	350	175
Sr	*>400*	175	275	246
F	*<25*	>400	<25	>400
Cl	*<25*	>400	200	48
SO4	*<25*	203	300	>400
IN	89	*<25*	100	*<25*
TN	*<25*	*<25*	*<25*	*<25*
DOC	148	86	65	<25

Table 7: Fitted semi-variogram ranked-ranges for each chemical species and sampling campaign at the 10 Km and 1Km sampling reaches.

Chemical Species	May 2006	Mar 2006	Apr 2007	Nov 2006
10 Km Sampling Reach				
SO/CL	1	4	3	2
Ca	1	3	4	2
K	1	2	4	3
Mg	1	3	4	2
Na	1	2	3	4
Si	1	1	4	3
Sr	3	1	4	2
F	1	3	2	4
Cl	1	3	2	3
SO4	1	4	3	2
IN	3	4	1	1
TN	4	1	2	3
DOC	2	1	4	3
Total Rank	21	32	40	34
1 Km Sampling Reach				
SO/CL	3	2	1	3
Ca	3	4	1	2
K	2	1	4	3
Mg	2	2	1	2
Na	1	2	4	3
Si	1	2	4	3
Sr	4	1	3	2
F	1	3	1	3
Cl	1	4	3	2
SO4	1	2	3	4
IN	3	1	4	1
TN	1	1	1	1
DOC	4	3	2	1
Total Rank	27	28	32	30

APPENDIX B: AN EMPIRICAL MODEL FOR PREDICTING FLOW PERMANENCE ON THE SAN PEDRO RIVER

Carlos D. Soto-López[1], Thomas Meixner[1] and Hoori Ajami[2]

[1] Department of Hydrology and Atmospheric Sciences

University of Arizona

1133 E James E Rogers Way

Building 11, Room 122

Tucson, Arizona, 85722, USA.

[2]Environmental Sciences

University of California

Riverside, CA, USA

To be submitted for publication to the Journal of Hydrology.

1 Abstract

In semi-arid streams and rivers streamflow permanence (perennial vs intermittent rivers segments) is a key hydrologic variable that controls the ecological structure and function, the biologic abundance and diversity, the vegetation type and structure, the primary production and biogeochemical processing rates of riparian ecosystems. Despite its importance streamflow permanence is a rarely recorded variable due to the significant deployment of resources needed to map this variable along a river. However, since 1999 and during the period of lowest flow, volunteers have surveyed and recorded the locations of wet and dry river sections along the San Pedro River National Conservation Area in Arizona. Here we make use of a logistic regression model to test if several geomorphic and hydrologic explanatory variables are significant predictors of streamflow permanence observed and recorded in the San Pedro River for the surveys years of 1999 through 2011. The results of this study show that variables that describe bedrock elevation, variables that describe the shape and width of the floodplain, variables that describe the land surface elevation and late spring streamflow are significant predictors of streamflow permanence in the San Pedro River. We argue, that these variables either directly or indirectly describe: the surface-groundwater-vegetation interaction of late spring baseflow, the shape and thickness of the aquifer underlying the river, and the channel morphology and its variation along the river. The logistic regression model was able to correctly predict 80.1-86.7% of the wet/dry locations of the study site during the validation period of 2006 to 2011 at a resolution of 10 meters using ten (10) hydrologic and geomorphic explanatory variables. Finally, the logistic regression model was also

able to show that increasing late spring streamflow would result in a downstream expansion of river segments classified as wet centered on areas that remain perennial.

2 Introduction

Arid and semiarid areas cover approximately one third of the earth's land surface [*Thomas,* 1989] and are characterized by potential evapotranspiration rates that exceed the precipitation rates that these areas receive. It is because of this lack of excess moisture that landscapes in these regions are dominated by ephemeral and intermittent streams with perennial streams forming only in locations where moisture is supplied by groundwater systems. During the dry season and in the absence of atmospheric inputs perennial flow in streams is sustained and controlled by baseflow inputs from aquifers. In turn, baseflow inputs are mainly controlled by the intersection of the regional and riparian groundwater table with the streambed [*Hedman and Osterkamp,* 1982; *Meinzer,* 1923]. These baseflow inputs are also controlled by the geology and geomorphology of the basin and stream, the hydrologic transport capabilities of the aquifer, land use characteristics of the basin, and climate [*Brutsaert,* 2005; *Meinzer,* 1923; *Price,* 2011]. Once the stream disconnects from its aquifer perennial streamflow will be controlled by the balance between upstream inputs, downstream outputs and infiltration. In other river systems spanning a range of climatic regimes, *Godsey and Kirchner* [2011] proposed that the locations where the streambed starts to become wet or dries out indicate a balance between upstream inputs, downstream outputs and subsurface transport capabilities.

The permanence of flow in streams is a critical variable that determines the ecological structure and function of riparian ecosystems. Intermittent and perennial semi-arid rivers create a hot spot of plant and animal biodiversity [*Naiman et al.,* 1993; *Patten,* 1998].

These ecosystems are needed by many species to complete their life cycles [*Brinson et al.,* 1981], create a critical layover for species migration [*Skagen et al.,* 1998], and enable mesic and hydric plant communities (Riparian Vegetation) to develop in an otherwise xeric landscape [*Patten,* 1998]. Furthermore, the presence or absence of streamflow in perennial semi-arid rivers (streamflow permanence) is a fundamental hydrologic variable in semi-arid rivers. It controls biotic diversity and abundance, vegetation types and structure, expansion and contraction of the ecosystem, primary production and biogeochemical processing rates [*Gomez et al.,* 2012; *Holmes et al.,* 1994; *Sponseller et al.,* 2010; *Stanley et al.,* 1997; *Stanley et al.,* 2004; *Stromberg et al.,* 2005; *Stromberg et al.,* 2010].

Although streamflow permanence is an important characteristic of a semi-arid stream, it is a rarely recorded variable because it requires a significant deployment of resources to map streamflow permanence along a river. Since 1999, on the third Saturday of June (the driest time of the year) a survey of flow permanence has been conducted along the San Pedro River National Conservation Area, Arizona, USA [*Turner and Richter,* 2011] (Figure 1). During this survey the locations of wet and dry river sections longer than 9.1m in length have been recorded by volunteers spearheaded by The Nature Conservancy and the Bureau of Land Management. In their analysis *Turner and Richter* (2011) showed that a large fraction of the river wet/dry status auto-correlates in time and that there is a positive correlation between the total number and length of wet river reaches and streamflow on the day of the survey. These correlations likely describe the degree of "wetness" that the system is currently in and suggests that, as a whole, flow

permanence in the San Pedro River depends on the long-term hydrologic conditions of the basin.

Research has shown that a large fraction of streamflow in the San Pedro River from the months of October to June is baseflow derived [Thomas and Pool, 2006]. Therefore, the height of the water table with respect to the streambed together with the hydraulic properties of the aquifer and streambed will play a major role in determining the amount of streamflow and locations of the river that remain wet or dry out during the driest period of the year. However, monitoring water table levels, hydraulic properties and streamflow on the entire river is a non-trivial measurement that requires a large investment in time and resources. In a similar semi-arid river system, researchers found that main stem drying patterns are primarily controlled by the degree of vertical or cross-sectional channel constriction and to a lesser degree the river reach type (i.e. riffle, run or pools) [Stanley et al 1997].

This project aims to answer the following questions. First, what physical, spatial and temporal properties of semi-arid river systems influence streamflow permanence? Two, how sensitive is streamflow permanence to changes in streamflow? Three, what do these results indicate about the underlying processes controlling streamflow permanence in arid and semi-arid regions?

We argue that major factors that control proximity of the water table to the ground surface (i.e.: bedrock topography, surface concavity, channel geomorphology and contributing area) as well as minor factors (i.e.: stream channel slope, stream channel sinuosity, flood plain width, streamflow and precipitation) predict the location and spatial distribution of streamflow permanence in the San Pedro River. These questions will be

answered by generating a logistic regression model with several geomorphic and hydrological explanatory variables, and testing if any of the explanatory variables used in the model are significant predictors of the wet/dry patterns observed in the stream using the Wet/Dry survey data collected from 1999-2011 [*Turner and Richter*, 2011]. That analysis will be followed by an overall assessment of the logistic regression, the fit of the model to actual outcomes, and an evaluation of its predicted probabilities. Finally, the calibrated and validated model will be used to assess the effects of future scenarios on the pattern of river reaches predicted wet by looking at historical highs, lows and average values for streamflow and precipitation in the basin.

3 Methods

3.1 Study Site

The study site consists of 80.6 kilometers of the San Pedro River inside the San Pedro River National Conservation Area (SPRNCA), located near the towns of Sierra Vista, Bisbee and Tombstone, Arizona (Figure 1). Inside SPRNCA, the river flows northward with an overall gradient of 2.43 m per kilometer and at the downstream end of SPRNCA the river drains an area of 5,011 km^2. The river flows along a variable depth alluvium filled extensional basin that is bounded by the Mule Mountains and Tombstone Hills on the east and by the Huachuca Mountains on the west with altitudes ranging from 1,524 to 2,256 m and from 1,524 to 2,896 m, respectively[*Pool and Coes,* 1999]. Inside SPRNCA the overall thickness of the alluvial deposits decreases as downstream distance increases and it ranges from zero (exposed bedrock) near the Tombstone Hills to 1.46 km at the upstream end of SPRNCA [Gettings and Houser, 2000].

3.2 Logit Model

A logistic regression model is part of a category of statistical models called generalized linear models. Generally, this model allows the prediction of a dichotomous outcome from a set of variables that may be continuous, categorical, discrete, or dichotomous. This type of model makes no particular assumption about the distributions of the independent variables. However it does assume that the distributions of the difference of the actual and predicted values, as well as the conditional mean of the dichotomous outcome are binomial. Specifically, the logistic regression models the probability (P) of a certain outcome. It takes the value 1 with a probability of success P, or the value 0 with probability of failure 1-P, such as presence/absence, success/failure or as in here Wet (1)/Dry (0). The relationship between the predictor and response variables is not a linear function in logistic regression (Equation 1). Instead, the logit transformation of P is used (Equation 2).

$$\mathrm{P} = \mathrm{Probability}(\mathrm{Y} = \mathrm{outcome\ of\ interest(wet)}|\mathrm{X} = X_i) = \frac{e^{c+\beta_1 X_1+\beta_2 X_2+\cdots+\beta_i X_i}}{1+e^{c+\beta_1 X_1+\beta_2 X_2+\cdots+\beta_i X_i}}$$

(Eq. 1)

$$\mathrm{Logit(Y)} = \mathrm{Ln(Odds)} = \mathrm{Ln}\left(\frac{P}{1-P}\right) = c + \beta_1 X_1 + \beta_2 X_2 + \cdots + \beta_i X_i \text{ (Eq. 2).}$$

Where, P is probability, c is the regression constant, β_i are the regression coefficients and X_i's are values for each explanatory variable. For a more in depth description, overview and application of the logistic regression please refer to [*Aldrich and Nelson,* 1984; *Hosmer and Lemeshow*, 2000; *Nerlove and Press*, 1973]. The null hypothesis (H_0) implicitly states that all β_i in the logistic regression model are equal to zero, while the

alternate hypothesis (H_a) states that at least one β in the set of explanatory variables is not equal to zero. Here, rejecting the H_0 means that the logistic regression equation is able to predict the probability that a particular location in the San Pedro River will be wet better than the overall observed fraction of wet locations in the wet/dry dataset.

3.3 Data sources and Data Management

In this investigation a logistic regression model was generated using several geomorphic and hydrological explanatory variables to predict the wet/dry status of the San Pedro River inside SPRNCA. Once created, the model was assessed by evaluating the significance of each variable in the model, the fit of the model to the actual outcomes and the model predicted probabilities. The model was then be used in conjunction with a series of alternate scenarios to assess the effects of hydro-climatological changes in the patterns of sections of the river predicted wet by the model. Before the model was generated all the explanatory variables were selected and processed to work within a logistic regression. Specifically, Matlab version 7.11 was used to create, calibrate and validate the logistic regression model using Matlab's generalized linear model fit (glmfit) function. ESRI's ArcGIS version 9.3 was used to create, pre-process, and format the datasets (Table 1) so that they conform to the requirements of Matlab's "glmfit" function. However, there are multiple statistics, mathematical and geographic information systems software packages capable of performing logistic regression analysis. Where necessary the specific commands used to perform certain key processes in Matlab or ArcGIS are mentioned as a reference.

A total of one response and 17 explanatory variables were initially selected and pre-processed to be part of the logistic regression model (Table 1). These variables were

chosen primarily because they were assumed to control water table elevations, and secondarily the spatial and temporal coverage of these variables matched that of the wet/dry dataset. Like *Turner and Richter* [2011] the linear geospatial representation of the San Pedro River inside SPRNCA from National Hydrography Dataset was used as the base location of the river for all analyses. The linear representation of the San Pedro River was converted to raster format with a per pixel resolution of 10m and during this process a unique identification number was assigned to each river pixel. Converting the linear representation of the San Pedro River into raster format resulted in 10,244 different pixels representing the river. In addition, three new Euclidean distance raster datasets with a resolution of 10m were created using the location of each USGS gauging station inside our study area. These new raster datasets describe the Euclidean distance between the location of each gauging station and any other point inside the study area (Table 1) and they were used to assign streamflow values to each river reach from its closest gauging station.

After pre-processing all explanatory and auxiliary variables, each individual river pixel was used to sample each response and explanatory variables as well as the Euclidean distance rasters using ArcGIS 9.3 “sample” function. The sample function generates a table that shows the pixel value in each different raster dataset (explanatory and auxiliary variables) that coincides with each river’s. The resulting table (input explanatory variable table) contained one column for each sampled raster and one row for each river pixel (10,244 rows in total).

3.4 Logistic Regression

Two steps were needed before the pre-processed explanatory variables were used in the logistic regression. First, the appropriate time period of all the explanatory variables with a temporal component (streamflow, precipitation) was identified. Second, multicollinear explanatory variables were identified and processed accordingly. Once these steps were completed the logistic regression process was completed and followed by an assessment of the regressed model performance.

After importing the input explanatory variable table, the optimal time period for calculating daily average streamflow across the three stations inside the study site was identified (Table 1). This calculation used the average daily streamflow across all three stations followed by the calculation of the 30-day, 60-day and 90-day moving averages of daily streamflow between October 1 and May 1 for each surveyed year. Finally, the correlation coefficient between moving average daily streamflow and the overall percentage of the study site classified as wet was calculated. Similarly, the optimal width and time for calculating total precipitation along the study site was identified by using 30-day, 60-day and 90-day moving integration windows together with a 7-month integration window between July 1st and December 31st. Once the total precipitation values for each integration window were calculated, the correlation coefficients between them and the overall percentage of the study site classified as wet for each surveyed year were then calculated. The integration periods for streamflow and precipitation that had the highest correlation with the overall percentage of the stream classified as wet were then selected as explanatory variables for the logistic regression.

In a logistic regression, multicollinearity between explanatory variables may cause an inflation of the regression coefficient standard error and a miscalculation in the sign and

magnitudes of regression coefficient estimates. Moderate to severe multicollinearity can lead to wrong conclusions about the relationships between the response and explanatory variables [*Belsley et al.*, 1980; *Greene,* 1993]. The Variance Inflation Factor (VIF) is commonly used to identify multicollinear explanatory variables. The VIF was calculated in three steps. First, ordinary linear least square regressions were created that have each explanatory variable as a function of all other explanatory variables, where n is the total number of explanatory variables. Then, for each linear regression the coefficient of determination (r_i^2) was calculated. Finally, the variance inflation factor for each explanatory variable (VIF_i) was calculated using the following relationship:$VIF_i = 1/(1 - r_i^2)$. The multicollinear variables were either removed or combined into a single variable (see 3.1). Once the multicollinear variables were removed or combined into a single variable, a logistic model was created and calibrated using the first 7 years of data (1999-2005) and validated using 6 years of data (2006-2011). Initially the model was created and calibrated using all the explanatory variables identified as not multicollinear and a constant term (full model) with Matlab's [*MathWorks*, 2012] "glmfit" function. A forward stepwise regression approach using the "sequentialfs" function in Matlab [*MathWorks*, 2012]was performed to test if a subset of the initial explanatory variables in the full model ("slimmer" model) has a comparative predictive power to that of the full model. The stepwise regression adds one explanatory variable at a time and checks to see if the addition of that variable significantly decreases the value of a diagnostic function. Here the deviance was used as the diagnostic function so that when an explanatory variable with no significant effect is introduced it reduces the deviance by an amount less

than that of an inverse chi-square (χ^2) distribution with one degree of freedom at 95% confidence or by an amount less than 3.842.

Once the logistic regression model was built and calibrated, the significance of the individual regression coefficients (β_i) was evaluated, the model predicted probabilities were dichotomized using optimal probability value and the model's skill was evaluated by computing model accuracy. The optimal probability value is defined as the threshold probability that maximizes both the true positive rate (TPR or Sensitivity) and the true negative rate (TNR or Specificity). TPR is defined as the ratio of locations correctly predicted wet to the total number of locations observed wet. Conversely, TNR is defined as the ratio of locations correctly predicted as dry to the total number of locations observed dry. The optimal probability value was determined by calculating the sensitivity and specificity for each probability cutoff value, and identifying the cutoff values where sensitivity equals specificity in the calibrated model.

Finally, an assessment of the model goodness of fit to data and its predictive abilities was done and will be presented in the supporting information document accompanying this manuscript (see supporting information).

3.5 Alternate Scenarios

Currently, there is not a hydro-climatological model available to predict changes in stream flow as a function of changes in precipitation and temperature. Therefore, historical streamflow and climatological records were used to generate a series of alternate scenarios to test the effects of hydro-climatological changes in the size and location of river reaches classified as wet by the logistic regression model. The only variables changed across alternate scenarios were streamflow and precipitation because

they were the only temporal variables used in the logistic model. A total of six different scenarios were created and these scenarios were based on the hydrologic (streamflow, USGS) and climatological (precipitation and temperature, VIC model) [*Maurer et al.*, 2002] datasets used in this study. The first scenario is based on zero flow and zero precipitation. The next three scenarios are based on the observed minimum, mean and maximum streamflow and associated precipitation values observed in the study area. The last two scenarios are based on the streamflow and precipitation values for the years with the hottest and coldest winters as recharge mainly occurs in winter [Wahi et al. 2008; Ajami et al. 2012]. Although, streamflow records for one of the stations extends to 1904 only the period of record from 1967 to 2011 was used to ensure that the temporal coverage all of the streamflow gauging stations and precipitation matched.

4 Results

4.1 Logistic Regression

The streamflow and precipitation periods important for predicting wet and dry locations along the river are not the immediate period preceding the survey but periods predating the survey date. The optimal integration window analysis for streamflow and precipitation suggested that a 30-day mean streamflow value for all stations between May 1 and May 30, and a 60-day total precipitation value between August 30 and October 28 had the highest correlation with the overall percentage of the study site classified as wet with r^2 values of 0.7577 and 0.7670, respectively (Figure 2 and Figure 3). Therefore, these two integration windows were used to create the temporal explanatory variables of streamflow and precipitation used in the logistic regression.

The multicollinear analysis showed that most of the VIF values of the initial 17 explanatory variables were between 1.0 and 3.0, with the exception of surface elevation (DEM), Mainstem Flow Accumulation, and streamflow at Charleston, Palominas and Tombstone. The process of removing or combining multicollinear variables resulted in 11 explanatory variables that were initially tested for the logistic regression model. These variables were: 1) Depth to Bedrock, 2) Change in Depth of Bedrock, 3) Slope of Depth of Bedrock, 4) Curvature of Depth of Bedrock, 5) Channel Sinuosity, 6) Floodplain Width, 7) Surface Elevation (LIDAR), 8) Surface Slope (LIDAR), 9) Surface Curvature (LIDAR), 10) Spatially allocated average daily streamflow (May-1 to May-30), and 11)Total Precipitation (Aug-30 to Oct-28). A final verification test showed that the VIF values for this set of 11 final explanatory variables were less than 2.1. There is no specific threshold to determine whether any given explanatory variable is highly multicollinear [*O'Brien*, 2007]. Therefore, the natural groupings of the VIF values were used to select the explanatory variables that had higher multicollinearity relative to rest. Only those explanatory variables that fell outside the initial 1.0 to 3.0 VIF range were further processed to avoid potential multicollinearity issues. First, to avoid multicollinearity issues with surface elevation only LIDAR elevation and its derived products (surface elevation, slope and curvature) were used as explanatory variables since the initial data set contained two sources that described surface elevation (LIDAR and a 30 m DEM). As a consequence the explanatory variables derived from DEM surface elevation (surface slope and surface curvature) were also eliminated from further analyses in the regression analysis. Second, VIF values for Mainstem Flow Accumulation suggested that it was highly multicollinear with one or more of the

remaining explanatory variables. Correlation coefficient values suggested that the high multicollinearity was being caused by a correlation between Mainstem Flow accumulation, depth to bedrock and surface elevation. As a result, Mainstem Flow Accumulation was removed and not used as an explanatory variable. Finally, the potential multicollinearity issues of all three explanatory variables of streamflow was prevented by spatially allocating to each river pixel the streamflow value of its closest gauging station using the Euclidian distance raster for each river pixel.

The initial set of 11 explanatory variables and a constant was used to generate a base logistic regression model (full model). However, a forward stepwise regression analysis identified that a subset of these variables without total precipitation had a similar predictive capability as the full model. Therefore, a final model was calibrated and validated using a constant value and all of the explanatory variables of the full model with the exception of total precipitation to predict streamflow permanence in the San Pedro River (

Table **3**). It is important to note that because of the elimination of total precipitation; spatially allocated average daily streamflow is the only temporal explanatory variable in the logistic regression model.

The Wald's χ^2 statistic with one degree of freedom (

Table **3**) was used to test each individual explanatory variable β value for significance. The Wald's χ^2 statistic showed that all 10 explanatory variables β values and the constant

term used in the saturated regression model are significant predictors of streamflow permanence (

Table **3**). According to the final model the ln(Odds) or $ln(p/(1-p))$ are directly related to sinuosity, surface elevation, spatially allocated mean daily streamflow, change in bedrock depth and curvature of depth to bedrock, and inversely related to depth to bedrock, floodplain width, surface slope, surface curvature and slope of` bedrock (p-value<0.0013). These coefficients were semi-standardized by multiplying them by the variable's standard deviation [*Kaufman,* 1996], thus allowing the determination of the relative importance of each coefficient in determining the predicted probability. The results show that surface elevation, depth to bedrock, spatially allocated streamflow, change in depth to bedrock and curvature of depth to bedrock are the top-five explanatory variables controlling the predicted probability in the logistic regression (

Table **3**).

4.2 Evaluation of the Model's Skill

The analysis for the logistic regression optimal probability value revealed that a cutoff value of 0.5332 maximized both the sensitivity and specificity of the model's dichotomized output (Figure 4). Using this value to dichotomize the model's output and evaluate the logistic regression model skill shows that during the validation period (2006-2011), the logistic regression model is able to correctly predict 80.1-86.7% of the wet/dry locations of the river (

Table **4**) when 52.8% of its wet/dry status (31.5% wet and 21.3% dry) remained constant during calibration. During the validation period the range of sensitivity and specificity were 77.5-92.6% and 73.2-87.2%, with average values of 84.0% and 81.9%, respectively. This indicates that overall the model is marginally better at predicting wet over dry locations in the river. In addition, the logistic regression does not show a particular bias in the prediction accuracy of wet versus dry locations, with wet classification being more accurate than dry classification 3 out of the 6 validation years.

The results show a spatial bias in the prediction errors where the model incorrectly predicts wet conditions in the middle 1/3 of the reach while it incorrectly predicts dry conditions in the upper and lower 1/3 of the reach (Figure 5). In addition, results show that the model predictive skill decreases in regions where the wet/dry conditions were not constant during the calibration period (i.e. gray regions coinciding with green regions, Figure 5). These regions account for 42.39% or 4,342 pixels out of all the pixels representing the river in the study site (10,244). In these regions during the validation period of 2006 to 2011, the model on average correctly predicted the wet dry status 70.5% of the time (SD=4.17%, min=65.7% and max= 76.3%). On the other hand, in regions where the wet/dry conditions were constant during calibration the model on average correctly predicted the wet/dry status 92.1% of the time (SD=1.92%, min=89.4% and max=94.3%) during the validation period of 2006 to 2011.

4.3 Alternate Scenarios

The alternate scenario analysis evaluated six different scenarios in the calibrated logistic regression model to assess the effects of changes in the amounts of streamflow on the size, and location of river reaches classified as wet by the logistic regression model.

Streamflow was the only explanatory variable that changed for each scenario used in this analysis (Table 5).

The results of the alternate scenario analysis showed that the total number of elements predicted wet are directly proportional to the average streamflow value used in each scenario to predict the river wet/dry status. This result was expected since the regression coefficient for streamflow is positive. The percentage of the elements in the study area classified as wet are 42.5%, 48.6%, 63.7%, 88.9%, 78.8% and 50.4% for scenarios A to F, respectively. The scenario with the smallest fraction of the study site classified as wet was the scenario of zero streamflow (scenario A, Figure 6) while the largest fraction of the study site classified as wet was associated with the scenario of maximum observed flow (scenario D, Figure 6). Increasing streamflow values from the zero flow scenario (scenario A) resulted in a northward expansion of the region predicted as wet (Figure 6). However, the region predicted wet did not expand upstream with increases in streamflow with the exception of the scenario of maximum observed flow (scenario D, Figure 6).

5 Discussion

5.1 The Predictive Capabilities of the Explanatory Variables and their Hydrologic Implications

In the San Pedro River, initial analysis suggested a positive and significant correlation between the overall extent of river recorded wet, daily average streamflow (May-1 and May-30) and mean total precipitation (Aug-30 to Oct-28) (Figure 2 and Figure 3). However, along the San Pedro River for any given year these two variables and their correlation with the extent of river recorded wet can only be used to predict the overall

fraction of the river classified as wet and not the particular locations of wet reaches. In groundwater-fed river systems like the San Pedro River researchers have shown that streamflow permanence is primarily controlled by factors that affect the height of the groundwater table relative to the streambed [*Brutsaert*, 2005; *Hedman and Osterkamp*, 1982; *Meinzer*, 1923; *Price*, 2011].

The results of this work demonstrate that a logistic regression model can be used to predict streamflow permanence of the San Pedro River in SPRNCA by using explanatory variables that directly or indirectly affect groundwater heights relative to the streambed. Specifically, this study shows that a logistic regression model utilizing 10 (

Table 3) out of the initial 17 explanatory variables (Table 1) are significant ($p<0.002$) predictors of streamflow permanence in the San Pedro River. Using those 10 explanatory variables and the optimal probability cutoff value (0.5332) the model is able to reasonably predict streamflow permanence of the San Pedro River in SPRNCA with an accuracy ranging from 80-87% (
Table **4**).

According to the logistic regression, there are 10 explanatory variables that are significant predictors of streamflow permanence (

Table 3). These variables can be divided into four classes and ranked by their average relative importance. These classes are: (1) the variable that describes streamflow (spatially allocated streamflow) with an average rank of 3, (2) variables that describe elevation and shape of bedrock (bedrock elevation, change in bedrock elevation, slope of

bedrock elevation, and curvature of bedrock elevation) with an average rank of 4.8, 3) variables that describe the shape of the floodplain channel (floodplain width and sinuosity) with an average rank of 6.5, and (4) variables that describe the elevation and shape of the land surface (surface elevation, surface slope and surface curvature) with an average rank of 6.7.

The results show that streamflow was the most important explanatory variable in predicting streamflow permanence and that higher streamflow values will lead to larger fractions of river identified as wet. This implies that in a groundwater dominated system like the San Pedro River [Thomas and Pool, 2006], streamflow not only describes the amount (magnitude) of water currently in the river but it serves as an indicator of the amount of water in the SA system. Interestingly, the analysis shows that timing is important, with streamflow 1.5 months before the survey best explaining streamflow permanence. This timing coincides with the onset of high evapotranspiration demands, caused by increasing temperatures, during the month of May. This streamflow-time relationship may imply that not only is the amount of water in the system important but the amount of water before increased ET withdrawals from the SA system with the onset of high temperatures and low humidity in June.

The second most important set of explanatory variables in predicting streamflow permanence is the variables that describe the elevation and shape of bedrock aquifer contact. When grouped together, these variables describe the shape and thickness of the aquifer system beneath the river. The results suggest that locations in the river with a thin aquifer, whose lower boundary gradually slopes upward as you move downstream and whose surface is concave up are more likely to be wet. These results imply that the

interactivity between the stream and its aquifer play an important role in streamflow permanence. In other words, with all other things being equal a vertically thinner and restricted aquifer is better able to stay saturated and connected to the stream.

The variables that describe the floodplain width and the sinuosity of the river are the third most important set of explanatory variables in predicting streamflow permanence. These variables of channel morphology and the results show that sections of river with a thinner and more sinuous floodplain are more likely to remain wet. The fact that these two morphological variables are important may imply that they serve as an indicator of riparian aquifer interactions, shallow aquifers (bedrock outcroppings), and/or the reach type (pool-run-riffle sequences). In the San Pedro River a more narrow and sinuous channel may enhance the lateral movement and storage of water from the stream to the riparian aquifer during periods of elevated streamflow. Once streamflow starts to decrease during the start of summer the stored water slowly returns to the river thus sustaining streamflow permanence. In addition, more narrow and sinuous channels in the San Pedro River are often associated with channel constriction due to bedrock outcroppings, which implies that channel morphology serves as an indicator of aquifer shape and thickness. Finally, sections of the San Pedro River with narrow floodplains and more sinuous profiles tend to describe sections of the river with pool-like characteristics. These sections are often the last parts of a river to lose surface water presence [Stanley et al 1997].

The final most important set of explanatory variables in predicting streamflow permanence are the variables that describe surface elevation. In other words, these variables describe the shape and form of the stream surface. The results suggest, that

stream locations with higher elevations, shallower slopes and with downward concavity are more likely to be wet. It is important to note that although this set of explanatory variables average rank is fourth, surface elevation actually is the single most important variable in the regression analysis with the other two (surface slope and surface concavity) ranking ninth and tenth. These results could be interpreted to imply that shape and form of the stream play a role in streamflow permanence similar to the channel morphology (discussed above). However, the large difference in ranks between each of the set members and the fact that surface elevation generally decreases as downstream distance increases may suggest that surface elevation acts like a positional variable rather than a geomorphological variable.

There are several steps that could be taken to increase logistic regression predictive model's skill. According to the regression analysis the explanatory variables that describe streamflow and the shape and thickness of the aquifer have high relative importance. However, the dataset from which these explanatory variables were derived has a coarse spatial resolution. For example, streamflow values for the entire study site were derived from three USGS stream gauging stations while depth to bedrock data was derived from a dataset with a spatial resolution of 1 km by 1km. In comparison, the logistic regression model predictions are based on a resolution of 10 m by 10m. This result suggests a more robust and higher resolution representation of surface flows and subsurface bedrock topography might increase the skill of the predictive model. Finally, it would be desirable to have a seasonal mapping of streamflow permanence to better fine-tune the small scale changes in wet/dry patterns and to test if the patterns and

relationships identified in this research hold true if the wet/dry mapping was performed during a different season (winter/wetter vs summer/dryer).

5.2 Alternate scenarios

The alternate scenario analysis together with the logistic regression model of the San Pedro River in SPRNCA show that the number and location of elements predicted as wet increase with increased average late spring streamflow value used in each scenario. This result was expected due to the fact that the coefficient of streamflow in the regression was positive and that streamflow was the only temporal explanatory variable in the regression. In addition, the results show that the expansion and contraction of the wet river segments is centered on an area that the yearly surveys suggest is mostly perennial. This area coincides with a region in the San Pedro River where the bedrock nears the surface resulting in decreased aquifer thickness.

The expansion and contraction of wet river segments due to changes in the amount of late spring streamflow and the relative importance of this explanatory variable in streamflow permanence implies that any anthropogenic or climatic changes that lead to lower baseflow discharges during this period may result in a more fragmented river and riparian ecosystem. In general, projecting into the future the effects of anthropogenic changes and climate change is not simple due to lack of consensus, information and/or large uncertainties. However, there is a current consensus about how the groundwater levels near the San Pedro River are threatened by an expanding cone of depression caused by groundwater withdrawals to the east of the river in the Fort Huachuca and Sierra Vista groundwater wellfields [*Gungle et al.*, 2016; *ADWR*, 2009]. The declining groundwater levels and the expansion of the cone of depression have been noted since the

1970's [*Gungle et al.*, 2016] and data has demonstrated that the cone of depression developing below Sierra Vista has expanded and deepened and it has altered the pre-development groundwater flow direction [*ADWR*, 2009]. *Gungle et al.* (2016) calculated a water-budget for the Sierra Vista Watershed, which contains roughly 3/4th of our study site, and estimated that the watershed in 2002 and 2012 was being overdrawn by 10200 and 5000 acre-feet, respectively. However, the change in the groundwater flow direction below the Sierra Vista and Fort Huachuca wellfields and the imbalance in the water-budget have not yet had a significant effect on the vertical hydraulic gradients near the stream or the lengths of wet reaches closest to the cone of depression [*Gungle et al.*, 2016].

If current withdrawals rates continue unchanged or even if they were to stop completely, this cone will eventually expand and intersect the river resulting in the aquifer capturing streamflow from the river (reversal of stream-aquifer flow) [*Barlow and Leake*, 2012]. The aquifer's baseflow discharge to the river will decrease when the cone of depression starts to capture streamflow. This will lead to a higher fraction of the river being observed as dry. That event is contingent on the idea that no actions will be made to stop the progression of the cone of depression or that natural or artificial recharge rates to the aquifer will either stay constant or decrease. The upper San Pedro watershed contains two facilities that recharge effluent to the aquifer, the City of Sierra Vista Underground Storage Facility (USF# 73-583024) and the Fort Huachuca Recharge faculty [*ADWR*, 2009]. Estimates show that these facilities recharged a combined total of 1300 and 3000 acre-ft of treated effluent water back into the Upper San Pedro River watershed in 2002 and 2012, respectively [*Gungle et al.*, 2016]. Although the amount of

artificial recharge more than doubled between the years 2002 and 2012, as it was mentioned earlier the water-budget for the Sierra Vista watershed was still in deficit. In fact, artificial recharge of treated effluent water in 2012 would have had to be to more than 8000 acre-feet in order to reach a balance in the watershed. This would mean artificially recharging more than 66.1% of the water pumped for rural, municipal and industrial uses [*Gungle et al.,* 2016].

5.3 Implications

One of the most important results derived from the data pre-processing and logistic regression analysis is the finding that a late spring 30-day integration window for average streamflow (May 1st to May 30th) in the San Pedro river had the most correlation with streamflow permanence and that it was a significant explanatory variable of streamflow permanence in a logistic regression. This result is important because it suggests that both the timing and magnitude of the streamflow as a proxy for streamflow permanence is important. For example, if the integration window were to be shifted towards the winter flow period it would imply that the hydrologic state of the basin and aquifer (supply) dictates streamflow permanence. This response would be caused by the fact that during this time period, riparian evapotranspiration demand is minimal, allowing for a recovery of near-stream groundwater levels [*Leenhouts et al.,* 2005]. On the other hand, if the period of highest correlation was shifted toward mid to late summer flow period it would imply that the riparian evapotranspiration demand dictates streamflow permanence because this period has the highest ET demand and lowest groundwater levels in the San Pedro River[*Leenhouts et al.,* 2005]. Therefore, the fact that late spring flows are the most correlated with streamflow permanence and that they are a significant predictor of

streamflow permanence implies that it is the interaction of both the hydrologic condition of the basin and the demands of the riparian vegetation that dictates streamflow permanence in the San Pedro River. These results suggest that vegetation plays an important role in the dynamics of streamflow permanence. Unfortunately, the results of this study do not allow for the determination of the magnitude of this influence on streamflow permanence.

The timing and amounts of precipitation in the San Pedro River basin could also vary due to climate change. However, there is a lack of consensus about the direction and magnitude of that change. [*Dixon et al.*, 2009] summarizes the current scientific consensus of why projecting the influence of climate change in rivers like the San Pedro is complicated. First, there is a large uncertainty in the magnitude, seasonality and direction of changes in precipitation even though temperatures are projected to increase. Second, climatic drivers in the region (North American Monsoon, orographic effects and multi-year atmospheric-oceanic tele-connections) are not well represented in current climate models [*Grimm et al.,* 1997; *Sheppard et al.,* 2002]. Lastly, the large scale heterogeneities in topography and rainfall generating storm events together with gradients in the seasonality of rainfall and its magnitude imply that the effects of climate change will not be uniform across the region [*Grimm and Fisher*, 1992]. *Dixon et al.*, [2009] generated a series of predictions based on several climatic scenarios, ranging from no change in climate to a warmer wetter climate with increases in precipitation. Their analyses showed that warming alone has little to no effects on the seasonality, frequency and magnitude of winter floods, but noted that changes in winter precipitation do lead to significant changes in those same parameters. In general, [*Dixon et al.*, 2009] observed

that, increases in winter precipitation would lead to increase frequency of winter floods, increase magnitude of floods and increased total discharge. In the case of a warm dry climate scenario [*Dixon et al.,* 2009] suggests that a reduction in winter precipitation would lead to a progressive elimination of winter floods. Recent modeling work has shown that yearly average precipitation in the semi-arid Southwest will slightly decrease towards the second quarter of this century (2031-2050) but then it is projected to increase during the last 30 years of this century (2071-2100) [*Niraula et al.,* 2017a]. Making use of Land-Surface Models and climatic predictions, modeling research has shown that the above referenced change in average yearly precipitation will be associated with a reduction in aquifer recharge through the end this century (2100) [*Niraula et al.,* 2017a; *Niraula et al.,* 2017b; *Serrat-Capdevila et al.,* 2007]. The apparent contradiction of more precipitation but less recharge is due to type and timing of recharge. In the San Pedro River, mountain system recharge (MSR) accounts for 60% of the total recharge to the aquifer [*Meixner et al.,* 2016]. In addition, MSR is more dependent on winter precipitation and temperatures [*Ajami et al.,* 2012]. The overall increase in temperatures and reduction in aquifer recharge would result in smaller late spring baseflow and higher evapotranspiration demands implying more sections could be observed as dry.

This study does not represent the first time streamflow permanence has been related to geomorphologic variables. [*Leenhouts et al.,* 2005], created a series of river reach classes inside SPRNCA based on streamflow permanence, floodplain channel width, and channel sinuosity. However, the association between geomorphology and streamflow permanence was based only on a single wet/dry survey year (2002) and it was used to study the relationship between water demand, water availability, water source and

riparian vegetation functioning in the San Pedro River and not to predict streamflow permanence. Besides highlighting the importance of geomorphic and hydrologic variables, our study highlights how increases in late spring streamflow lead to a northward expansion (or decreases of late spring streamflow lead to a southward contraction) of river reaches classified as wet and that this expansion/contraction is centered on an area that yearly surveys suggest is mostly perennial. These results suggest that with an overall increase in baseflow to the stream, dry locations are more likely to become wet if they have upstream reaches that are wet. This implies that under a scenario of increasing river discharge intermittently-wet sections will become perennial first when compared to more intermittently-dry sections

In semi-arid river systems like the San Pedro River the contraction of wet river reaches is concentrated on sections that have a higher susceptibility for drying caused by river flow structures, hydrologic conditions, geologic setting, and geomorphic features which varies in time and space [*Stanley et al.,* 1997]. In other river systems, Godsey and Kirchner [2011] proposed that the locations where the streambed starts drying or wetting indicates a balance between upstream inputs, downstream outputs and SA exchanges. Therefore, wet river reaches could serve to quickly identify locations in the river that are actively interacting with the riparian or basin aquifers. Simple water balance dictates that these interactions would range from upward interaction (groundwater discharge) at the head of a wet reach to downward interaction (groundwater recharge) at the end of a wet reach. The identification of these locations and interactions are significant because research has shown that they are biogeochemical hotspots and drivers of nutrient cycling

in the stream and hyporheic zone [*Dent and Grimm*, 1999; *Dent et al.*, 2001; *Holmes et al.*, 1994; *Jones et al.*, 1995a; *Jones et al.*, 1995b; *Meixner et al.*, 2012].

Streamflow permanence, drying events and the expansion and contraction of wet river reaches have important biological implications to the macroinvertebrate and plant communities of the stream ecosystem. Streamflow permanence or more specifically, drying event conditions have been shown cause declines in macroinvertebrate biodiversity (alpha-diversity) in streams [*Datry et al.*, 2014; *Wood and Armitage*, 2004], act as ecological biodiversity filters of macroinvertebrates [*Bogan and Lytle*, 2011; *Leigh and Datry*, 2017] and be a strong primary determining factor of macroinvertebrate biodiversity (alpha-diversity) [*Leigh and Datry*, 2017]. This implies that a transition to a more intermittent San Pedro River would result in lower biodiversity of macro invertebrates and create strong barriers to the reestablishment of communities in dry areas as they wet-up. In the San Pedro River, [*Stromberg et al.*, 2005] described a spatial and temporal relationship between streamflow permanence and the composition and response of streamside herbaceous cover. Specifically, she observed spatial and temporal gradients of hydric, mesic and xeric plant communities following the river degree of flow and intermittency, with hydric and mesic plant communities decreasing with increased intermittency and decreased flow rates. The implications of this result are important to successful river restoration efforts in ground-water dominated river systems. In the San Pedro River [*Katz et al.*, 2009], identified streamflow as a key factor controlling herbaceous plant communities and on positive outcome of riverine restoration efforts (i.e. hydrologic and vegetation conditions of the restored sites matches those of a perennial reference site). Her results show that restoration efforts on one of the two sites were not

successful but more importantly the failed restoration site was upstream of perennially wet reach whereas the successful restoration site was downstream of a perennial wet reach. Integrating the results of [*Katz et al.*, 2009] and those of this study suggest that hydric and mesic plant communities would then expand or contract following the downstream expansion and contraction of wet river reaches.

6 Conclusion

In this study the logistic regression analysis was used to investigate which physical, spatial and temporal properties of the San Pedro River influence streamflow permanence, how sensitive is streamflow permanence to streamflow changes and what do the results suggest about the underlying processes controlling streamflow permanence. This study shows that a logistic regression using ten (10) hydrologic and geomorphic explanatory variables can be used to predict streamflow permanence on the San Pedro River National Conservation Area. The resulting predictive model was able to correctly predict 80.1-86.7% of the wet/dry locations of the study site during the validation period of 2006 to 2011 at a resolution of 10 meters. According to the logistic regression analysis, late spring streamflow as well as variables that describe bedrock elevation, variables that describe the shape and width of the floodplain and variables that describe the land surface elevation are significant predictors of streamflow permanence in the San Pedro River. In addition, the logistic regression showed that an increase in late spring streamflow lead to a downstream expansion of the wet segments of the river centered on areas that are perennial. Finally, the explanatory variables in the predictive model directly or indirectly describe: the surface-groundwater-vegetation interaction of late spring baseflow, the

shape and thickness of the aquifer underlying the river, the channel morphology and how it varies along the river, and the shape and form of the stream surface.

The findings of this study highlight a predictive relationship between streamflow permanence and several hydro-geomorphic factors. With these relationships several key processes controlling streamflow permanence can be suggested. Although not part of this study's objectives, the available data and current physical understanding prevent the authors from proposing the processes controlling streamflow permanence. In its simplest form streamflow permanence is controlled by the imbalance between inputs and outputs of water to the stream, the hydraulic transport properties of the streambed and its aquifer (Godsey and Kirchner, 2011). Therefore, future studies should focus on investigating these process-level controls and how they are affected by the hydro-geomorphic factors identified in this study.

7 Acknowledgments

"LIDAR data were provided by the USDA-ARS, Tucson, AZ, and the University of Florida with funding assistance from the EPA, and the U.S. Dept. of Defense Legacy Program. Processing of the LIDAR data was done by M. Durcik and A. Farid while supported by SAHRA (Sustainability of semi-Arid Hydrology and Riparian Areas) under the STC Program of the National Science Foundation, Agreement No. EAR-9876800." Additional support was provided by NSF –EAR 1038938.

8 References

Arizona Department of Water Resources (ADWR). 2009. Arizona Water Atlas: Southeastern, Arizona Planning Area. Volume 3.

Ajami, H., T. Meixner, F. Dominguez, J. Hogan, and T. Maddock III (2012), Seasonalizing Mountain System Recharge in Semi-Arid Basins-Climate Change Impacts, *Ground Water, 50*, 585-597.

Aldrich, J. H., and F. D. Nelson (1984), Linear Probability, Logit, and Probit Models, Sage Publications, Beverly Hills.

Barlow, P.M., and Leake, S.A., 2012, Streamflow depletion by wells—Understanding and managing the effects of groundwater pumping on streamflow: U.S. Geological Survey Circular 1376, 84 p.

Belsley, D. A., E. Kuh , and R. E. Welsch (1980), *Regression Diagnostics : Identifying Influential Data and Sources of Collinearity*, Wiley, New York.

Brinson, M. M., National Water Resources Analysis Group (U.S.), Eastern Energy and Land Use Team., and U.S. Fish and Wildlife Service. (1981), Riparian Ecosystems : Their Ecology and Status, Eastern Energy and Land Use Team [and] National Water Resources Analysis Group, U.S. Fish and Wildlife Service, Kearneysville, W. Va.

Bogan, M. T. and D. A. Lytle (2011), Severe drought drives novel community trajectories in desert stream pools, *Freshwat. Biol., 56*, 2070-2081.

Brutsaert, W., (2005), Hydrology : An Introduction, Cambridge University Press, Cambridge; New York.

Datry, T., S. T. Larned, K. M. Fritz, M. T. Bogan, P. J. Wood, E. I. Meyer, and A. N. Santos (2014), Broad-scale patterns of invertebrate richness and community composition in temporary rivers: effects of flow intermittence, *Ecography, 37*, 94-104.

Dent, C. L. and N. B. Grimm (1999), Spatial heterogeneity of stream water nutrient concentrations over successional time, *Ecology, 80*, 2283-2298.

Dent, C. L., N. B. Grimm, and S. G. Fisher (2001), Multiscale effects of surface-subsurface exchange on stream water nutrient concentrations, *J. N. Am. Benthol. Soc., 20*, 162-181.

Dixon, M. D., J. C. Stromberg, J. T. Price, H. Galbraith, A. K. Fremier, and E. W. Larsen (2009), Potential effects of climate change on the upper San Pedro riparian ecosystem, in *Ecology and Conservation of the San Pedro River*, edited by J. C. Stromberg and B. Tellman, University of Arizona Press, Tucson.

Gettings, M. E. and B. B. Houser (2000), Depth to bedrock in the Upper San Pedro Valley, Cochise County, southeastern Arizona, *U. S. Geological Survey Open-File Report, 00-138, Version 1.0*.

Godsey, S., J.W. Kirchner (2011), Dynamic, discontinuous stream networks and their sensitivity to climate change *(Invited),* Abstract H53P-02 presented at 2011 Fall Meeting, AGU, San Francisco, Calif., 5-9 Dec.

Gomez, R., M. Isabel Arce, J. Javier Sanchez, and M. del Mar Sanchez-Montoya (2012), The effects of drying on sediment nitrogen content in a Mediterranean intermittent stream: a microcosms study, Hydrobiologia, 679, 43-59.

Greene, W. H., (1993), *Econometric Analysis*, Prentice Hall, Englewood Cliffs, NJ.

Grimm, N. B., A. Chacon, C. N. Dahm, S. W. Hostetler, O. T. Lind, P. L. Starkweather, and W. W. Wurtsbaugh (1997), Sensitivity of aquatic ecosystems to climatic and anthropogenic changes: The Basin and Range, American Southwest and Mexico, *Hydrol. Process., 11*, 1023-1041.

Grimm, N. B. and S. G. Fisher (1992), *Responses of Arid-Land Streams to Changing Climate*, 233 pp.

Gungle, B., J. B. Callegary, N. V. Paretti, J. R. Kennedy, C. J. Eastoe, D. S. Turner, J. E. Dickinson, L. R. Levick, and Z. P. Sugg (2016), Hydrological conditions and evaluation of sustainable groundwater use in the Sierra Vista Subwatershed, Upper San Pedro Basin, southeastern Arizona, Scientific Investigations Report, 106.

Hedman, E. R. and W. R. Osterkamp (1982), Streamflow characteristics related to channel geometry of streams in western United States, USGS Water Supply Paper, 2193.

Holmes, R. M., S. G. Fisher, and N. B. Grimm (1994), Parafluvial nitrogen dynamics in a desert stream ecosystem, J. N. Am. Benthol. Soc., 13, 468-478.

Hosmer, D. W. and S. Lemeshow (2000), Applied Logistic Regression, 397 pp., Wiley.

Jones, J. B.,Jr, S. G. Fisher, and N. B. Grimm (1995a), Nitrification in the hyporheic zone of a desert stream ecosystem, *J. N. Am. Benthol. Soc., 14*, 249-258.

Jones, J. B.,Jr, S. G. Fisher, and N. B. Grimm (1995b), Vertical hydrologic exchange and ecosystem metabolism in a Sonoran Desert stream, *Ecology, 76*, 942-952.

Katz, G. L., J. C. Stromberg, and M. W. Denslow (2009), Streamside herbaceous vegetation response to hydrologic restoration on the San Pedro River, Arizona, *Ecohydrology, 2*, 213-225.

Kaufman, R. (1996), Comparing effects in dichotomous logistic regression: A variety of standardized coefficients, Soc. Sci. Q., 77, 90-109.

Leenhouts, J. M., J. C. Stromberg, and R. L. Scott (2005), Hydrologic Requirements of and Consumptive Ground-Water Use by Riparian Vegetation along the San Pedro River, Arizona, *U. S. Geological Survey Scientific Investigations Report, 2005-5163*.

Leigh, C. and T. Datry (2017), Drying as a primary hydrological determinant of biodiversity in river systems: a broad-scale analysis, *Ecography, 40*, 487-499.

MathWorks (2012), MATLAB, *R2012a*.

Maurer, E., A. Wood, J. Adam, D. Lettenmaier, and B. Nijssen (2002), A long-term hydrologically based dataset of land surface fluxes and states for the conterminous United States, *J. Clim., 15*, 3237-3251.

Meinzer, O. E. (1923), Outline of ground-water hydrology, with definitions, Geological Survey Water Supply Paper, 494, 71.

Meixner, T., P. Brooks, J. Hogan, C. Soto, and S. Simpson (2012), Carbon and Nitrogen Export from Semiarid Uplands to Perennial Rivers: Connections and Missing Links, San Pedro River, Arizona, USA, *Geography Compass, 6*, 546-559.

Meixner, T. et al. (2016), Implications of projected climate change for groundwater recharge in the western United States, *Journal of Hydrology, 534*, 124-138.

Naiman, R., H. Decamps, and M. Pollock (1993), The Role of Riparian Corridors in Maintaining Regional Biodiversity, Ecol. Appl., 3, 209-212.

Nerlove, M., and S. J. Press (1973), Univariate and Multivariate Log-Linear and Logistic Models, Rand Corp., Santa Monica, Calif.

Niraula, R., T. Meixner, F. Dominguez, N. Bhattarai, M. Rodell, H. Ajami, D. Gochis, and C. Castro (2017a), How Might Recharge Change Under Projected Climate Change in the Western US?, *Geophys. Res. Lett., 44*, 10407-10418.

Niraula, R., T. Meixner, H. Ajami, M. Rodell, D. Gochis, and C. L. Castro (2017b), Comparing potential recharge estimates from three Land Surface Models across the western US, *Journal of Hydrology, 545*, 410-423.

O'Brien, R. M. (2007), A caution regarding rules of thumb for variance inflation factors, *Qual. Quant., 41*, 673-690.

Patten, D. (1998), Riparian ecosystems of semi-arid North America: Diversity and human impacts, Wetlands, 18, 498-512.

Pool, D. R. and A. L. Coes (1999), Hydrogeologic investigations of the Sierra Vista subwatershed of the Upper San Pedro Basin, Cochise County, southeast Arizona: Water Resources Investigation Report, 99-4197, 41 p.

Price, K. (2011), Effects of watershed topography, soils, land use, and climate on baseflow hydrology in humid regions: A review, Prog. Phys. Geogr., 35, 465-492.

Serrat-Capdevila, A., J. B. Valdés, J. G. Pérez, K. Baird, L. J. Mata, and T. Maddock (2007), Modeling climate change impacts – and uncertainty – on the hydrology of a riparian system: The San Pedro Basin (Arizona/Sonora), *Journal of Hydrology, 347*(1), 48-66.

Sheppard, P., A. Comrie, G. Packin, K. Angersbach, and M. Hughes (2002), The climate of the US Southwest, *Clim. Res., 21*, 219-238.

Skagen, S. K., C. P. Melcher, W. H. Howe, and F. L. Knopf (1998), Comparative Use of Riparian Corridors and Oases by Migrating Birds in Southeast Arizona, Conserv. Biol., 12, 896-909.

Sponseller, R. A., N. B. Grimm, A. J. Boulton, and J. L. Sabo (2010), Responses of macroinvertebrate communities to long-term flow variability in a Sonoran Desert stream, Global Change Biol., 16, 2891-2900.

Stanley, E. H., S. G. Fisher, and N. B. Grimm (1997), Ecosystem expansion and contraction in streams, Bioscience, 47, 427-435.

Stanley, E., S. Fisher, and J. Jones (2004), Effects of water loss on primary production: A landscape-scale model, Aquat. Sci., 66, 130-138.

Stromberg, J. C., K. J. Bagstad, J. M. Leenhouts, S. J. Lite, and E. Makings (2005), Effects of stream flow intermittency on riparian vegetation of a semiarid region river (San Pedro River, Arizona), River Research and Applications, 21, 925-938.

Stromberg, J. C., S. J. Lite, and M. D. Dixon (2010), Effects of Stream Flow Patterns on Riparian Vegetation of a Semiarid River: Implications for a Changing Climate, River Res. Appl., 26, 712-729.

Thomas, D. S. G. (Ed.) (1989), Arid Zone Geomorphology, Belhaven Press ; Halsted Press, London; New York.

Turner, D. S. and H. E. Richter (2011), Wet/Dry Mapping: Using Citizen Scientists to Monitor the Extent of Perennial Surface Flow in Dryland Regions, Environ. Manage., 47, 497-505.

Wahi, A. K., J. F. Hogan, B. Ekwurzel, M. N. Baillie, and C. J. Eastoe (2008), Geochemical quantification of semiarid mountain recharge, Ground Water, 46, 414-425.

Wood, P. and P. Armitage (2004), The response of the macroinvertebrate community to low-flow variability and supra-seasonal drought within a groundwater dominated stream, *Arch. Hydrobiol., 161*, 1-20.

9 List of Figures

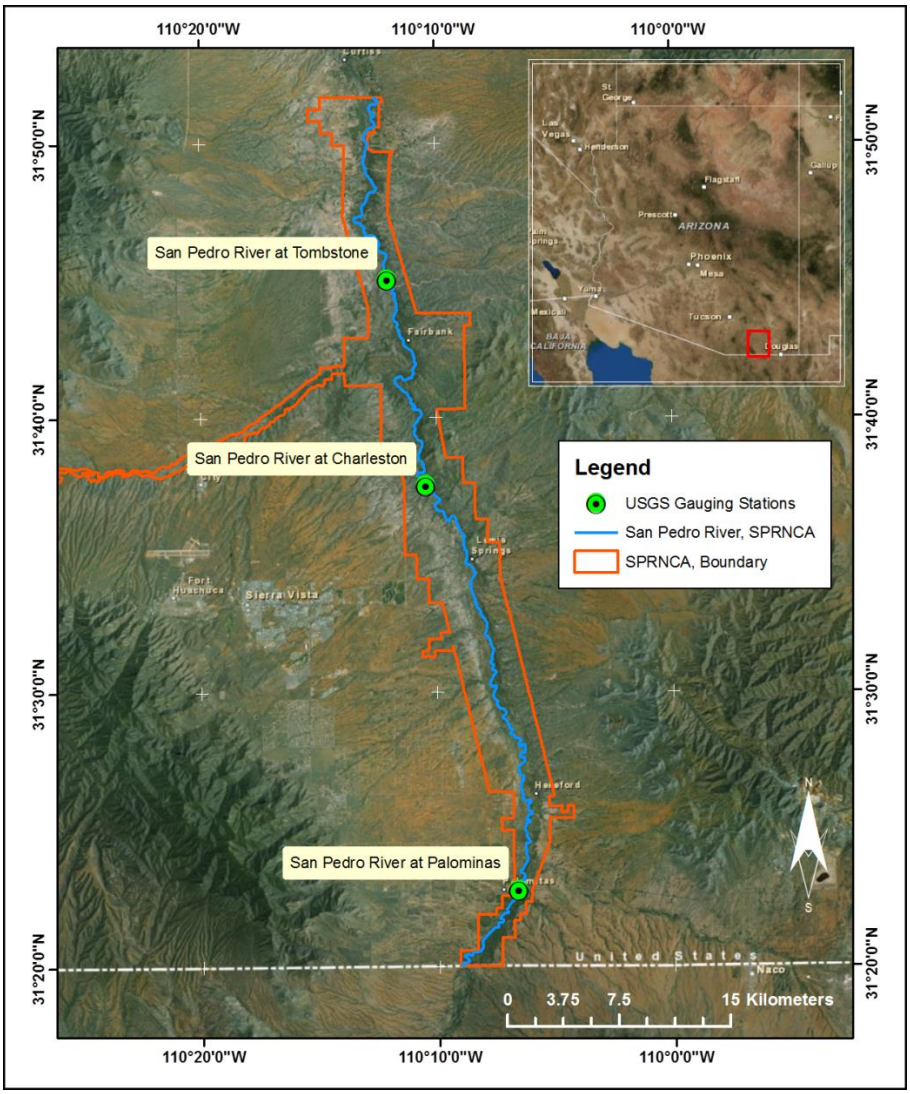

Figure 1: Map of study site showing the San Pedro River inside the SPRNCA boundary.

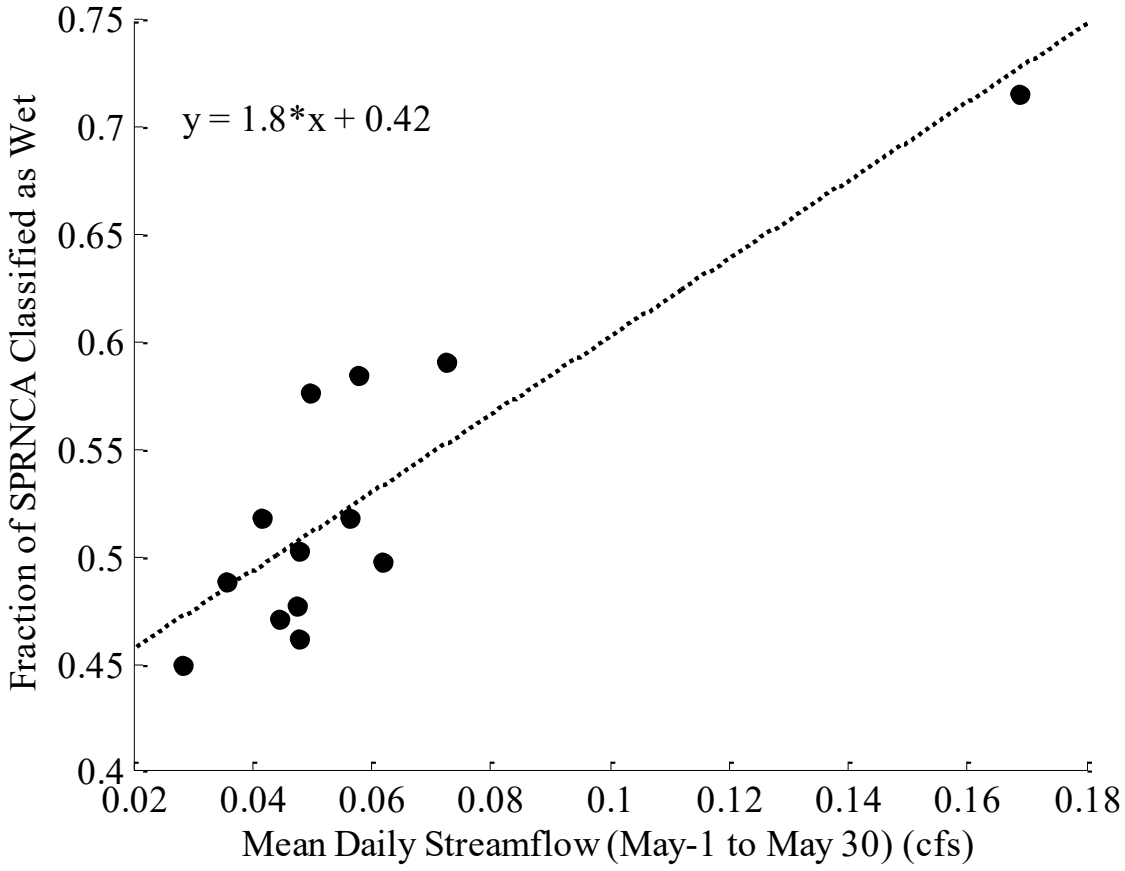

Figure 2: Wetted fraction of SPRNCA as a function of the mean daily discharge for the gauging station in Palominas, Charleston and Tombstone (May, 1999-2011). P-value<0.001, r^2=0.7577

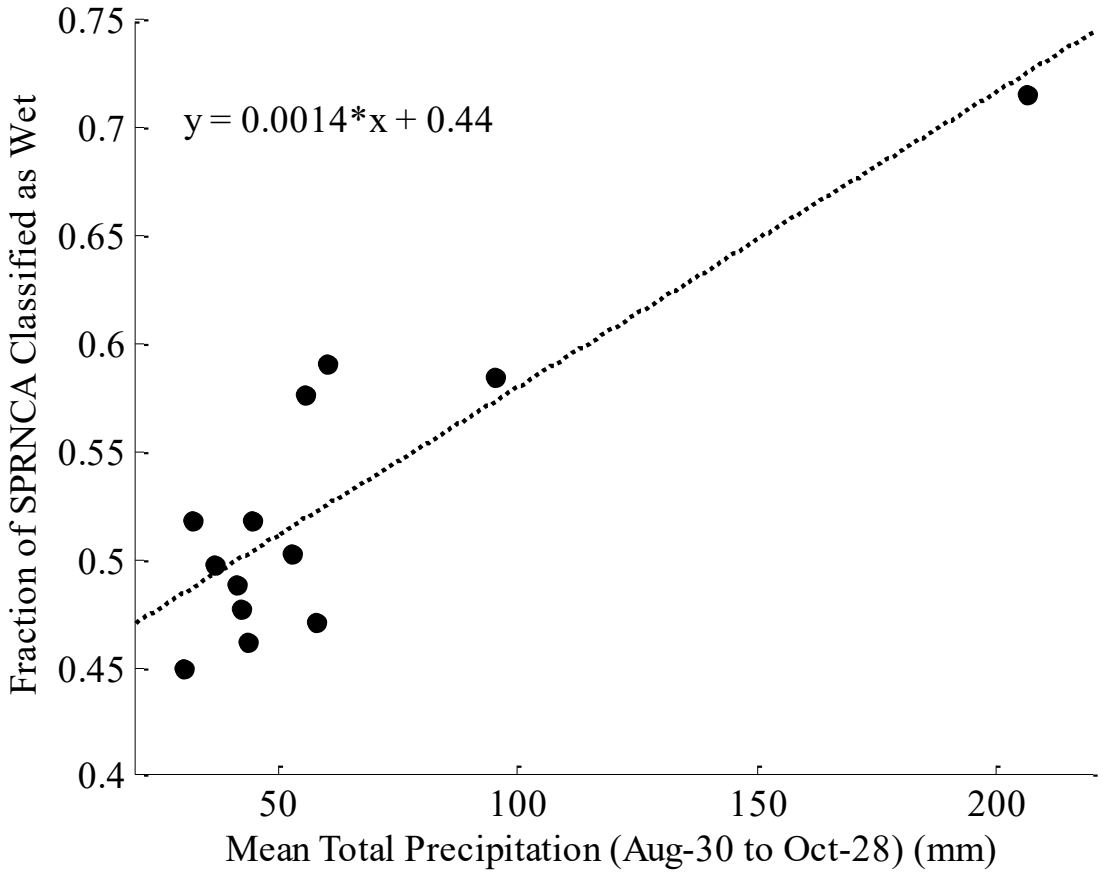

Figure 3: Wetted fraction of SPRNCA as a function of mean total precipitation (1999-2011?). P-value<0.001, r^2=0.7620

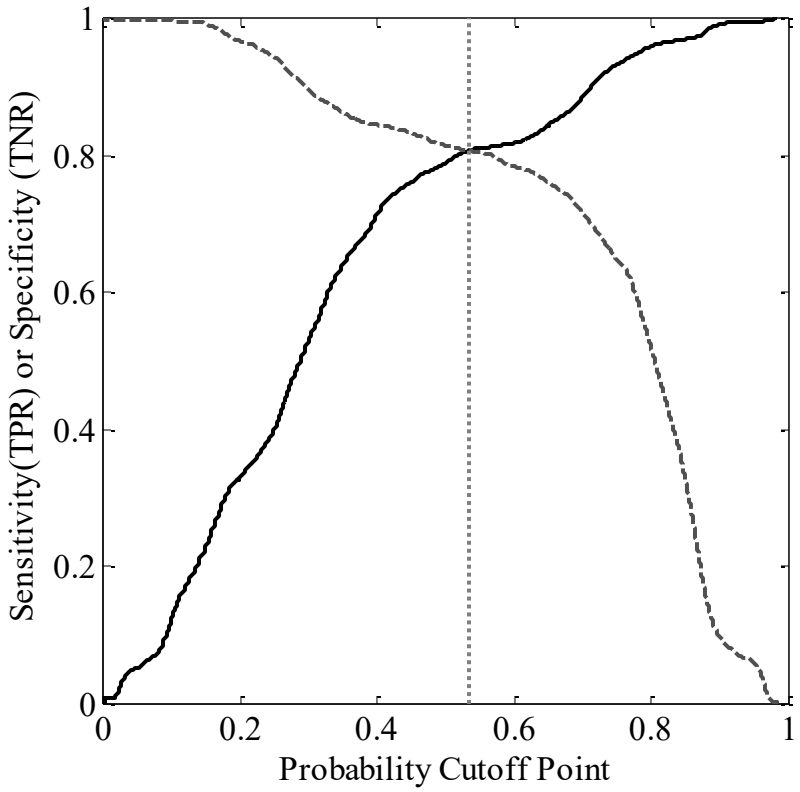

Figure 4: Plot of Sensitivity (dark solid line) and Specificity (light dashed line) as a function of the probability cutoff value used to classify wet/dry location. The vertical dotted line represents the optimal probability cutoff value (0.5332) where both sensitivity and specificity are equal and thus maximized.

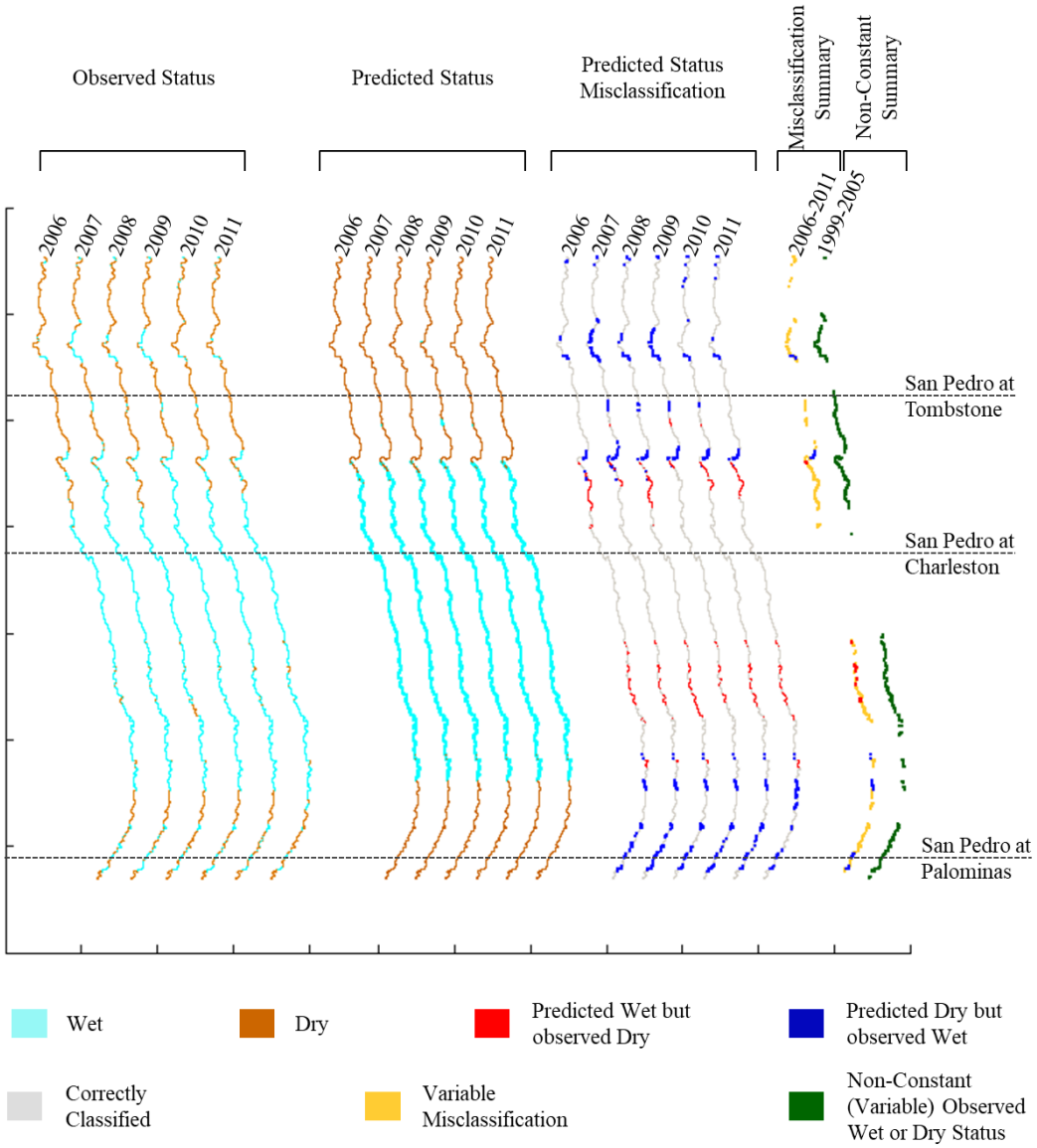

Figure 5: A graphical representation of the predictive capabilities of the San Pedro River Wet/Dry logistic regression model for the validation period of 2006-20011. The first set of six river traces represent the observed wet/dry statues for the validation period,. The second set represents the model prediction for the validation period while the thrid set of six river traces represent the model misclassification for the same period. The first river trace of the fourth set represents the combination of the predicted status misclassification for 2006-2011. The final trace represent the locations were the river wet/dry status was not constant during the calibration period of 1999-2005.

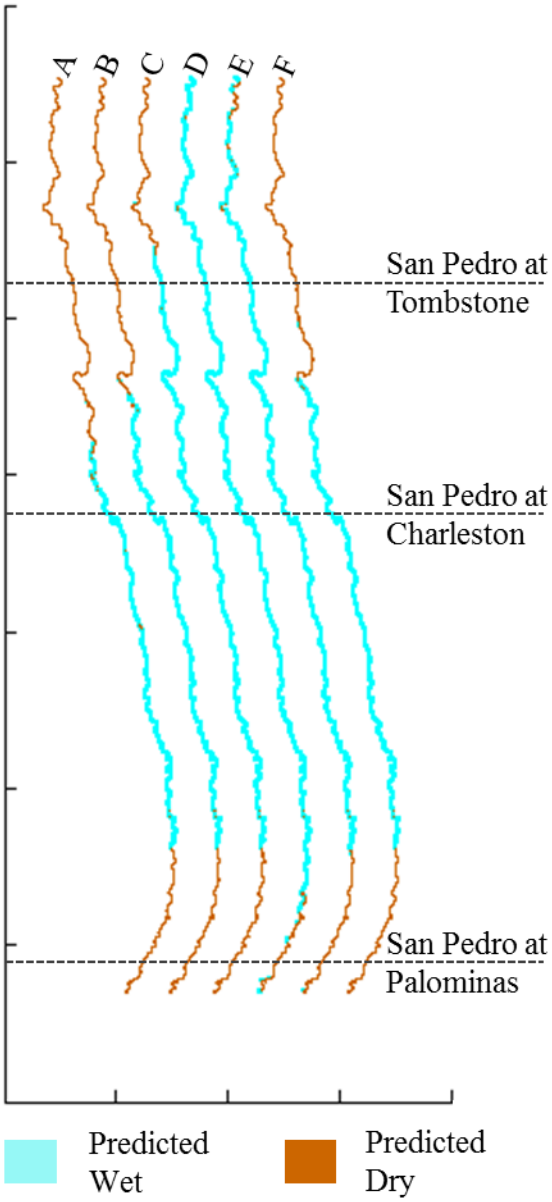

Figure 6: Graphical representation of the predicted wet/dry status of the San Pedro River based on six different alternate stream flow scenarios: A) zero flow, B) minimum flow, C) mean flow, D) maximum flow, E) flow after the coldest winter and F) flow after the hottest winter for each gauging station.

10 List of Tables

Table 1: List of variable names, type, source, processing method and resolution.

Variable Name	Variable Type	Source	Processing	Resolution
1999-2011 San Pedro River Wet/Dry Dataset	Response	[*Turner and Richter*, 2011]	Vector Data converted to raster format using ArcGIS 9.3 feature to raster function.	10 m
Depth of Bedrock	Explanatory	[*Gettings and Houser*, 2000]	None, original dataset.	1000 m
Change in Depth of Bedrock	Explanatory	Depth of Bedrock	Difference between San Pedro River main stem upstream and downstream pixels.	1000 m
Slope of Depth of Bedrock	Explanatory	Depth of Bedrock	Calculation of Slope using ArcGIS 9.3 slope function.	1000 m
Curvature of Depth of Bedrock	Explanatory	Depth of Bedrock	Calculation of Curvature using ArcGIS 9.3 Curvature function.	1000 m
Channel Sinuosity	Explanatory	National Hydrography Dataset, 1:24,000-scale, US Geological Survey, http://nhd.usgs.gov	Linear representation of San Pedro River inside SPRNCA was divided in 1,000 m long reaches and sinuosity was calculated as reach length divided by straight line endpoint distance of each reach. The dataset was then converted to raster format.	30 m

Table 1: *(Continued)*

Variable Name	Variable Type	Source	Processing	Resolution
Surface Elevation (LIDAR)	Explanatory	San Pedro River 2003 LIDAR Dataset http://newims.hwr.arizona.edu/SAHRA/GeoDB/PublicUSPdata.html	None, original dataset.	1 m
Surface Slope (LIDAR)	Explanatory	Surface Elevation (LIDAR)	Calculation of Slope using ArcGIS 9.3 slope function.	1 m
Surface Curvature (LIDAR)	Explanatory	Surface Elevation (LIDAR)	Calculation of Curvature using ArcGIS 9.3 Curvature function.	1 m
Surface Elevation (DEM)	Explanatory	1 arc-second (30 m) Digital Elevation model for the San Pedro River , US Geological Survey, http://ned.usgs.gov/	None, original dataset.	30 m
Surface Slope (DEM)	Explanatory	Surface Elevation (DEM)	Calculation of Slope using ArcGIS 9.3 slope function.	30 m
Surface Curvature (DEM)	Explanatory	Surface Elevation (DEM)	Calculation of Curvature using ArcGIS 9.3 Curvature function.	30 m

Table 1: *(Continued)*

Variable Name	Variable Type	Source	Processing	Resolution
Streamflow at Palominas (average daily)	Explanatory	National Water Information System, USGS 09470500 San Pedro River At Palominas, AZ, US Geological Survey, http://waterdata.usgs.gov/	Euclidian distance raster was created based on the location of this station using ArcGIS 9.3 Euclidean Distance function. All further grouping done in Matlab 7.11	10 m
Streamflow at Charleston (average daily)	Explanatory	National Water Information System, USGS 09471000 San Pedro River At Charleston, AZ, US Geological Survey, http://waterdata.usgs.gov/	Euclidian distance raster was created based on the location of this station using ArcGIS 9.3 Euclidean Distance function. All further grouping done in Matlab 7.11	10 m
Streamflow at Tombstone (average daily)	Explanatory	National Water Information System, USGS 09471550 San Pedro River near Tombstone, AZ, US Geological Survey, http://waterdata.usgs.gov/	Euclidian distance raster was created based on the location of this station using ArcGIS 9.3 Euclidean Distance function. All further grouping done in Matlab 7.11	10 m
Total Daily Precipitation	Explanatory	VIC Model 8th Degree Meteorological Forcing Data (Daily Precipitation), 1949-2010 [*Maurer et al.*, 2002]. http://www.cbrfc.noaa.gov/devel/vic_8d_forc/	Unique identification grid linking the daily data with the spatial location of the river was converted to raster format using ArcGIS 9.3 feature to raster function. All further grouping done in Matlab 7.11	380 m

Table 1: *(Continued)*

Variable Name	Variable Type	Source	Processing	Resolution
Floodplain Width	Explanatory	Surface Elevation (LIDAR)	Manual digitization of the bank-full floodplain using the LIDAR dataset in ArcGIS 9.3	10 m
Main Stem Flow Accumulation	Explanatory	Surface Elevation (DEM)	Main Stem Flow Accumulation raster was created using the Flow Accumulation tool in ArcGIS 9.3	10 m

Table 2: Mean and Standard Deviation of the Data Set use to Calibrate the San Pedro Wet/Dry Logistic Regression

Status	Total Sample (N)	Depth to Bedrock	Sinuosity	Floodplain Width	Surface Elevation (LIDAR)	Surface Curvature (LIDAR)
Wet	38830	2.67E-01 (4.01E-01)	1.25E+00 (2.11E-01)	1.80E+02 (9.52E+01)	1.22E+03 (7.39E+01)	5.91E+00 (6.04E+00)
Dry	32878	4.84E-01 (5.25E-01)	1.24E+00 (2.78E-01)	1.96E+02 (9.93E+01)	1.19E+03 (1.19E+02)	5.43E+00 (6.11E+00)
All	71708	3.67E-01 (4.74E-01)	1.25E+00 (2.44E-01)	1.87E+02 (9.74E+01)	1.21E+03 (9.91E+01)	5.69E+00 (6.08E+00)

Table 2: *(Continued)*

Status	Total Sample (N)	Surface Curvature (LIDAR)	Spatially Allocated Mean Daily Streamflow (5/1 to 5/30)	Change in Depth to Bedrock	Slope of Depth to Bedrock	Curvature of Depth to Bedrock
Wet	38830	-3.61E-01 (1.34E+01)	8.47E-02 (7.46E-02)	2.39E-02 (6.70E-02)	2.99E-03 (3.84E-03)	1.85E-07 (8.38E-06)
Dry	32878	-2.88E-02 (1.27E+01)	3.64E-02 (5.43E-02)	4.53E-03 (7.13E-02)	3.54E-03 (3.57E-03)	2.05E-06 (1.04E-05)
All	71708	-2.09E-01 (1.31E+01)	6.26E-02 (7.03E-02)	1.50E-02 (6.97E-02)	3.24E-03 (3.73E-03)	1.04E-06 (9.39E-06)

Table 3: San Pedro River Wet/Dry Logistic Regression Parameters

Explanatory Variable	β	*SE* β	Semi-Standardized $\beta_{ss} = \beta * SD$	Wald's χ^2	*df*	*p-value*	β Lower 95%	β Upper 95%	Relative Importance
Intercept	-31.2125	0.3087	N/A	10222	1	<.0001	-31.8187	-30.6086	N/A
Variables that describe streamflow									
Spatially Allocated Streamflow (May-1 to May-30)	10.9371	0.1707	0.7689	4103.6	1	<.0001	10.6031	11.2724	3
Variables that describe the elevation and shape of bedrock									
Depth to Bedrock	-2.4838	0.0284	-1.1781	7645.5	1	<.0001	-2.5396	-2.4282	2
Change in Depth to Bedrock	5.1644	0.2091	0.3597	609.88	1	<.0001	4.7550	5.5747	4
Curvature of Depth to Bedrock	21484.2189	1167.5334	0.2018	338.59	1	<.0001	19196.1039	23772.8292	5
Slope of Depth to Bedrock	-27.0760	3.5510	-0.1009	58.14	1	<.0001	-34.0499	-20.1301	8
Variables that describe shape of floodplain channel									
Flood Plain Width	-0.0020	0.0001	-0.1987	371.15	1	<.0001	-0.0022	-0.0018	6
Sinuosity	0.6880	0.0423	0.1679	264.93	1	<.0001	0.6052	0.7709	7
Variables that describe the elevation and shape of the land surface									
Surface Elevation (LIDAR)	0.0257	0.0003	2.5499	9555.4	1	<.0001	0.0252	0.0262	1
Surface Slope (LIDAR)	-0.0051	0.0016	-0.0312	10.5	1	0.0012	-0.0082	-0.0020	9
Surface Curvature (LIDAR)	-0.0023	0.0007	-0.0305	10.38	1	0.0013	-0.0038	-0.0009	10

Table 4: Observed and Predicted Wet/Dry Status Frequency (percent) for each validation year (2006-2011) using the San Pedro River Logistic Regression Model using the probability cutoff value of 0.5332

	Validation Year								
	2006			2007			2008		
	Predicted Dry	Predicted Wet	Total	Predicted Dry	Predicted Wet	Total	Predicted Dry	Predicted Wet	Total
Observed Dry	4513 (44.1%)	1124 (11.0%)	5637 (55.0%)	3783 (36.9%)	474 (4.6%)	4257 (41.6%)	4348 (42.4%)	1160 (11.3%)	5508 (53.8%)
Observed Wet	746 (7.3%)	3861 (37.7%)	4607 (45.0%)	1384 (13.5%)	4603 (44.9%)	5987 (58.4%)	874 (8.5%)	3862 (37.7%)	4736 (46.2%)
Total Correct	4513 (85.8%)	3861 (77.5%)	8374 (81.7%)	3783 (73.2%)	4603 (90.7%)	8386 (81.9%)	4348 (83.3%)	3862 (76.9%)	8210 (80.1%)

	Validation Year								
	2009			2010			2011		
	Predicted Dry	Predicted Wet	Total	Predicted Dry	Predicted Wet	Total	Predicted Dry	Predicted Wet	Total
Observed Dry	3804 (37.1%)	388 (3.8%)	4192 (40.9%)	4428 (43.2%)	714 (7.0%)	5142 (50.2%)	4350 (42.5%)	1007 (9.8%)	5357 (52.3%)
Observed Wet	1191 (11.6%)	4861 (47.5%)	6052 (59.1%)	649 (6.3%)	4453 (43.5%)	5102 (49.8%)	741 (7.2%)	4146 (40.5%)	4887 (47.7%)
Total Correct	3804 (76.2%)	4861 (92.6%)	8665 (84.6%)	4428 (87.2%)	4453 (86.2%)	8881 (86.7%)	4350 (85.4%)	4146 (80.5%)	8496 (82.9%)

Table 5: Streamflow values used in the alternate scenarios analysis.

Gauging Station	Scenario A Zero Flow (M^3/s)	Scenario B Minimum flow (M^3/s)	Scenario C Mean flow (M^3/s)	Scenario D Maximum flow (M^3/s)	Scenario E Flow after the coldest winter (M^3/s)	Scenario F Flow after the hottest winter (M^3/s)
Charleston	0	6.940E-02	2.265E-01	1.053E+00	2.741E-01	1.410E-01
Palominas	0	0	1.560E-02	8.440E-02	2.920E-02	2.000E-03
Tombstone	0	5.660E-04	1.472E-01	4.899E-01	2.503E-01	4.160E-02

APPENDIX C: EFFECTS OF MEASUREMENT RESOLUTION ON THE ANALYSIS OF TEMPERATURE TIME SERIES FOR STREAM-AQUIFER FLUX ESTIMATION

Carlos D. Soto-López[1], Thomas Meixner[1] and Ty P.A. Ferré[1]

[1] Department of Hydrology and Water Resources

University of Arizona

1133 E James E Rogers Way

Building 11, Room 122

Tucson, Arizona, 85722, USA.

An edited version of manuscript was published on Water Resources Research. Copyright (2011) American Geophysical Union

Soto-Lopez, C. D., T. Meixner, and T. P. A. Ferré (2011), Effects of measurement resolution on the analysis of temperature time series for stream-aquifer flux estimation, Water Resour. Res., 47, W12602, doi:10.1029/2011WR010834.

To view the published paper, go to:

https://agupubs.onlinelibrary.wiley.com/doi/pdf/10.1029/2011WR010834

1 Abstract

From its inception in the mid 1960's, the use of temperature time series (thermographs) to estimate vertical fluxes has found increasing use in the hydrologic community. Beginning in 2000, researchers have examined the impacts of measurement and parameter uncertainty on the estimates of vertical fluxes. To date, the effects of temperature measurement discretization (resolution), a characteristic of all digital temperature loggers, on the determination of vertical fluxes has not been considered. In this technical note we expand the analysis of recently published work to include the effects of temperature measurement resolution on estimates of vertical fluxes using temperature amplitude and phase shift information. We show that errors in thermal front velocity estimation introduced by discretizing thermographs differ when amplitude or phase shift data are used to estimate vertical fluxes. We also show that under similar circumstances sensor resolution limits the range over which vertical velocities are accurately reproduced more than uncertainty in temperature measurements, uncertainty in sensor separation distance, and uncertainty in the thermal diffusivity combined. These effects represent the baseline error present and thus the best-case scenario when discrete temperature measurements are used to infer vertical fluxes. Errors associated with measurement resolution can be minimized by using the highest resolution sensors available. But, thoughtful experimental design could allow users to select the most cost-effective temperature sensors to fit their measurement needs.

2 Introduction

The use of temperature time series (thermographs) to infer fluxes between a stream and an aquifer was first proposed by *Stallman* (1965). Constantz and Anderson made

major advances in the use of temperature methods for hydrology in the early 1980's and both reviewed the field recently (*Anderson*, 2005; *Constantz*, 2008). Over the past three decades, the approach has found widespread use in the hydrologic community, as evidenced by the high number of citations of their original work (> 120). There have been continuous efforts to improve the accuracy and robustness of the inferred fluxes. Notably, *Niswonger (2000)* provided an estimate of the impacts of temperature measurement and parameter uncertainty (thermal conductivity and heat capacity) on estimating a specific flux value. More recently, *Shanafield* (2011) conducted an analysis of the impacts of temperature measurement uncertainty, uncertainty in thermal properties (thermal diffusivity), and experimental design (separation distance) on a large range of vertical fluxes using the method proposed by *Hatch et al.* (2006). Their work described limitations in the range of upward and downward fluxes for which the method can be used. We extend the analyses of *Niswonger* (2000) and *Shanafield* (2011) to examine the impacts of measurement discretization (resolution) on the accuracy of flux estimates. We also suggest a revised approach to the analysis of thermographs to improve the robustness and accuracy of flux estimates.

Traditionally, vertical fluxes have been estimated by forward modeling of thermographs coupled with estimation of thermal and hydraulic parameters. *Hatch et al.* (2006) provides a simple and clear explanation of the use of thermographs measured at depth to infer steady-state water fluxes based on the analytical solution to the approach of *Stallman* (1965) and later modified by *Hatch et al.* (2006) to include the effects of thermal dispersion in the direction of flow. The method proposed by *Hatch et al. (2006)* used observed ratios of amplitude (amplitude ratio, AR) and changes in phase (phase

shift, $\Delta\varphi$) of thermographs at two depths beneath the stream-streambed interface to solve directly for vertical flux. *Hatch et al. (2006)* demonstrated that amplitude ratios alone could be used to accurately estimate both the direction and magnitude of small fluxes, but phase shift data can only be used to estimate the flux magnitude. In a recent paper, *Shanafield et al.* (2011) showed that degradation of the temperature time series with random, Gaussian measurement error and uncertainty in the parameters of depth and thermal conductivity significantly reduces flux estimate accuracy.

While previous work has improved our understanding of the impacts of random errors, the practical selection of a sensor often rests on the desired measurement resolution. Specifically, measurement resolution is a well-defined quantity that describes how an instrument truncates and rounds measured values. While manufacturers commonly report both sensor resolution and accuracy, price is often more dependent on the resolution capabilities of the sensor than any other characteristic [*Johnson et al.*, 2005]. In this work, we focus on the effects of temperature measurement discretization (resolution), which were not considered by *Shanafield et al*. (2011) and suggest a modified approach to flux estimation.

3 Method

Our analysis follows closely that of *Shanafield et al* (2011). We use Stallman's analytical solution as modified by *Hatch et al.* (2006) to generate synthetic thermographs at two depths (0.1 and 0.35 m) beneath the stream-streambed interface in response to a range of synthetic thermal front velocities (-4 to 4 m/d, negative is downward and positive is upward) and a daily sinusoidal surface temperature signal generated at one-minute intervals for a system with a thermal diffusivity of 0.075 m^2/d. We repeat this

over different upper boundary temperature signal amplitudes (1 to 5 °C). Extending the work of *Shanafield et al* (2011), we subject the signal to different levels of rounding. That is, we use a sequence of discretization intervals that round temperature measurements to the nearest resolution interval ranging from 0.01 to 0.50 °C. We then estimate the vertical thermal front velocities using the discretized thermographs. These are then compared to the known synthetic velocities to show the impacts of measurement resolution on the accuracy of upward and downward flux estimates.

As with *Shanafield et al*. (2011), velocities in this paper refer to thermal front velocities (v) and not fluid flux (v_f). Thermal front velocity is equal to fluid flux divided by the ratio of volumetric heat capacity of a water-saturated medium to the volumetric heat capacity of water (γ).

4 Results and Discussion

The data shows that the bias on predicted velocities derived from amplitude ratio and phase shift values is a function of the resolution value used to discretize the thermographs and the amplitude of the temperature variation at the upper boundary (not shown). However, we found that the introduced bias was the same in conditions where the ratios of resolution value to upper boundary amplitude value were equal. For example, the bias introduced on predicted velocities derived from thermographs discretized at 0.05 °C and 0.25 °C were the same when the amplitude of the upper boundary temperature was 1 °C and 5 °C, respectively. This finding allows us to simplify the presentation and discussion of our results by introducing a new parameter, the ratio of temperature sensor resolution to upper boundary amplitude (RSRA) as $RSRA = Res/A_0$. Where, Res is the temperature sensor resolution and A_0 is the amplitude of temperature variation at the upper boundary.

RSRA defines the minimum amplitude ratio that a pair of sensors can detect and record given their resolution and the range of the diurnal temperature signal. Any amplitude ratio that is smaller than RSRA will result in temperature variations that are less than the instrument resolution, effectively losing the signal because the thermographs remain constant with respect to time.

Emulating the *Shanafield et al.* (2011) model and parameters, and introducing discretization (sensor resolution) to synthetic thermographs produced large estimation errors when using amplitude ratio as a predictor (Figure 1 A and 1B) but introduces small errors when using phase shift as a predictor (Figure 1C and 1D). In particular, discretization reduces the range of thermal velocities that can be inferred accurately due to signal loss (amplitude ratio < RSRA) (Figure 1B and 1D). The large impact of sensor resolution can be explained by the way discretization affects thermographs. Discretization errors artificially increase or decrease the thermograph's amplitude by as much as half the discretization interval. This artificial change is not constant and it is a function of the velocity magnitude and measurement depth. The effect of this artificial change in the thermograph amplitude is reduced when the amplitude of the un-rounded thermograph increases and/or when sensor resolution decreases, with the most accurate estimates occurring when RSRA approaches zero (Figure 1A). This result suggests that the accuracy of estimated vertical velocities using amplitude ratio will not remain constant in time since surface water temperature amplitude changes with time and environmental conditions. For example, if velocity estimates are done for data collected during a 5-day period in which the stream-water temperature amplitude steadily decreases from 5 °C to 1 °C our results suggest that the accuracy of estimated velocities

using amplitude ratio as a predictor will decrease. The artificial increase or decrease of the thermograph's amplitude due to rounding errors has little to no effect on the thermograph's phase shift, thus making phase shift-based estimates of vertical velocity very accurate across much of the test space (Figure 1C). However, such determinations are very sensitive to the sampling interval used [*Hatch et al.*, 2006]. Here, we sampled data at 1min intervals to focus on the effects of rounding error itself. If the sampling interval does not change with time our results suggest that the accuracy of estimated vertical velocities using phase shift will remain constant in time except for the complications noted by *Shanafield et al.* (2011) and *Hatch et al.* (2006).

Our analysis shows that discretization of temperature measurements significantly impacts the estimation accuracy of vertical velocities. When the effects of measurement discretization are compared to the effects of parameter and measurement uncertainty we find that measurement discretization has a larger impact on velocity estimation than parameter and measurement uncertainty. We examined velocities over the range of -4 to 4 m/d, the same range used by *Shanafield et al.* (2011). Reproducible velocities are those velocities estimated from discretized thermographs whose values are within 10% of the actual velocity. Our results show that discretizing thermographs with a 0.15 °C resolution interval and using amplitude ratio as predictor of velocities reduced the range of reproducible velocities to just 23% of the total range examined (Figure 1B, when RSRA=0.15). On the other hand, we found that discretizing thermographs with a 0.15 °C resolution interval and using phase shift as predictor of velocities reduced the range of reproducible velocities to 49% of the total range examined (Figure 1D, when RSRA=0.15). In both cases the majority of this reduction is caused by signal loss due to

discretization of the thermographs (Figure 1B and 1D). Also, this reduction on the range of reproducible velocities was larger than the reductions derived from *Shanafield et al.* (2011) when introducing uncertainty in temperature measurements, uncertainty in sensor separation distance, or uncertainty in the thermal diffusivity. When these sources of uncertainty are combined the range of reproducible velocities is reduced to 31% and 34% when using amplitude ratio and phase shift, respectively [Table 1; *Shanafield et al*., 2011]. These results suggest that under similar circumstances temperature measurement discretization (resolution) of 0.15 °C is as important as the introduction of uncertainty in temperature measurements, uncertainty in sensor separation distance, and uncertainty in thermal diffusivity because it has a greater impact on the range of vertical velocities that can be accurately reproduced, especially when using amplitude ratio as a predictor. Finally, we argue that the effects of measurement discretization shown here represent the primary source of error in all time-series based estimates of velocity. These errors will be compounded, but their pattern should still hold, when uncertainty in temperature measurements, uncertainty in parameters, and non-ideal field conditions are considered.

5 Implications

Recognizing the impacts of resolution, measurement error, and parameter uncertainty on the amplitude and phase responses reported here and in the literature can be used to tailor the experimental design to reduce the bias of flux estimates, i.e., sensor selection, sensor placement and range of fluxes to estimate. Specifically, our results and those of *Shanafield et al.* (2011) show clearly that estimates of flux using phase shift are far less susceptible to these limitations. In fact, amplitude ratio information is only needed to infer the direction of flow, which requires that the flux magnitude be estimated with less

than 100% relative error. Our analysis suggests that the near neutral region of -0.3 to 0.3 m/d encompasses the range of velocities most affected by changes in the discretization magnitude and upper boundary temperature amplitude, which causes a miscalculation of the directionality of flow. This zone also includes the large biases associated with the sensitivity of thermal front velocities to changes in phase shift in the near neutral regions reported by *Hatch et al. (2006).* Making use of these characteristics, we recommend using phase shift information independently to estimate flux magnitude and the amplitude ratio information only to determine the direction of flow.

To use phase shift as an accurate predictor of vertical velocities and avoid the interference of discretization errors with the determination of phase shift, we define the minimum detectable amplitude ratio (AR_{min}) as $(1.5 \times RSRA)$. AR_{min} is more conservative than RSRA but also defines the minimum amplitude ratio that a pair of sensors can detect and record given a sensor's resolution and the diurnal temperature signal. Therefore, to be able to observe a measurable temperature variation, the amplitude ratio (AR) for a given soil thermal diffusivity (K_e), thermal front velocity (v) and separation distance (Δz) (Eq. 1) must be greater than or equal to AR_{min} ($AR \geq AR_{min}$).

$$AR(K_e, v, \Delta z) = \left(\frac{v\Delta z}{2K_e} - \frac{\Delta z}{2K_e}\sqrt{\frac{\alpha+v^2}{2}}\right) \quad (1);$$

Where, $k_e = \lambda_0 / \rho c + \beta |v_f|$ (effective thermal diffusivity), ρc is heat capacity of the saturated sediment-fluid system, $\alpha = \sqrt{v^4 + (8\pi \cdot k_e/\tau)^2}$, τ is period of oscillation, λ_0 is medium's baseline thermal conductivity with no fluid flow, and β is longitudinal thermal dispersivity.

Using equation 1, a response surface can be developed that describes amplitude ratio as a function of separation distance, thermal front velocity and thermal diffusivity. The response surface can then be used to estimate the ranges of thermal front velocities and separation depths that can be observed given an AR_{min} and the soil thermal diffusivity (Figure 2). In general, soils with a low thermal diffusivity, coupled with low upper boundary temperature amplitude and coarse sensor resolution will result in a very restricted range of upward velocities that could be inferred using temperature as a tracer of vertical fluxes because most upward fluxes will have an AR that is smaller than AR_{min}. Any AR that is smaller than AR_{min} will result in temperature variations that are less than the instrument resolution and thus effectively constant with respect to time.

For example, assume a user wants to quantify the vertical direction and magnitude of velocities in a streambed with a thermal diffusivity (K_e) of 0.075m^2/d using a temperature sensor with a 0.5 °C resolution during a time period in which the minimum expected stream water temperature amplitude is 2.5°C. These conditions lead to a calculated AR_{min} equal to 0.3. This information used in conjunction with a response surface generated from Eq. 1 can be used to answer two types of questions. First, under ideal conditions what is the maximum separation distance allowable in order to quantify a specific range of velocities using only two sensors (Case 1)? If, for example, the user wants to estimate velocities in the -1 to 1 m/d range, then the maximum separation distance allowed between the sensors should not exceed 8 cm. Secondly, under ideal conditions what range of velocities can be inferred from paired temperature measurements separated by a specific distance (Case 2)? In this case, assume that because of design limitations the user separates two sensors by a distance equal to 30 cm. Again figure 2 shows, only

velocities larger than 0.4 m/d in the downward direction can be estimated. This analysis can be duplicated using any range of sensor resolution, upper boundary temperature amplitude, separation distance, vertical velocities, and/or thermal diffusivities to fit the user needs. We have created a MATLAB script that will run this analysis using user-defined values for these parameters and it is available as an electronic supplement to this note.

6 Conclusions

We have extended *Shanafield et al.* (2011) analysis to include the effects of temperature measurement resolution (rounding error) on estimates of vertical thermal front velocity from paired streambed thermographs. Our analysis has shown that temperature measurement discretization (sensor resolution) introduces large estimation errors when amplitude ratio is used as a predictor of vertical thermal front velocities, but introduces little to no errors when using phase shift as a predictor. The different response to discretization between amplitude ratio and phase shift is mainly caused by the artificial change in the thermograph's amplitude introduced by the discretization process. This artificial change in the thermograph's amplitude and its effect on determinations of thermal front velocity depends on the magnitude of the discretization interval and the actual amplitude of the thermograph. These observations suggest that the use of phase shift as a predictor of vertical thermal front velocities will result in more accurate estimates when compared to the use of amplitude ratio as a predictor. Therefore, we recommend using amplitude ratio to estimate the directionality of flow and phase shift to estimate the magnitude of velocity. Our recommendation relies on the validity of the assumption that enough information is contained in the discrete (rounded) streambed

thermograph to calculate its amplitude and avoid the interference of rounding errors with the determination of phase shift. As a result, we defined a new parameter named AR_{min} and argue that in order to observe a measurable temperature variation, the amplitude ratio for a given soil thermal diffusivity, velocity and separation distance must me greater than or equal to $AR_{min.}$

7 Acknowledgements

Carlos Soto-López was supported by the National Science Foundation Graduate Research Fellowship (NSFGRFP), Dr. Meixner was supported by Sustainability of semi-Arid Hydrology and Riparian Areas (SAHRA) under the STC Program of the National Science Foundation (EAR-9876800) and by the Environmental Protection Agency Science to Achieve Results (EPASTAR R833025) and, Dr. Ferré was supported by the National Science Foundation under Grant No. EAR 07-53521 awarded to the Consortium of Universities for the Advancement of Hydrologic Science, Inc. Any opinions, findings, conclusions or recommendations expressed in this publication are those of the authors and do not necessarily reflect the views of the supporting entities.

8 Reference List

Anderson, M. P. (2005), Heat as a Ground Water Tracer, Ground Water, 43, 951-968.

Constantz, J. (2008), Heat as a tracer to determine streambed water exchanges, Water Resour. Res., 44.

Hatch, C. E., A. T. Fisher, J. S. Revenaugh, J. Constantz, and C. Ruehl (2006), Quantifying surface water-groundwater interactions using time series analysis of streambed thermal records: Method development, Water Resour. Res., 42.

Johnson, A. N., B. R. Boer, W. W. Woessner, J. A. Stanford, G. C. Poole, S. A. Thomas, and S. J. O'Daniel (2005), Evaluation of an Inexpensive Small-Diameter Temperature Logger for Documenting Ground Water-River Interactions, Ground Water Monit. Remediat., 25, 68-74.

Niswonger, R. G. and J. L. Rupp (2000), Monte Carlo analysis of streambed seepage rates, in Riparian Ecology and Management in Multi-Land use Watersheds, edited by P. J. Wigington and R. C. Beschta, pp. 161-166, American Water Resources Association, Middleburg, VA.

Shanafield, M., C. Hatch, and G. Pohll (2011), Uncertainty in thermal time series analysis estimates of streambed water flux, Water Resour. Res.,47, W03504, doi:10.1029/2010WR009574

Stallman, R. W. (1965), Steady 1-Dimensional Fluid Flow in a Semi-Infinite Porous Medium with Sinusoidal Surface Temperature, Journal of Geophysical Research, 70, 2821-2827.

9 List of Figures

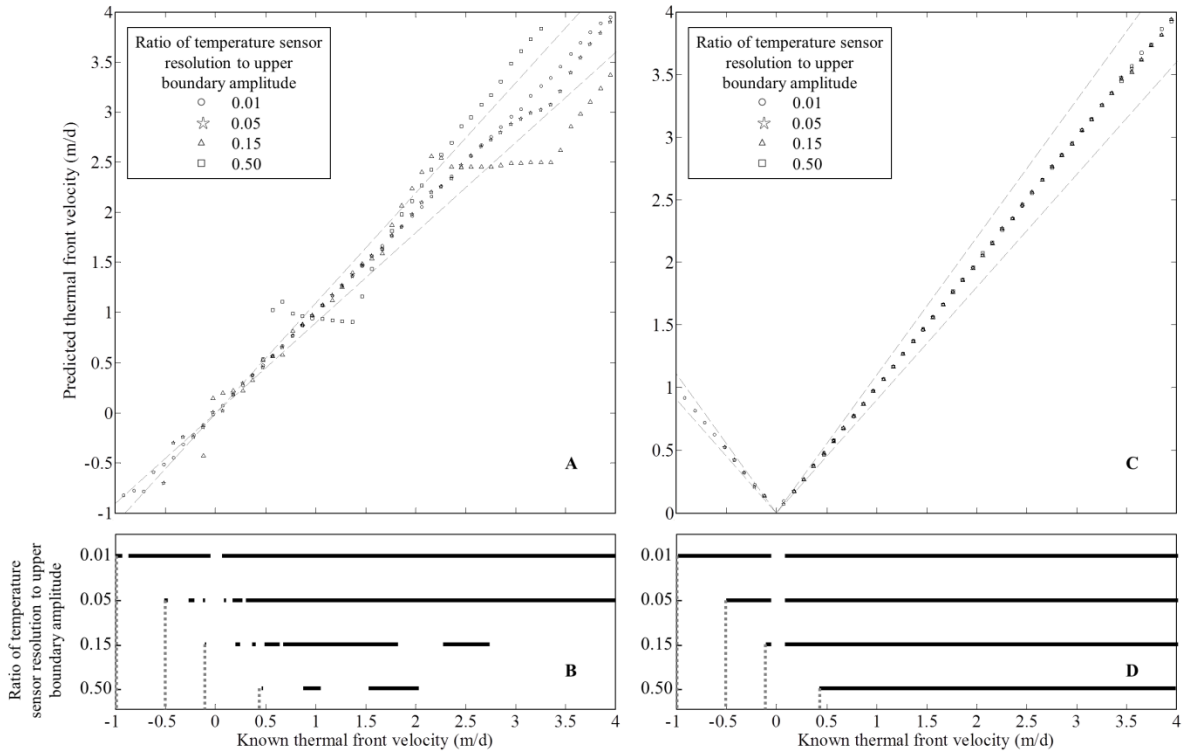

Figure 1: A) Known versus predicted thermal front velocities derived for four different values of RSRA using AR values derived from discretized synthetic thermographs at 0.1 and 0.35m as a predictor. B) Simplified representation of panel A showing the range of thermal front velocities (in black) where the predicted values have an absolute error less than 10%. C) Known versus predicted thermal front velocities derived for four different values of RSRA using $\Delta\varphi$ values derived from discretized synthetic thermographs at 0.1 and 0.35m as a predictor. D) Simplified representation of panel C showing the range of thermal front velocities (in black) where the predicted values have an absolute error less than 10%. Note, on A and C diagonal dashed lines represent the upper and lower boundary of the region of low prediction bias (± 10 %); on B and D the vertical dotted lines represent the threshold where signal loss occurs because AR<RSRA.

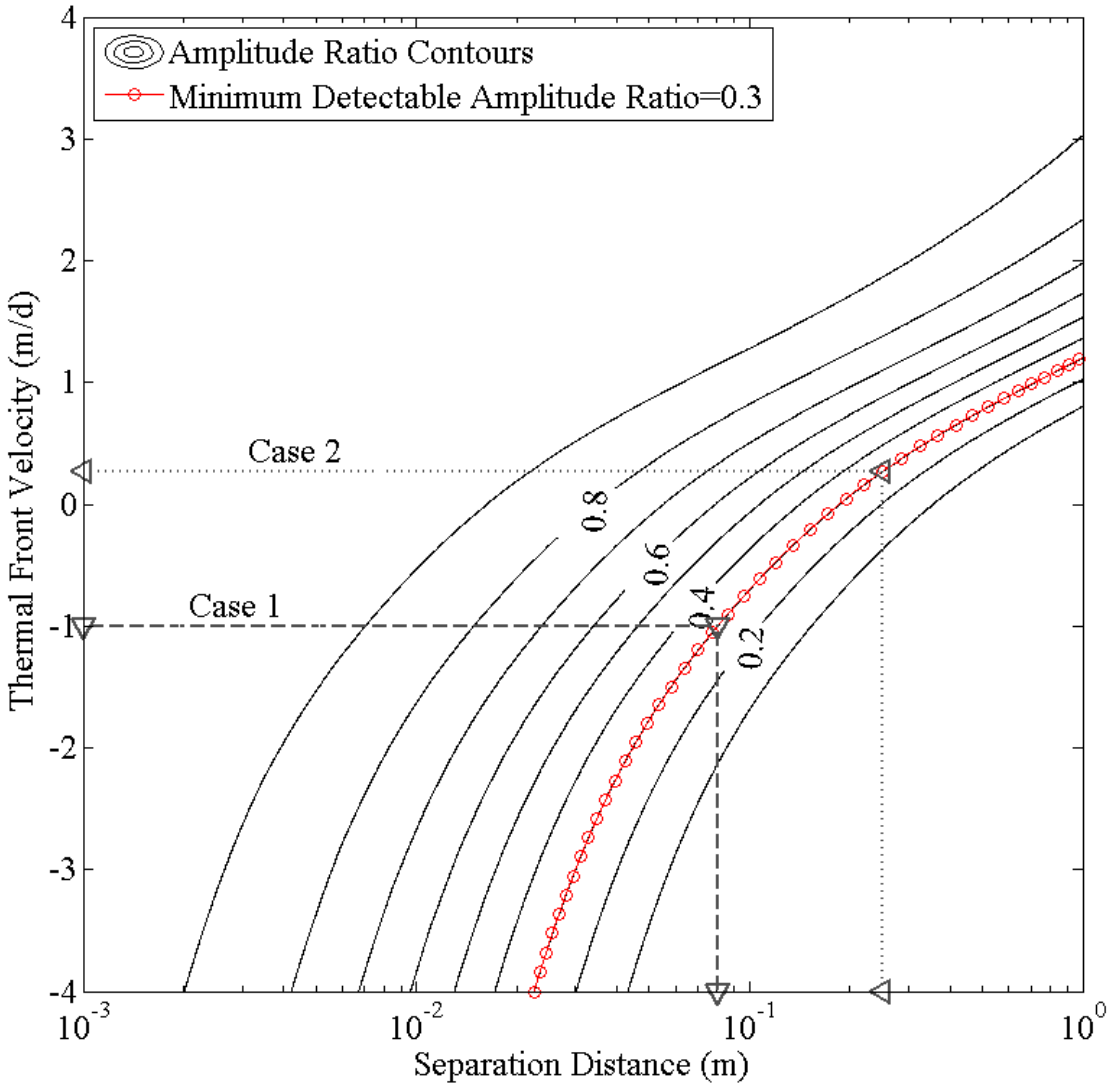

Figure 2: Example of amplitude ratio (AR) curves as a function of separation distance and thermal front velocity using a thermal diffusivity value of 0.075 m^2/d. Each contour interval represents the Amplitude Ratio (AR) value that would be observed at a specified separation distance and thermal front velocity. The figure has overlaid the values described in the example used in this note.

APPENDIX D: SAMPLING SITES COORDINATES AND GEOCHEMICAL DATASET FROM THE SAN PEDRO RIVER NATIONAL CONSERVATION AREA USED IN APPENDIX A

1 San Pedro River: Metals, Nutrient and Anion Dataset

The electronic link listed below contains the entire dataset of the chemical species measured for all the samples collected as described in Appendix A. Note that not all chemical species were used for completing Appendix A. However, they are included here as a complete dataset.

https://goo.gl/ZW8v4G

https://drive.google.com/open?id=1MAB_jbUVkbXVFWOX2Hcck4_qWRAAIRFg

The dataset contains the following information columns:

1. Sampling Date (MM/DD/YYYY): Contains the date the sample was taken.
2. Numerical Sample Code: An internal code to help quickly identify the sampling scale and sampling station. The integer digits identify the sampling scale, whereas the decimal digits identify the sampling station. Where the integers 10, 1, 100 and 40 represent the sampling scales of 10 Km, 1 Km, 100 m and 40 m, respectively,
3. Sampling Campaign Code: An internal code to help quickly identify the sampling campaign that each sample belongs to. Where the number 1 is March 2006, number 2 is May 2006, number 3 is November 2006 and number 4 is April 2007

4. Sample Name: The internal sampling names used to identify locations and samples. Note, sampling 20-C is the intersection of AZ Highway 90 with the San Pedro River (31° 33.115'N, 110° 8.314'W). For location information see
5. Sampling Reach Scale: The sampling scale for each sample
6. Sample Position Distance (meters): The number of downstream meters from the 40-S sampling point. It extends all the way to 10000 meters.

The remaining columns of the table contain the concentration values in milligrams per liter (mg/L) for the 26 chemical species listed below. Note that N/A means that the concentration could not be determined.

1. Aluminum [Al]
2. Arsenic [As]
3. Boron [B]
4. Barium [Ba]
5. Calcium [Ca]
6. Copper [Cu]
7. Iron [Fe]
8. Potassium [K]
9. Lithium [Li]
10. Magnesium [Mg]
11. Manganese [Mn]
12. Sodium [Na]
13. Nickel [Ni]
14. Silica [Si]
15. Strontium [Sr]
16. Zinc [Zn]
17. Dissolved Organic Carbon [DOC]
18. Total Nitrogen[TN]
19. Flouride Ion [F-]
20. Chloride Ion [Cl-]
21. Nitrite Ion [NO_2-]
22. Bromide Ion [Br-]
23. Nitrate Ion [NO_3-]
24. Sulphate Ion [SO4]
25. Sulphate:Chloride Ratio [SO_4/CL]
26. Inorganic-N [NO_3-N + NO_2-N]

2 San Pedro River Sampling Locations Dataset

The electronic links listed below contains a Google Earth KML file with the coordinates and names for the sampling locations at the 10 Km, 1 Km and 100 m referred in the section listed above (San Pedro River: Metals, Nutrient and Anion Dataset) and thus described and used in Appendix A.

https://goo.gl/NBpxPV

https://drive.google.com/open?id=1VRoVoEfBsQzxMCMC8TAbDYjiFzoGBzNU

APPENDIX E: SUPPORTING INFORMATION FOR AN EMPIRICAL MODEL FOR PREDICTING FLOW PERMANENCE ON THE SAN PEDRO RIVER (APPENDIX B)

1 Assessment of the Calibrated Logistic Regression Model

Once the logistic regression model is built and calibrated the model's fit to the data and predictive abilities was evaluated, the statistical significance of the logistic regression model with all its explanatory variables (using saturated model) over the intercept-only regression (null model) was tested using the likelihood ratio test. This comparison was followed by an evaluation of the model's goodness-of-fit by means of the Wald's χ^2 statistic, the Hosmer-Lemshow (H-L) test [*Hosmer and Lemeshow,* 2000] and Point Biserial Correlation (R_{pb}) values. Lastly, the model's wet/dry predicted probabilities were evaluated by means of several measures of association, between the model's predicted probabilities (continuous), the model's predicted wet/dry outcome (discrete) and the actual wet/dry status of the river during calibration and validation periods.

Six measures of association are used in this study and they describe how concordant or discordant the predicted probabilities are in relation to the actual wet/dry status of the river. Here a measure was deemed concordant when locations that were observed wet also have the highest predicted probability or predicted outcome, and discordant when the opposite is true. Including the previously used R_{pb}, these measures are: 1) c-statistic also known as concordance index or as the ROC-Area Under Curve (ROC-AUC), 2) Point Biserial Correlation (R_{pb}), 3) Goodman and Kruskal's Gamma, 4) Kendall's Tau-b, 5) Stuart's Tau-c and 6) Somer's D. Besides the differences in interpretation and calculation of each of these measures, the main difference between the c-statistic and R_{pb} with the

other measures is the type of input data needed to calculate them. The first two measures (c-statistic and R_{pb}) compare the actual dichotomous(nominal) outcome versus the continuous probabilities predicted by the logistic regression model. The last four measures compare the actual dichotomous (nominal) outcome versus the predicted dichotomized outcome based on thresholding the logistic regression model predicted probabilities using the optimal probability value.

1.1 General Model Evaluation and Goodness of Fit

The results show that the wet/dry predictive capabilities of the logistic regression model are significant when compared to the intercept-only model, that all 10 of the explanatory variables used in the logistic regression model are significant predictors of streamflow permanence and that a Hosmer-Lemshow test was significant. The statistical significance of the improvement of the logistic regression model (saturated model) over the intercept-only regression (null model) was tested using the likelihood ratio test. A likelihood ratio test showed that improvement of the logistic regression model (saturated model) over the intercept-only regression (null model) was significant with a p-value less than 0.001 (Table 4). The null model regression yielded a value for the constant of 0.1664. Using this constant in Eq. 1 yields a probability of a location being classified as wet of 0.5415, which is equal to the ratio of the wet elements to the total elements ($N_{wet}/N_{Total} = 32878/71708 = 0.5415$) in the wet/dry dataset for the calibration period (Table 2).

The statistical significance of the model's goodness-of-fit between the predicted probabilities and the actual wet/dry status of the river was tested using Hosmer-Lemshow (H-L) test (Table S1) [*Hosmer and Lemeshow*, 2000]. The results of the H-L test for this

model returned a χ^2 value of 2932.4 which at 8 degrees of freedom was significant ($p<0.001$). The Point Biserial Correlation (R_{pb}) value, a descriptive measure of the model goodness-of-fit (wet/dry status vs. predicted probability), during calibration was equal to 0.6472, when squared (R_{pb}^2) this value is equal to 0.4187 (Table S2). In general this implies that approximately 42% of the variation observed in the wet dry patterns is explained by the predicted probability values of the logistic regression.

1.2 Evaluation of the Model's Predicted Probabilities

The logistic model quality and predicted probabilities were evaluated by comparing the amount of association between the model's predicted probabilities (continuous), the model's predicted wet/dry outcome (discrete) and the actual wet/dry status of the river during calibration and validation periods. In general these measures of association show that higher predicted probabilities from the logistic regression model tend to be associated with locations observed wet in the stream. Analysis of the predicted probabilities during calibration showed that the optimal probability value was equal to 0.5332 (Figure 4). This value was used to dichotomize the predicted probabilities in order to calculate the measures of association and estimate model skill. The Receiver Operator Curve or ROC (Figure S1 and Figure S2) was obtained by plotting sensitivity against 1-specificty for all possible probability cutoff values. The ROC is derived from radar signal analysis and describes the models ability to discriminate that a wet location will have a higher probability than a dry location. The integration of the ROC (ROC-AUC) yields the c-statistic or concordance index. The c-statistic value for the calibration period (Figure S1 and Table S2) was equal to 0.8686, which means that for 86.86% of all possible pairs of locations (wet/dry) the model assigned a higher probability to the

locations which were wet. The c-statistic values during the validation period (Figure S2 and Table S2) ranged from approximately 84% to 90%. With the exception of the Goodman and Kruskal's Gamma, which ranges from 0.89-0.95, all other nominal versus nominal measures of association are in close agreement with correlation values between 0.60 and 0.73 (Table S2).The main reason for the difference in magnitude between Goodman and Kruskal's Gamma and the other three nominal versus nominal correlation values is that ties are ignored during the calculation of Goodman and Kruskal's Gamma.

2 Does the Logistic Regression Model Fit the Data?

The logistic regression model was assessed in stages. First evaluating the general null hypothesis (Ho1) of a logistic regression model was rejected. This hypothesis states all regression coefficients (βi) in the logistic regression model are equal to zero while the alternate hypothesis (Ha1) states that at least one βi in the set of explanatory variables is not equal to zero. In other words, a logistic regression model (saturated model) is said to be better if it provides a significant improvement over the intercept-only model (null model). The null model contains no explanatory variables, just a constant, and all observations according to this model would be predicted into the largest class in the dataset (i.e. wet) with a probability equal to the ratio of wet location to total elements (0.5415). To test this hypothesis the likelihood ratio test was used. The results of the likelihood ratio test showed that the improvement was significant ($p<0.001$) and allows for the rejection of the null hypothesis and accepts the alternate hypothesis (Ha,) that at least one β in the set of explanatory variables is not equal to zero. This result suggests that the saturated model is better than the mean at predicting the wet/dry status of the

river. In other words, the logistic regression model allows a better discrimination of the wet/dry status of the river when compared to the discrimination obtained by predicting that all sections of the river will follow the largest class in the dataset (wet prediction). However, this test only evaluates the model as a whole and does not test whether the coefficients of each explanatory variable are significantly different than zero. The Wald's $\chi 2$ test was used to check if a variable coefficient was different from zero. The test showed that all 10 explanatory variables and the constant term were significant predictors ($p<0.002$) of the wet/dry locations in the river (

Table 3). This result allows us to further strengthen the rejection of the general null hypothesis of logistic regression.

The second stage in the model evaluation involved testing for the statistical significance of the logistic regression model's goodness-of-fit between the predicted probabilities and the actual wet/dry status of the river using the Hosmer-Lemshow test (H-L test). For this test the null hypothesis (Ho2) states that the model fits the data whereas the alternate hypothesis (Ha2) states the model does not fit the data. The results of the H-L test for this model were significant ($p<0.001$). Therefore, the H-L test rejects the null hypothesis suggesting that the model does not fit the data. This result implies that the residuals are systematic and larger than the variation of the model [Hosmer and Lemeshow, 2000]. Besides the H-L test we used of the Point Biserial Correlation (R_{pb}) to evaluate the model's goodness of fit. The R_{pb} is similar to the Pearson correlation but is used when one of the variables is dichotomous (actual wet/dry) while the other is continuous (predicted probability). The low R_{pb} correlation values observed (R_{pb}~ 0.65,

Table 6) suggest that only a small portion of the variation observed in the wet dry patterns is explained by the predicted probability values of the logistic regression. The low correlation between the predicted and the actual wet/dry status of the stream further explain the rejection of the Hosmer-Lemeshow null hypothesis (Ho2). However, the close agreement amongst all the correlation values (Table S2) is indicative of a positive and consistent association between the actual and predicted wet/dry status. The lack of fit between the model and the data might be explained by the lack of other important explanatory variables or by the lack of detail of the variables used. We argue that if the level of detail (resolution) of the depth to bedrock were to be increased the fit between the model and the data would increase. Yet, this idea can't be confirmed with the datasets currently available.

Although the results of the H-L test and R_{pb} suggested that the model did not fit the data well. They cannot be interpreted to mean that the model performance is less than optimal. The third and final stage in the model evaluation involved the assessment of model performance. Four measures of model performance were used in this study. The first, the c-statistic is a standard measure that describes the degree of discrimination of the model or the likelihood that a location predicted as wet has a higher probability than one predicted dry. More importantly, the c-statistic measures the overall accuracy of a logistic regression independently of a classification probability cutoff point [*J. M. DeLeo*, 1993]. The second, model skill describes the overall fraction of correct predictions in a binary classification. Finally, sensitivity and specificity describes the fraction of true positives (wet) and true negatives (dry) in a binary classification. As opposed to the c-statistic these last three measures depend directly on the optimal classification probability

cutoff point of 0.5225 chosen earlier. The results showed that during the validation periods the c-statistic values ranged from approximately 84% to 90% (Table S2). This result implies that during validation 84 to 90 percent of the times a randomly selected wet location will have a higher probability value than a randomly selected dry location. Also, during the validation period the model skill ranged from approximately 80 to 87% with an average sensitivity and specificity equal to 84.0% and 81.9%, respectively (Table **4**). This result implies that during each validation year the logistic regression model correctly predicted the wet/dry status of 80 to 87 percent of sites modeled and that the model is marginally better at predicting wet over dry locations in the river. According to Hosmer and Lemeshow (2000) the c-statistic values derived from the results of the logistic regression analysis are considered to be an excellent discrimination rate and near the maximum limit of achievable in a logistic regression. In fact, Hosmer and Lemeshow (2000) state that is extremely unusual and nearly impossible to calibrate models with c-statistics greater than 0.9.

3 References

J. M. DeLeo (1993), Receiver operating characteristic laboratory (ROCLAB): Software for developing decision strategies that account for uncertainty, 1993 (2nd) International Symposium on Uncertainty Modeling and Analysis.

Hosmer, D. W. and S. Lemeshow (2000), Applied Logistic Regression, 397 pp., Wiley.

4 List of Figures

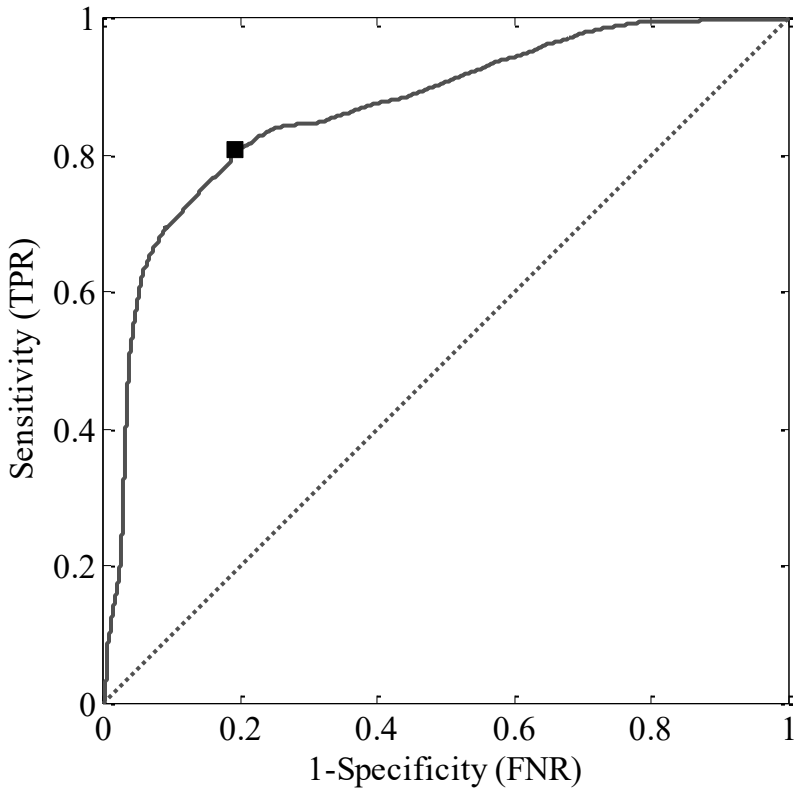

Figure S1: Receiver Operator Curve (ROC) for Wet/Dry Logistic regression during the calibration period (1999-2005). The black square represent the sensitivity and "1-specificity" value for the optimal cutoff point identified in Figure 4. The area under the curve (ROC-AUC, concordance index or c-statistic) is 0.8686.

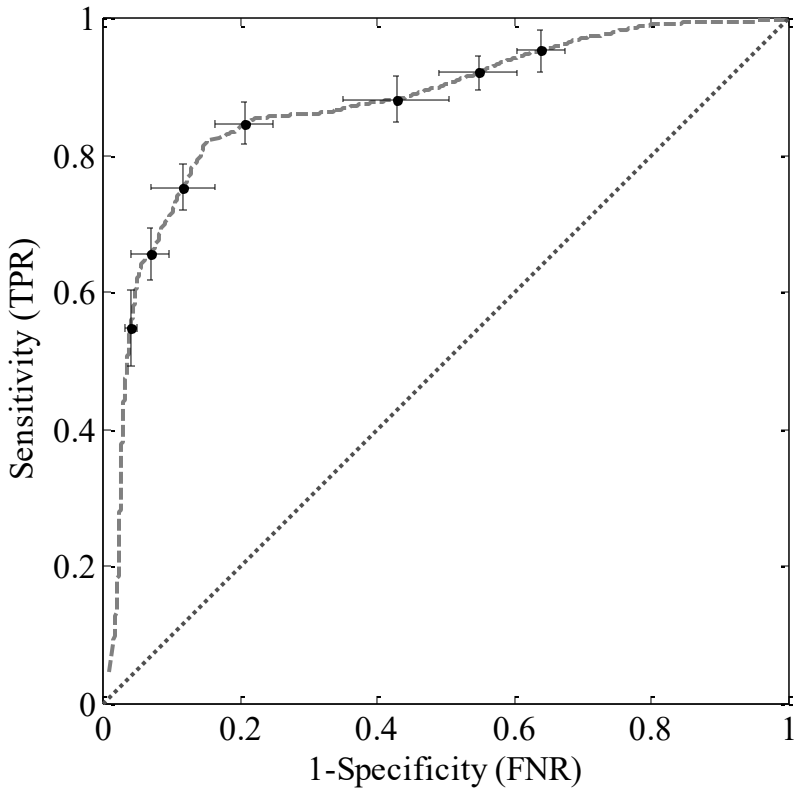

Figure S2: Average Receiver Operator Curve (ROC) for the validation dataset (2006-2011) of the San Pedro River Wet/Dry Logistic Regression Model. The average ROC curve was obtained by averaging both the sensitivity and 1-specificty values based on their probability cutoff value for each validation year. The black squares and error bars represent one standard deviation around the mean value of the sensitivity and 1-specificity with equal probability cutoff value for each validation year. The area under the curve (ROC-AUC, concordance index or c-statistic) for each of the validation years was 0.8668, 0.8465, 0.8293, 0.8767, 0.9007 and 0.8884

5 List of Tables

Table S1: Overall Model Evaluation and Goodness-of-fit test for the San Pedro River Wet/Dry Logistical Regression.

	Log Likelihood					
	Reduced Model (Constant Only)	*Full Model*	*Difference*	*χ^2*	*df*	*p-value*
Overall Model Evaluation						
Likelihood Ratio Test	-49456.9	-35415.3	-14041.6	28083.20	10	<.0001
Goodness-of-fit tests						
Hosmer & Lemeshow				2932.4	8	<.0001

Table S2: Association Statistics of Actual versus Predicted Wet/Dry Status during Calibration and Validation period of the San Pedro River Wet/Dry Logistic Regression Model

Name	Calibration	Validation					
	1999-2005	2006	2007	2008	2009	2010	2011
Nominal (Actual) Vs. Continuous (Predicted)							
Concordance Index (c-statistic or ROC-AUC)	0.8686	0.8760	0.8380	0.8459	0.8674	0.8962	0.8879
Point Biserial Correlation	0.6472	0.6704	0.6332	0.6172	0.6746	0.7343	0.7038
Nominal (Actual) Vs. Nominal (Predicted)*							
Goodman and Kruskal's Gamma	0.8924	0.9082	0.9274	0.8861	0.9512	0.9541	0.9205
Kendall's Tau-b	0.6136	0.6357	0.6481	0.6032	0.6991	0.7340	0.6597
Stuart's Tau-c	0.6107	0.6322	0.6387	0.6014	0.6872	0.7339	0.6590
Somer's D	0.6123	0.6327	0.6388	0.6016	0.6876	0.7340	0.6590

*For calculating these values the continuous probability values were converted into nominal values (1=Wet and 0=Dry) by thresholding the data using the optimal probability cutoff point (0.5332) identified in Figure 4

APPENDIX F: AUXILIARY MATERIAL FOR EFFECTS OF MEASUREMENT RESOLUTION ON THE ANALYSIS OF TEMPERATURE (APPENDIX C)

1 Introduction

This appendix contains the Matlab script code used to generate amplitude ratio values as a function of thermal front velocity, separation depth and thermal diffusivity. This script is made available as an electronic supplement to APPENDIX C: EFFECTS OF MEASUREMENT RESOLUTION ON THE ANALYSIS OF TEMPERATURE TIME SERIES FOR STREAM-AQUIFER FLUX ESTIMATION and it will generate and plot data similar to Figure 2 of APPENDIX C using equation 1 of said appendix. This figure allows the user to answer two types of questions (Q1 and Q2).

Q1) Under ideal conditions what is the maximum separation distance allowable in order to quantify the specified range of thermal front velocities using only two sensors?

Q2) Under ideal conditions what range of velocities can be inferred from paired temperature measurements separated by a specific distance?

Note that any contours that fall below the red contour (Minimum detectable Amplitude Ratio) will result in temperature variations that are smaller than the detection limit of the instrument. Therefore, to be able to observe a measurable temperature variation, the amplitude ratio (AR) for a given soil thermal diffusivity (Ke), velocity (v) and separation distance (z) must me greater than or equal to ARmin (red contour).

2 MatLab Code: Script to generate Amplitude Ratio Values as a Function of Thermal Front Velocity, Depth and Thermal Diffusivity

Code can also be downloaded from http://onlinelibrary.wiley.com/doi/10.1029/2011WR010834/full#footer-support-info by accessing the supporting information section.

```
%% Script to generate Amplitude Ratio Values as a Function of Thermal Front Velocity,
Depth and Thermal Diffusivity
% Version 2.0 Created by Carlos D. Soto Lopez using MATLAB R2010B,
% April 2011
%% Description

% This script is made available as an electronic supplement to Soto-Lopez
% et al. (in press) and it will generate and plot data similar to Figure 2
% of Soto-Lopez et al. (in press) using equation 1 of said paper.  This
% figure allows the user to answer two types of question.

%Q1)Under ideal conditions what is the maximum separation distance
%allowable in order to quantify the specified range of thermal front
%velocities using only two sensors?

%Q2)Under ideal conditions what range of velocities can be inferred from
%paired temperature measurements separated by a specific distance?

% Note that any contours that fall below the red contour (Minimum
% detectable Amplitude Ratio) will result in temperature variations that
% are smaller than the detection limit of the instrument. Therefore, to be
% able to observe a measurable temperature variation, the amplitude ratio
% (AR) for a given soil thermal diffusivity (Ke), velocity (v) and
% separation distance (z) must me greater than or equal to ARmin
% (red contour).
clc
clear all
close all
%_____
___%
%% ******************USER CONTROL
INPUTS**********************************
%General Constants

minz=0.001;                 %Minimum Separation Depth in meters
maxz=5;                     %Maximum Separation Depth in meters
```

```
minv=-4;                  %Minimum Thermal front Velocity positive is
                         % downward direction, m/d
maxv=4;                   %Maximum Thermal front Velocity positive is
                        % downward direction, m/d
tau=1;                    %Period of oscilation in days
ke=0.075;                 %Effective Thermal diffussivity m2d-1
Res=0.15;                 %Sensor Resolution in Deg C

Ao=1;                   %Minimum upper boundary Temperature
                       % Amplitude in Deg C
xlog=1;                   %If you want the output figure to have log
                       %x-axis.  0=no, 1=yes
%_____________________________________________________________________
____
%The following variables are needed to anwer the following questions
%-------------------------------------------------------------------------
%Q1)Under ideal conditions what is the maximum separation distance
%allowable in order to quantify the specified range of thermal front
%velocities usingonly two sensors? (positive is downward direction, m/d)
Vminrange=-1;             %Minimum Thermal front Velocity search
                       %range positive is downward direction, m/d
Vmaxrange=1;              %Maximum Thermal front Velocity search
                       %range positive is downward direction, m/d

%Q2)Under ideal conditions what range of velocities can be inferred from
%paired temperature measurements separated by a specific distance? (meters)
SepDis=0.25;              %Maximum separation distance (meters)
% downward direction, m/d
%_____________________________________________________________________
___%
%% Initalization of Variables
z=(minz:(maxz-minz)/2000:maxz);  %Separation Depth Vector in meters
v=(minv:(maxv-minv)/2000:maxv);  %Thermal front velocity Vector positive is
                          % downward direction, m/d
AR=zeros(length(z),length(v));  %Initalizing Amplitude Ratio Variable
ARmin=Res*1.5/Ao;  %ARmin Value
%Check if parameters are inside boundaries.
if ARmin>1
   disp('ARmin is greater than 1 please check and re-run function')
   return
end
if SepDis>maxz
   disp('The selected maximum separation distance is larger than parameter maxz.')
   disp('Either decrease parameter SepDis or increase parameter maxz')
   return
end
```

```
SearchVrange=min([Vminrange...  %Minimum Thermal velocity for answering Q1
   Vmaxrange]);
SearchSepDis=SepDis;         %Maximum separation distance for answerign Q2
%% Generate AR Values using Equation 3 of Soto-Lopez et al. (2011)

for indx2=1:length(z)%To loop around all depth values
   alpha=sqrt(v.^4+(8*pi()*ke/tau)^2);
   a=(v.*z(indx2)/(2*ke));
   b=(z(indx2)/(2*ke));
   c1=sqrt((alpha+v.^2)/2);
   AR(indx2,:)=exp(a-b*c1);
end

%_____
____
%% Calculation of values for answering Q1 and Q2
w=contourc(z,v,AR',[ARmin ARmin]);
zp=w(1,2:w(2,1)+1);          %This generates an array with separation
%                        depth coordinates of the ARmin threshold
vp=w(2,2:w(2,1)+1);          %This generates an array with thermal front
%                        velocity coordinates of the ARmin threshold
vpindxq1=find(vp>=SearchVrange,1,'first');
Q1ans=zp(vpindxq1); %This is the Answer for Q1
zpindxq2=find(zp>=SearchSepDis,1,'first');
Q2ans=vp(zpindxq2); %This is the Answer for Q2
Q1ansp=round(Q1ans*1000)/1000; %Rounded Answer for printing Q1
Q2ansp=round(Q2ans*1000)/1000; %Rounded Answer for printing Q2
%In case search for Q1ans fall outside limits
if isempty(Q1ans)
   disp(['For velocities between ',num2str(Vminrange), ' and ',...
      num2str(Vmaxrange),' m/d,'])
   disp(['the maximum separation distance exceeds ',...
      'parameter value maxz.'])
   disp('!!!!!Setting distance value to maxz and corresponding velocity to the maximum
VELOCITY')
   disp('in the MINIMUM DETECTABLE AR CURVE!!!!!')
   disp('PRESS ENTER TO ACKNOWLEDGE')
   pause
   Q1ans=maxz;
   vpindxq1=length(vp);
   Q1ansp=Q1ans;
end
%% Graphical Output
close all
% Create Figure
scrsz = get(0,'ScreenSize');
```

```
figure1=figure('OuterPosition',[1 scrsz(4)*.05 scrsz(3)/2 scrsz(4)*.9]);
% Create axes
if xlog==1
   axes1=axes('Parent',figure1,'XScale','log',...
      'Position',[0.10 0.17 0.80 0.78],...
      'Layer','top');
   sp=260;
else
   axes1=axes('Parent',figure1,...
      'Position',[0.10 0.17 0.80 0.78],...
      'Layer','top');
   sp=350;
end
% Plot and label AR data
box(axes1,'on');
hold(axes1,'all');
hold on
[C,h]=contour(z,v,AR','LineColor', 'k');
clabel(C,h,'LabelSpacing',sp, 'FontSize',10);
set(h,'ShowText','on','TextStep',get(h,'LevelStep')*2)
% Plot ARmin Contour
plot(zp(1),vp(1),'r-o');
plot(zp,vp,'r');
plot(zp(1:40:end),vp(1:40:end),'ro')
% Label Axes
xlabel('Separation Distance (m)')
ylabel('Thermal Front Velocity (m/d)')
title(['Amplitude Ratio Contours for a Soil with Thermal Diffusivity ',...
   'equal to ',num2str(ke),'m/d ^2'])
legend('Amplitude Ratio Contours',['Minimum Detectable Amplitude Ratio='...
   num2str(ARmin)],'Location','NorthWest')
%Plot visual representation of Q1ans and Q2ans
plot([minz Q1ans],[vp(vpindxq1) vp(vpindxq1)],'--','Marker','v','MarkerSize',11)
plot([Q1ans Q1ans],[vp(vpindxq1) minv],...
   '--','Marker','v','MarkerSize',11)
plot([SearchSepDis SearchSepDis],[minv Q2ans],':m', 'Marker','<','MarkerSize',11)
plot([minz SearchSepDis],[Q2ans Q2ans],':m', 'Marker','<','MarkerSize',11)
% Create textbox
annotation('textbox',[.12 .035 .654 .064],'String',...
   {['Analysis using a temperature sensor with resolution =', ...
   num2str(Res),'^oC and upper boundary amplitude =',num2str(Ao),'^oC.']...
   ,['For thermal front velocities between ',num2str(Vminrange),...
   ' and ',num2str(Vmaxrange),' m/d, the maximum separation distance <= ',...
   num2str(Q1ansp),' m.'],['With a Separation Distance of ',...
   num2str(SearchSepDis),'m only thermal front velocities >= ',...
   num2str(Q2ansp),' m/d can be estimated.']},'FitBoxToText','on',...
```

```
    'BackgroundColor',[1 1 1]);
hold off
xlim([0.001 1])
ylim([-4 4])
%--------------------------------------------------------------------------
```